WELL INTEGRITY DIAGNOSTICS FOR SUSTAINED CASING PRESSURE AND FAULTY GAS-LIFT VALVES BASED ON PRESSURE TRANSIENT MODELING

A Dissertation

by

TONY ROCHA-VALADEZ

Submitted to the Office of Graduate and Professional Studies of
Texas A&M University
in partial fulfillment of the requirements for the degree of

DOCTOR OF PHILOSOPHY

Chair of Committee,	M. Sam Mannan
Co-Chair of Committee,	A. Rashid Hasan
Committee Members,	Charles J. Glover
	James C. Holste
Head of Department,	M. Nazmul Karim

December 2014

Major Subject: Chemical Engineering

ABSTRACT

A problem frequently present in the oil and gas industry is the difficulty of measuring well integrity parameters; particularly, for high-pressure high-temperature wells. For this reason, many relevant parameters, indicators of the integrity of the well, are not directly measured but rather qualitatively estimated by testing response variables, sometimes, unfortunately, without understanding the correlation between the key parameter and the response variable. This research presents methodologies to quantitatively evaluate well integrity in wells with sustained casing pressure (SCP) and gas-lifted wells with faulty gas-lift valves (GLV). The phenomenon occurring during these well integrity issues were modeled using the thermodynamic properties and transport phenomena occurring inside the wellbore. Well integrity denotes the ability to maintain intentional isolation between the formation and the well. The consequences of not detecting and managing well integrity issues can go from the activation of rupture discs to a release of oil/gas, fire and/or explosion during a blowout.

For the SCP problem, the developed analytic model has been validated against field data and compared to other numerical models showing similar performance. The SCP model allows for early time data to be used to accurately predict the leak's severity by estimating a seepage factor, which is akin to permeability, to account for leakage occurring through the imperfect cement sheath. In comparison to current practices, the model shortens the testing time and reduces the risk from gas accumulation and pressure buildup, making it an inherently safer testing procedure.

The methodology developed to assess wellbore annular integrity, during gas-lift operations, has been compared to acoustic well sounding (AWS) data from different wells. The model divides the well into small elements and estimates average properties which are used to quantify the total amount of mass and hydrostatic pressure in the annulus at any given time. This methodology accurately tracks casinghead pressure and liquid level increase. When fluid intrusion occurs mostly through the gas-lift valve, the model allows estimating the damage coefficient of the faulty GLV. This coefficient serves as a quantitative parameter for GLV replacement; being independent of acoustic well sounding devices. This methodology has the advantages of easy and quick implementation, being accurate, not requiring any specialized equipment, and providing a quantitative damage parameter for the GLV.

To my wife, Irma Angelica,

to my son Iker, and my daughter Mia…

with all my love.

ACKNOWLEDGEMENTS

I would like to express my gratitude to my committee chair, Dr. Mannan, for letting me be part of the MKOPSC and providing support and guidance throughout the course of my studies. His professionalism and leaderships skills are worthy of admiration. To my co-chair, Dr. Hasan, for all the advice, suggestions and technical expertise that made this research possible. His knowledge and brilliance was a great inspiration. To my committee members, Dr. Glover and Dr. Holste, for their valuable comments, support and constructive suggestions.

I would like to acknowledge my team leader and mentor, Dr. Mentzer. His teachings have impacted me in both my professional and personal life. Thank you, specially, for reminding me of putting "first things first".

I also need to recognize the help from many other people from the Chemical Engineering Department and MKOPSC, Towanna Arnold, Valerie Green, Donna Startz, Tricia Hasan and students from the department and friends from the MKOPSC. They have all contributed to make this work possible.

Finally I wish to express my love and gratitude, to my wife Angelica, for believing and encouraging me in every step of the way. To my son, Iker, and daughter, Mia, for being my greatest source of motivation. My family: Moms, Pops, Toño y Rosa, Lucy, Wendy y Alberto, Julio, Suegrita Irma, compadre Jorge y Lore. Thank you.

TABLE OF CONTENTS

Page

LIST OF FIGURES

Page

Page

LIST OF TABLES

Page

1. INTRODUCTION: WELL INTEGRITY PROBLEMS AND RELEVANCE[*]

Along with the increasing demand for hydrocarbons and other sources of energy, the methods for satisfying our energy needs have become more complex. In the case of oil and gas, exploration and production has gone to deep waters and wells are drilled several miles into the earth's core. Nonetheless, we must obtain the hydrocarbons in a safe manner and without negative environmental impacts. The application of technical, operational and organizational solutions to reduce risk of uncontrolled release or intake of formation fluids through the life cycle of a well is known as Well Integrity, as defined by the NORSOK (2004) D-10 standard. The consequences from not achieving well integrity can be catastrophic, both for fluids entering the well in an uncontrolled manner or fluids being unintentionally released to the formation. A blowout is an uncontrolled release of oil and/or gas from a well after hydrocarbons enter the well and pressure control systems fail (Watson et al., 2003); the consequences of such events can result in loss of human life, property and environmental damage. On the other hand, if drilling fluids leak outside the well, the risk of fracturing the formation can have harsh environmental impacts, such as contamination of aquifers from drilling fluids or gas migration.

In the oil field glossary, the gap between two tubes or casings is called the annulus. The casing is the steel pipe cemented in place with the objective of stabilizing

[*] Part of this section is reprinted with permission from "Rocha-Valadez, T., Mentzer, R. A., Hasan, A. R., & Mannan, M. S. (2014). Inherently Safer Sustained Casing Pressure Testing for Well Integrity Evaluation. *Journal of Loss Prevention in the Process Industries, 29*, 209-215." Copyright 2014, Elsevier

the wellbore. The cementing operation is performed to place a cement sheath around a casing fixing the surrounding formation and the casing together. The main objectives of the cement are to provide zonal isolation, support the casing and protect it from corrosive fluids. Depending on the depth of the well there will be several casings in contact with the formation, some of them will be filled with cement, others can be filled with a combination of cement and drilling mud. Figure 1.1, shows a schematic of a well along with its nomenclature.

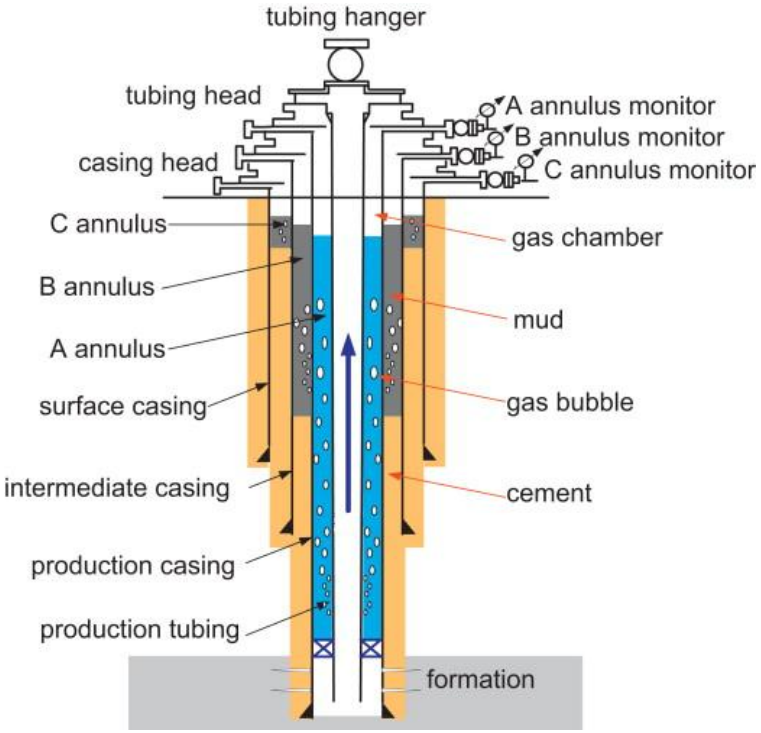

Figure 1.1. Annulus schematic of a well. From Zhu et al. (2012)

1.1. Sustained Casing Pressure

Sustained casing pressure (SCP), exhibited by many wells, is defined as any measurable casing pressure that rebuilds after being bled down, attributable to cause(s) other than artificially applied pressures or temperature fluctuations in the well. Gas leakage, leading to SCP, may occur through the poor cement bond between the casing and the formation, packer, and/or the casing itself. Figure 1.2 shows a pictorial description of the most common problems leading to SCP, including several cementing problems. The migrated gas percolates through the mud or annular liquid column, thereby forming a gas cap above it. The pressure of the gas cap can reach dangerous levels if not properly controlled. Figure 1.3 presents the typical configurations of wells where gas migration or SCP can occur (Zhu et al., 2012). Generally, as the depth of the well increases, the probability of cementing to the surface, from intermediate casing and forward, decreases. This usually occurs given that the cementing to the surface would result in higher material and equipment costs.

Studies submitted to the Mineral Management Service (MMS), currently the Bureau of Ocean Energy Management, Regulation and Enforcement (BOEMRE) (Bourgoyne Jr. et al., 2000; Wojtanowicz et al., 2001), show that the casings most heavily affected, by SCP problems in the US, are the production and intermediate casings. In the report by Wojtanowicz et al. (2001), 85% of the analyzed wells presented SCP problems in at least one casing. Besides the studies and regulations in the United States, issues with casing integrity have been documented in other countries. For instance, a systematic well integrity study by Watson and Bachu (2009) showed that

over 64% of 20,725 wells in a tested area of Alberta, Canada, experienced leakage through the surface-casing vent. The major contributing cause to these leaks was cited to be poorly cemented casings. A study of gas wells by Zhu et al. (2012), performed in Chongqing, China, showed that 92.3% of the studied wells exhibited SCP problems, most of them in two of more casings. Vignes and Aadnoy (2010) explored the well integrity issues of Norway's offshore setting involving 406 wells. Their findings suggested that 18% of the wells have had integrity failures, issues, or uncertainties and 7% of these were shut-in because of well integrity issues.

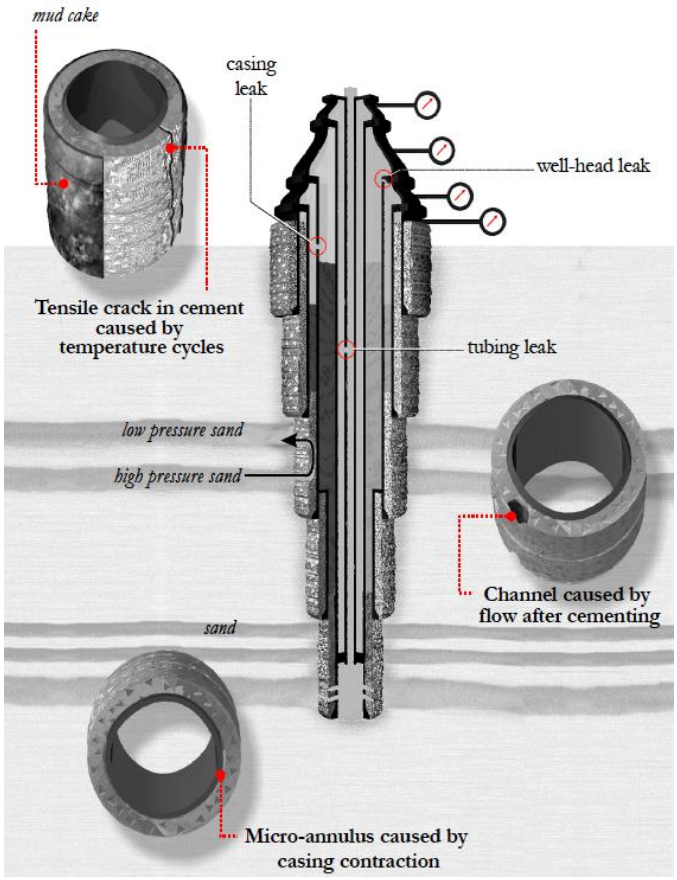

Figure 1.2. Origins of sustained casing pressure. From (Bourgoyne Jr. et al., 2000)

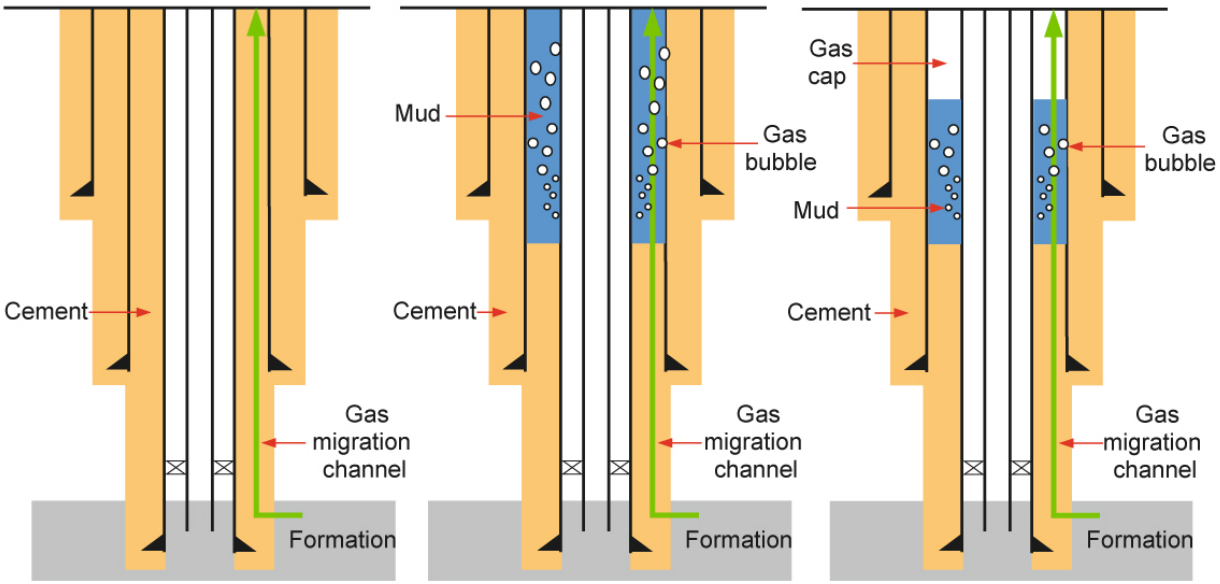

Figure 1.3. Gas migration in different well configurations. From (Zhu et al., 2012).

1.2. Gas-Lift Valve Leakage

The most well-suited artificial lifting technique for deep-water wells is gas lifting (Takacs, 2005) and, as of 2012, was present in 10% of all producing wells in the world (Rigzone, 2012). This technique is commonly implemented when there is insufficient reservoir pressure to lift the column of liquid to the surface. The reduction of fluid density with injected gas enables the lifting. A gas-lifted well consists of an inner pipe called production tubing that connects the reservoir to the surface. Surrounding the production tubing there is another pipe called the production casing. In gas lifted wells, gas is typically injected through the A-annulus into the production tubing as close to the

well bottom as possible. However, in many cases more than one gas-lift valve (GLV) is needed to unload liquid in the annulus at the startup phase. The mixture of oil and gas decreases the overall density of the mixture allowing the oil to rise to the surface. Figure 1.4 shows a typical configuration of a gas lift well along with the all the GLVs.

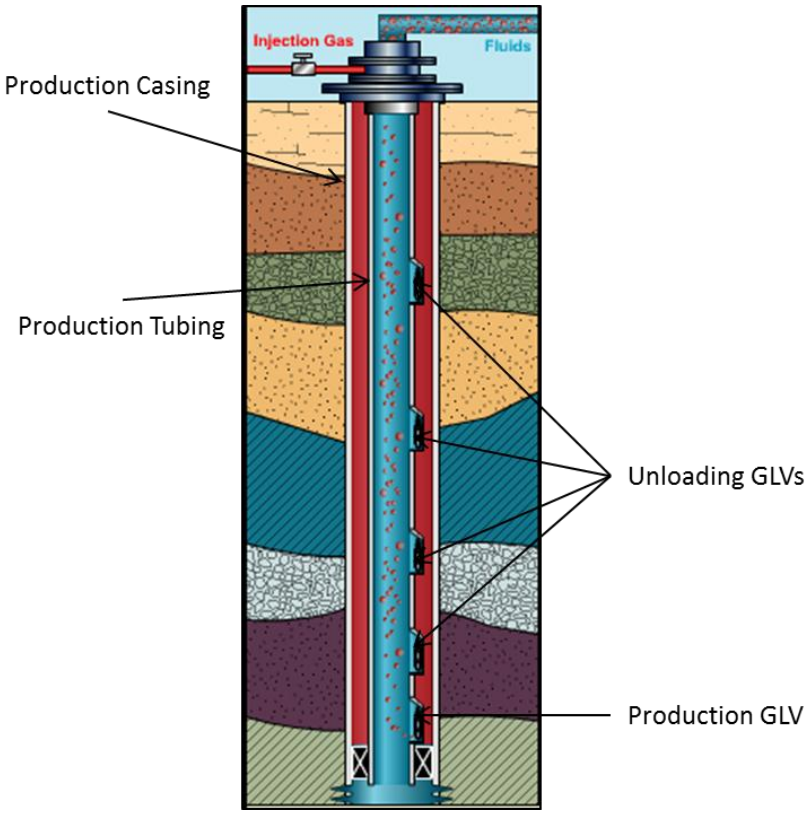

Figure 1.4. Schematic of gas-lift well.

The most commonly used GLV is the injection gas pressure operated (IPO) bellows valve. This is a one-way valve that allows gas to pass through to the tubing but prevents oil from returning to the annulus (Economides et al., 1993). GLVs should, in

principle, prevent the tubing fluid from flowing into the annulus even when pressure differential exists toward the annulus. This situation occurs when the annulus pressure is bled off upon well shut-in. The integrity of GLV may deteriorate over time because of erosion, or it may fail to close because of stuck debris, incorrect injection pressure, improper bellows pressure or corrosion of valve stem (Gilbertson, 2010). If hydrocarbons flow through the wrong path they can reach the wellhead and create an undesired accumulation of high-pressure combustible material; a serious safety issue. The UK's Health and Safety Executive (HSE) published a semi-permanent circular concerning the hazards from gas-lift operations (HSE, 2012), where the main hazard comes from the accumulated gas and the malfunction of mechanical barriers such as gas-lift valves. Typical gas-lift operations require the pressurization of the annulus gas inventory, commonly natural gas, to pressures greater than 1,500 psi, reaching inventories greater than 2 or 3 tons. Needless to say, loss of containment of this inventory could result in tragedy. Additionally, when liquid invades the annulus, a procedure called liquid unloading takes place to get rid of liquid in the annulus through the GLV by injecting high pressure gas. This practice further damages the GLV leading to erosion or check valve problems (Posenato & Rosa, 2012). Figure 1.5 shows GLV components damaged by liquid flow erosion.

Figure 1.5. Damaged components of gas-lift valves from liquid flow. From (Posenato & Rosa, 2012).

1.3. Motivation

Well integrity issues, such as sustained casing pressure and gas-lift valve leakage, are of interest from a process safety and production perspective. As many studies show (Bourgoyne Jr. et al., 2000; Vignes & Aadnoy, 2010; Watson & Bachu, 2009; Wojtanowicz et al., 2001; Zhu et al., 2012) SCP is a worldwide problem that affects the first layer of protection against hydrocarbon intrusion. This issue is not limited to wells that produce oil and gas but also wells that are used for CO_2 applications such as enhanced oil recovery or gas sequestration. Several authors (D'Alessio et al., 2011; Huerta et al., 2009; Loizzo et al., 2011; Tao et al., 2012; Tao et al., 2010) have shown that the phenomena occurring in these wells is fundamentally similar to those in oil and gas. A model to predict SCP would be of benefit to the wells with this problem and could serve as basis for a faster and safer testing procedure.

Gas lift is the most widely used artificial lift method used in enhanced oil recovery, being used in 10% of the oil wells as of 2012 (Rigzone, 2012). Given that

currently no safeguard exists in the GLV to prevent product passage in the event of check valve failure, the proper testing and functioning of the valve becomes even more important. Current testing methods for estimating the damage to GLV consist in pulling the GLV out of the well and inspecting it *off-situ,* deeming the valve temporarily useless and changing it for a tested valve or a new valve. Modeling of the phenomena occurring during this leak intrusion could help design *in-situ* GLV tests that would result in an economic and safety advantage to the operators.

1.4. Problem Statement

Current models to predict SCP (Nishikawa, 1992; Xu, 2002; Zhu et al., 2011), require an iterative numerical solution and, from an operator point of view, could be hard to implement or use. Somei's model, although useful, was never validated against field data and, given that most casings are not cemented to the top, the use of this model is limited to mostly surface casings. Xu's model is based on a system with a mud column above the cement. It assumes that the pressure exerted by the mud column varies as it is compressed. The last assumption requires careful scrutiny given that, for compressible fluids, a decrease in volume will result in an increase in density as long as the mass remains the same. Zhu's, model requires rigorous numerical calculations, high-level programming skills to implement the finite difference method, and is very time consuming. Finally, none of these models have incorporated any further risk analysis or consequence estimation of the wellhead pressures attained during testing periods. In order to improve SCP testing the objective will be to use fundamental equations from the

transport phenomena and thermodynamics occurring in the well, to develop robust analytic models which can represent the SCP behavior and are easily implemented, preferably in an Excel Spreadsheet. Additionally, a consequence analysis of conditions in the well will help establish a safe pressure range where the testing of SCP can be performed.

Because of the well-integrity concern, suspected GLVs can be retrieved with a wireline for inspection, maintenance or replacement when the need arises. Criteria for repair, testing and setting of GLVs, as well as specification of the equipment, are available through recommended practices of the American Petroleum Institute (API, 2008a, 2008b). However, a testing procedure or criteria for determining when a GLV should be pulled out of the well is not specified and would most likely be covered by Annular Casing Pressure Management (API, 2006) practices such as API RP90. Challenges that are carried with current pressure transient tests include: dangerous pressure build-ups, erosion to the GLV, damaging the mechanical integrity of the annulus and future need of liquid unloading. Furthermore, bringing GLVs to the surface merely for inspection is time consuming, resulting in production loss and operational expenses. A novel method is proposed in this research that provides *in-situ* estimates of leak rates through the GLV aided by acoustic well sounding to determine liquid level and flow monitoring during draw down or build up tests.

1.5. Research Scope and Significance

This research focuses on developing models that estimate important well integrity parameters that are, otherwise, hard or impossible to do by *in-situ* testing. Since the scope of the research mostly focuses on annular integrity, the application of the models can encompass both oil and gas wells for onshore and offshore settings. The models will be limited, however, to the phenomena occurring from the point of intrusion of hydrocarbons in the well, to the top of the well, known as wellhead or casinghead.

The purpose of this research is to improve understanding and modeling of the phenomena that present a risk to the integrity of wells. In a much broader sense, the goal will be to develop models that are accurate, economically feasible and less invasive, that can predict key well integrity parameters to facilitate or improve the design of safer operating and testing procedures.

1.6. Deepwater Horizon Oil Spill – A Case Study

The Deepwater Horizon Oil spill serves as example to provide a real-world background on the dangers of not achieving well integrity. The Deepwater Horizon oil spill happened in the Gulf of Mexico. On the 20th of April 2010, high-pressure natural gas from the well expanded into the drilling riser and was released onto the drilling rig where it ignited and exploded engulfing the drilling rig. This incident took the lives of 11 workers, injured 17 others and resulted in approximately 4.9 million barrels of oil spilled; the largest offshore oil spill in history. There are several investigation reports of this incident (BP, 2010; Deepwater Horizon Study Group, 2011; National Oil Spill

Commission, 2011; U.S. CSB, 2014a, 2014b). After cementing operations, a negative pressure test was carried out to determine if the well was sealed. However, the cement did not bond properly and mechanical barriers failed, allowing oil and gas to flow into the production tubing. The hydrocarbons entered the well undetected and reached the surface. Well control was lost and efforts to close the blowout preventer failed after the gas and oil had ignited on the rig and caused an explosion. There are several barriers that failed and their failure aligned in such a way that the worst possible outcome resulted. Figure 1.6 depicts the alignment of these barrier failures.

As shown in Figure 1.6 there are eight key events that, eventually resulted in the fire and oil spill. The events, in a chronological order, are the following (BP, 2010):

1. The annulus cement slurry did not seal the formation.
2. The shoe track, one-way valve, failed to isolate the hydrocarbon.
3. The negative-pressure test was accepted without establishing well integrity.
4. Hydrocarbon leakage was not detected or recognized until the hydrocarbons were in the riser.
5. Well control responses were inadequate.
6. Diversion to the mud gas separator caused gas venting onto the rig.
7. Fire and gas protection systems were insufficient to prevent hydrocarbon ignition.
8. The blowout preventer failed to seal the well.

Even though the avoidance of any of the previous failures would have resulted in the prevention of this disaster, the best practice would be to stop hydrocarbons intake as

early in the process as possible. In this particular case by achieving well integrity the hydrocarbons would not have entered the well. This example shows how, two of the main components, cement and mechanical barriers, are key to successfully achieve well integrity. SCP can result from improper cementing or damaged cement. GLV leakage, in the other side, can be caused by a variety of reasons resulting in the inability of the one-way valve to close properly.

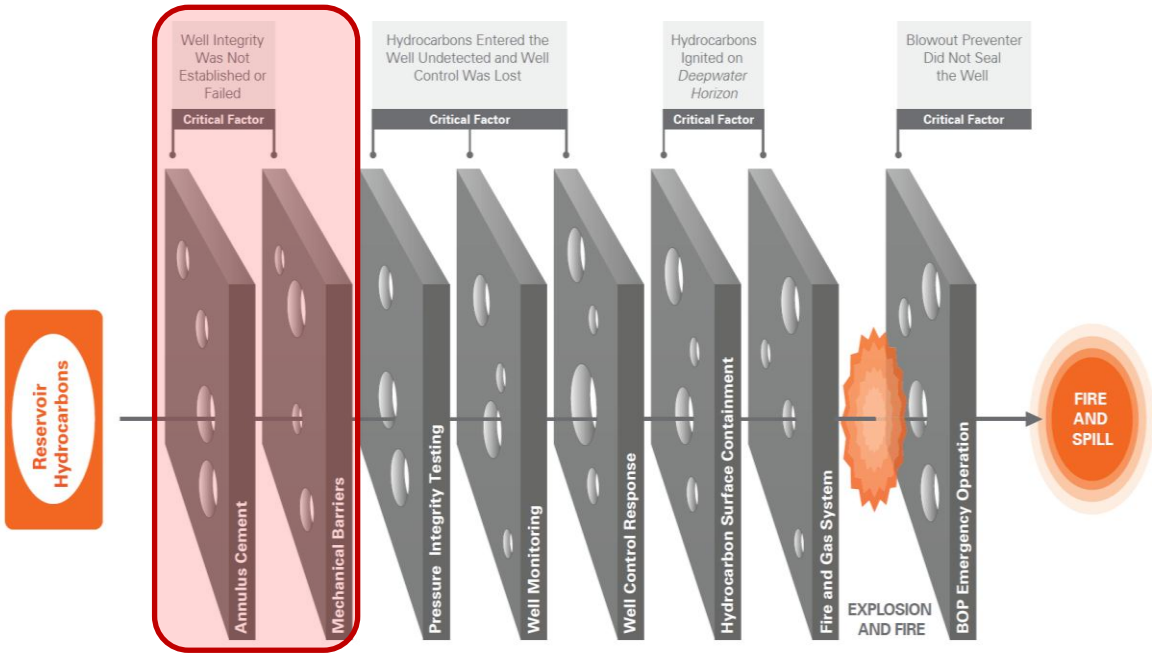

Figure 1.6. Barrier failure in the Deepwater Horizon oil spill. From BP (2010)

1.7. Organization of Dissertation

Section 1 of this dissertation provides the motivation for this research. It presents some basic information regarding the design of a well and its components. The two main

problems, SCP and faulty GLV, are introduced. The problems of current methodologies to estimate SCP and quantify GLV leak severity are described, helping to set the objectives and scope of research.

The following sections, although following the journal article style format, are organized in the same way as the strategy to develop and validate the testing methodologies. That is, in one section we present the model development along with validation and in the following section we present the applicability and describe its use to enhance current practices for detecting well integrity issues in wells with sustained casing pressure or wells with faulty gas-lift valves.

In this context, section 2 describes the development of an analytical expression to model sustained casing pressure and provides comparison against data from different oil and gas wells and is compared against previously developed numerical models. It is also shown that the model is robust enough to be able to accurately predict pressure profiles with early-time data.

Section 3 uses the model developed in section 2 and compares its performance against current U.S. regulatory practices. The time it takes to run a test is compared by analyzing the amount of gas accumulated during these tests. In order to have a sense of the risk present from the gas inventories accumulated during the tests, a risk analysis using the TNT equivalency method is performed.

Section 4 introduces the methodology used to estimate the thermodynamic properties of the gas in the annulus of a gas-lifted well. Two main temperature profiles can occur during this test, a linear temperature gradient or polytropic temperature

profile. These profiles are assumed for the full depth of the well, along with estimated pressure profile, and used to estimate the mass of gas in the annulus. This section shows that by knowing certain variables of the system, the changes in the gas chamber can be calculated to track the changes with respect to time. Data from four wells are reproduced using the methodology presented in this section.

Section 5 makes use of the methodology on section 4 and proposes the introduction of two new variables, exiting gas flow from the casinghead and damage discharge coefficient of the GLV. By introducing these two variables, one of which can be controlled and measured, the degrees of freedom needed to know the gas properties are satisfied. This test is validated by comparing the estimated flow rates provided by a vendor that used AWS, same set of data as section 4. This section also explains how this test can serve as quantitative criteria to decide whether a GLV presents enough damage that it should be replaced or not.

Section 6 gives overall conclusions from this dissertation and provides recommendations for potential future work on the topic of well integrity assessment of sustained casing pressure annuli and faulty gas-lift valves in gas-lift operations.

2. MODELING THE SUSTAINED CASING PRESSURE PHENOMENA*

2.1. Introduction

SCP in one or more casing strings indicates potential wellbore safety concerns during hydrocarbon production. If the induced heat transfer of the producing fluid in the tubing string triggers a rise in annular pressure, this issue is mitigated by reducing the production rate, using insulating material, such as vacuum-insulated tubing, synthetic foam, and burst disc to minimize heat transfer. Many studies (Azzola et al., 2007; Bellarby et al., 2013; Hasan et al., 2010; Oudeman & Kerem, 2006) have addressed this concern, which is termed as annular-pressure buildup (APB). In contrast, if physical hydrocarbon leaks are causing a pressure increase in the annular string, the well integrity issue merits a different treatment. As discussed by Bourgoyne Jr. et al. (2000), the tubing leak into Annulus-A appears to be the main reason for SCP. In fact, flow rates through tubing (Bourgoyne Jr. et al., 2000) leaks can escalate rapidly in the presence of produced sand. Therefore, the leak rate is just as important as the magnitude of the pressure increase in ascertaining the potential hazard. Because SCP detection triggers well-intervention operations and the consequent well shut-in or loss of production for an indefinite period, a strong incentive exists for periodic well integrity assessment.

In light of the above, many field operators have adopted safety measures that evolved with time. For instance, Anders et al. (2008) chronicled various well integrity

* Part of this section is reprinted with permission from "Rocha-Valadez, T., Hasan, A. R., Mannan, M. S., & Kabir, C. S. (2014). Assessing Wellbore Integrity in Sustained Casing Pressure Annulus. *SPE Drilling & Completion, 29* (01), 131-138." Copyright 2014, SPE.

operations at the Prudhoe Bay field in Alaska. Particularly, wells were designed to handle acceptable limits of 2,000 psig in Annulus-A, 1,000 psig in Annulus-B, and 500 psig in the subsequent annuli. In this context, American Petroleum Institute (API) recommends a bleed-off and buildup test when the annulus pressure exceeds 100 psig (API, 2006).

Diagnostic testing for SCP is required in the US. Kinik and Wojtanowicz (2011), make three qualitative inferences to define the risk of SCP: (1) If an annulus shows no pressure buildup from zero WHP after the bleedoff test, the annulus does not have SCP; (2) If the zero annulus pressure increases to a finite safe value within 24 hours following the bleedoff, the annulus is considered to have an *acceptable* leak rate and barriers for pressure containment are considered *adequate*; (3) If the WHP does not bleed to 0 psig in 24 hours, pressure containment barriers may have partially failed and the leak rate may be unacceptable (Kinik & Wojtanowicz, 2011).

Although useful, these guidelines appear arbitrary and require thorough vetting. Accordingly, efforts have been made to run tests that provide quantitative measures. For instance, Nishikawa (1992), modeled the late gas migration through an annulus cemented to the surface. He considered gas migration as vertical flow through permeable porous media and analyzed the effects of cement porosity, temperature, and gas specific gravity on SCP. He concluded that low porosity, low temperature, and low gas gravity would increase SCP. Unfortunately, the model's results were never verified with field data. Furthermore, because most intermediate casings are not cemented to the surface, this model's applicability is severely limited.

For casings that are filled with cement and mud sections, a variety of numerical solutions have been developed and used by several authors (Huerta et al., 2009; Tao et al., 2010; Xu, 2002; Xu & Wojtanowicz, 2001; Zhu et al., 2011). Xu and Wojtanowicz (2001) and Xu (2002) studies, explored the effects of parameters that are usually unknown for most wells. These parameters include but are not limited to the presence and volume of a gas cap at casinghead, height of the mud column, and gas permeability through the cement column. These parameters were regressed with the model to match the pressure rise in the annulus. However, these parameters were recognized by other authors (Bourgoyne Jr. et al., 1999; Wojtanowicz et al., 2001) who attributed the SCP buildup pattern to the parameters of cement, mud, and the gas invasion zone.

The model by Xu (2002) requires an iterative solution with a constant formation pressure assumption. Mud is treated as a constant density, slightly compressible fluid. In addition, it was postulated that gas from the formation would leak through the cement, travel to the top of the mud column, and accumulate in a gas chamber above it. The pressure at the cement top is calculated by adding the pressure of the gas at the top of the mud and the pressure of the mud column itself. We also note that the model by Xu (2002) assumes the pressure exerted by the mud column varies as it is compressed. The last assumption requires careful scrutiny. Zhu et al. (2011) developed another numerical model that coupled gas migration momentum with a heat transfer balance which is solved by the finite difference method giving good agreement with data from one well. Xu's model was modified and adapted by Huerta et al. (2009), and later by Tao et al.

(2010), to study wells in gas reservoirs to explore potential candidacy for CO_2 sequestration giving good fit for wells with SCP problems due to CO_2 migration.

2.2. Model Formulation

The model as sketched in Figure 2.1 shows a gas cap of length L_g, a mud column of length L_f, and a cemented section of height L_c. The formation gas seeps through the cement and percolates up the mud column into the gas cap, compressing the mud column and accumulating at the top because of buoyancy. This model's implicit assumption is that the well produces at a stable rate to ensure the fluctuating tubular flow condition does not induce any heat transfer that will influence the outcome of the SCP test.

At the beginning of the test, the casing is fully open and the pressure is bled to a certain initial pressure, p_o. The instant the annular casing-head valve is closed, the gas bubbles will percolate up the mud column. We assumed the gas leaking through the cement will move up the mud column and will displace the same amount of gas from the top of mud column and into the gas cap. In that sense one can presuppose that the gas emerging out of the cement will affect the gas cap instantaneously. The gas-cap volume will increase with time because of the slight compressibility of the mud and the mud-column length will decrease slowly with time. However, because the mud is enclosed in the annulus, the mass of mud remains constant; therefore, the pressure exerted by the mud column will remain constant.

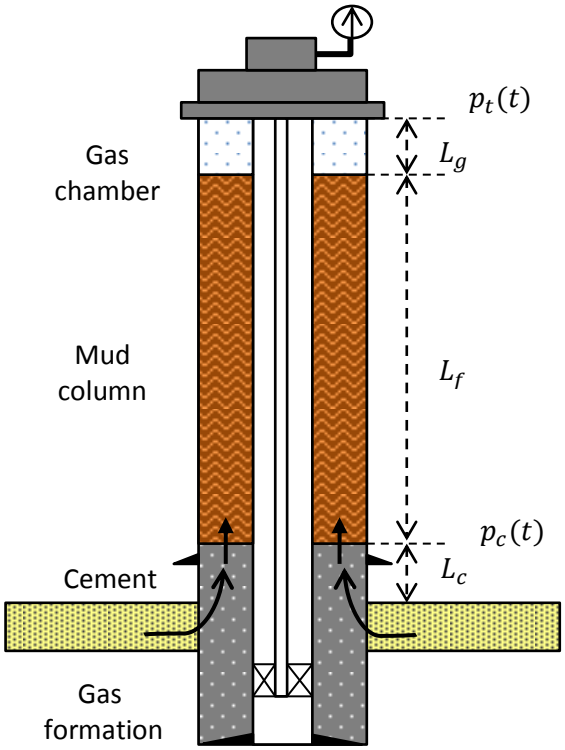

Figure 2.1. Schematic of the cement/mud annular system. (Rocha-Valadez et al., 2014b)

The gas flow through the cement may be written as follows:

$$q = \frac{0.003164kAT_{sc}}{L_c \mu_i Z_i p_{sc} T}\left(p_f^2 - p_c^2\right) \tag{2.1}$$

where q is in Scf/D, k is in md, μ is in centipoise, and pressures are in psia. Note that we prefer to use the term seepage factor, k_s, to account for leakage of any type including that through the imperfect cement sheath. The conversion factor of k in md to k_s in ft^2 is 1.06235×10^{-14}. The seepage factor can also serve as an indicator of the cement integrity,

making it a potential safety performance indicator as suggested by several authors (Hopkins, 2012; Mannan et al., 2014; Skogdalen et al., 2011; Vinnem, 2010).We use the gas law, $n = pV/(ZRT)$, to relate gas influx rate to the gas pressure rate of change in the gas-cap. The change in the gas-cap volume is accounted for by the compressibility of the mud column. Appendix A shows the steps leading to the differential equation governing the transient behavior of casing pressure, which is reproduced below:

$$\frac{\mathrm{d}p}{\mathrm{d}t} = \frac{\dfrac{0.003164kAT_{wh}}{L_c\mu_i Z_i T}\left(p_f^2 - (p + 0.052\rho_m L_f)^2\right)}{V_i + c_m V_m p\left(1 + \dfrac{1}{1 + c_m p}\right)} \tag{2.2}$$

The analytical solution of Equation 2.2 is expressed by the following equation in terms of the independent variable, *t*:

$$t = \frac{\{(\alpha - 1)V_i - \alpha\beta V_m\}\tanh^{-1}\left(\dfrac{p + b}{p_f}\right)}{p_f d(\alpha - 1)} + \frac{c_m V_m\left\{2\ln[1 + c_m p] + (2 - \alpha)\ln\left[p_f^2 - (p + b)^2\right]\right\}}{2d(\alpha - 1)} \tag{2.3}$$

For ease of arriving at a solution, Equation 2.3 is written in terms of the independent time variable rather than the customary dependent variable. Besides estimating the annular pressure rise and the attendant gas influx rate, one can calculate

the cement-seepage factor, k_s, which is akin to permeability. The analytic model presented in this work allows for rapid estimation of the seepage factor for a given data set. Because the pressure-time expression is nonlinear, we used the generalized reduced gradient (GRG) method to estimate k_s. The objective function for the optimization was to minimize the mean-squared error (MSE), similar to the variance of the estimator, [24], which is defined as:

$$MSE = \frac{1}{n}\sum_{i=1}^{n}\left(\hat{Y}_i - Y_i\right)^2 \tag{2.4}$$

where $\hat{Y}$ is the vector of n predictions and Y is the vector of true values. The constraint for the cement-seepage factor k_s, is that the value must be positive.

Another advantage of the analytic form of the solution is that the maximum attainable casinghead pressure, p_{max}, can be estimated corresponding to the infinite shut-in time. Once the model parameters are estimated, Equation 2.3 can be used for that purpose. However, the maximum casinghead pressure can also be evaluated by setting the derivative equal to zero, leading to the following expression:

$$\frac{0.003164kAT_{wh}}{L_c\mu_i Z_i T}\left(p_f^2 - (p_{\max} + 0.052\rho_m L_f)^2\right) \to 0$$

$$p_{\max} + 0.052\rho_m L_f \to p_f \tag{2.5}$$

Equation 2.5 makes intuitive sense because when the sum of casinghead pressure and the pressure exerted by the mud column (= $0.052\rho_m L_f$) equals the formation pressure

p_f, there is no pressure differential available for gas to seep into the annulus; that is, the maximum casing pressure has been attained.

2.3. Model Validation with Field Examples

This section presents the analysis of two sets of wells: oil and gas wells. The two oil producing wells were discussed initially by Xu and Wojtanowicz (2001) and Xu (2002), and more recently by Huerta et al. (2009). In addition, Huerta et al. (2009) and Tao et al. (2012) probed the application of the same model in gas wells to test the well integrity issues in the context of possible CO_2 sequestration.

2.3.1. Analysis of Oil Wells

Figure 2.2 presents history matching of data collected over 300 days and forecasting for Well 23, reported earlier in Xu's dissertation (2002). Only cement-seepage factor adjustment and initial gas-cap height were sought to obtain this match; we assumed that formation pressure, p_f, cemented length, L_c, and total well depth L, are known with reasonable confidence. The relevant parameters are shown in Table 2.1. Note that the seepage factor is inversely proportional to the volumetric rate of gas that permeates the cement. There are two reasons for the significant differences between the parameter values calculated by our model and those reported by Xu. The primary reason appears to be the imprudent use of the cement-top pressure, p_c, instead of the standard pressure, p_{sc}, to convert the gas seepage rate into molal rate in Equation A.2. The second reason is the way the mud-column height and the hydrostatic pressure are treated. In the

proposed method, the hydrostatic pressure of the mud column is considered to be constant throughout, which is consistent with APB analysis induced by heat transfer.

Figure 2.3 presents the results of Well 24 where near-stabilization of pressure occurs in 33 days, as signified by the low-gas influx rate. This example is also taken from Xu's dissertation (2002). Table 2.2 captures the basic input parameters for both wells.

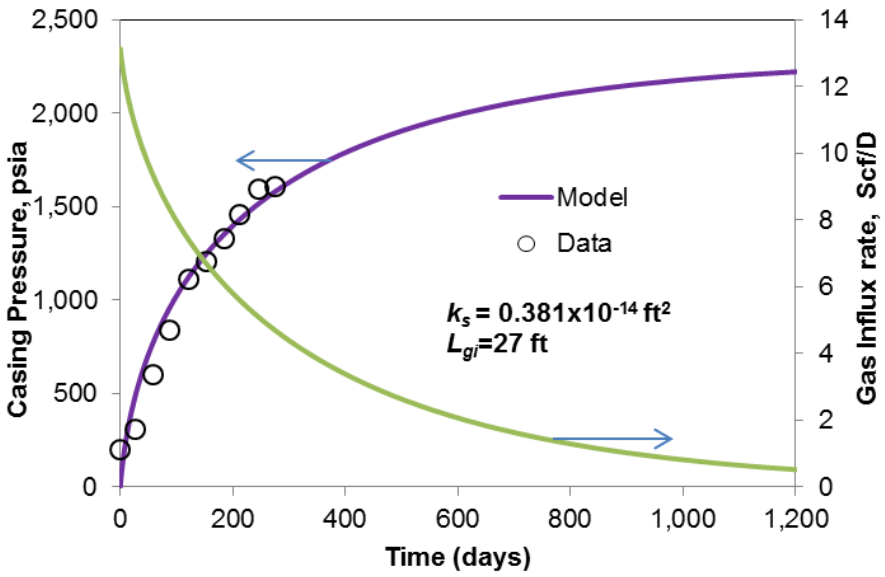

Figure 2.2. Modeling SCP data and future prediction for Well 23.

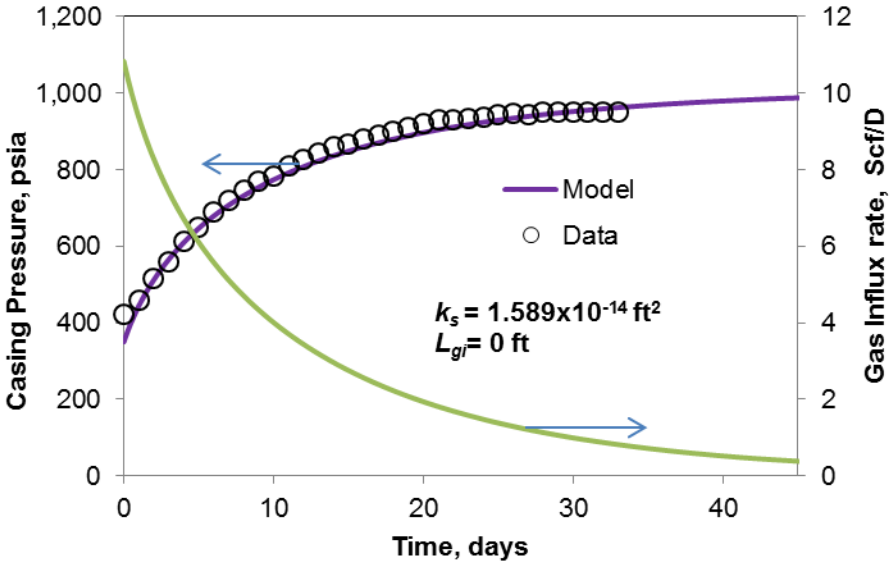

Figure 2.3. Modeling SCP data and future prediction for Well 24.

Table 2.1. Study results for Wells 23 and 24

	Well 23			**Well 24**		
Model Parameters	Xu (2002)	Huerta et al. (2009)	This study	Xu (2002)	Huerta et al. (2009)	This study
p_f, psia	6,600	6515	6,600	6,362	6330	6,362
Initial L_t, ft	27	-	27	0	-	0
c_m, psi^{-1}	4.0E-6	-	4.0E-6	1.5E-6	-	1.5E-6
k, md	**0.001**	**0.403**	**0.3586**	**0.003**	**0.94**	**1.496**
k_s, ft^2			**0.381x10^{-14}**			**1.687x10^{-14}**

Besides the seepage factor, given the uncertainty in reservoir pressure and the initial gas-column height, we performed a systematic study to explore the range of solutions obtained with multivariate regression analyses. We examined three cases by increasing the number of unknown variables in the parameter optimization process: (1)

seepage factor (k_s), (2) seepage factor and the initial gas-column length (L_{gi},), and (3) three variables, k_s, L_{gi}, and formation pressure (p_f). As both Table 2.3 and Figure 2.4 illustrate, increasing the number of unknowns did not change the solution outcome markedly. This finding was reassuring given the uncertainty in field data.

Table 2.2. Input parameters for studied wells

	Well 23	**Well 24**
T_{wb}, °R	575	552
T, °R	630	584
T_{wh}, °R	520	520
T_{sc}, °R	491.7	491.7
D_1, ft	0.829	0.829
D_2, ft	0.583	0.635
L_c, ft	1,821	3,217
Initial L_f, ft	8,273	6,433
ρ, lbm/gal	10	16
μ_g, cp	0.02	0.015
$p_{sc,}$ psia	14.7	14.7
Z-factor	0.86	0.92

Table 2.3. Multivariate regression analysis

Case Number	***k*, md**	**k_s, ft^2**	**p_f, psia**	**L_{gi}, ft**	**MSE**
1	1.490	1.583E-14	6,362	0	2.62
2	1.867	1.983E-14	6,332	0	1.675
3	2.579	2.740E-14	6,325	3	1.515

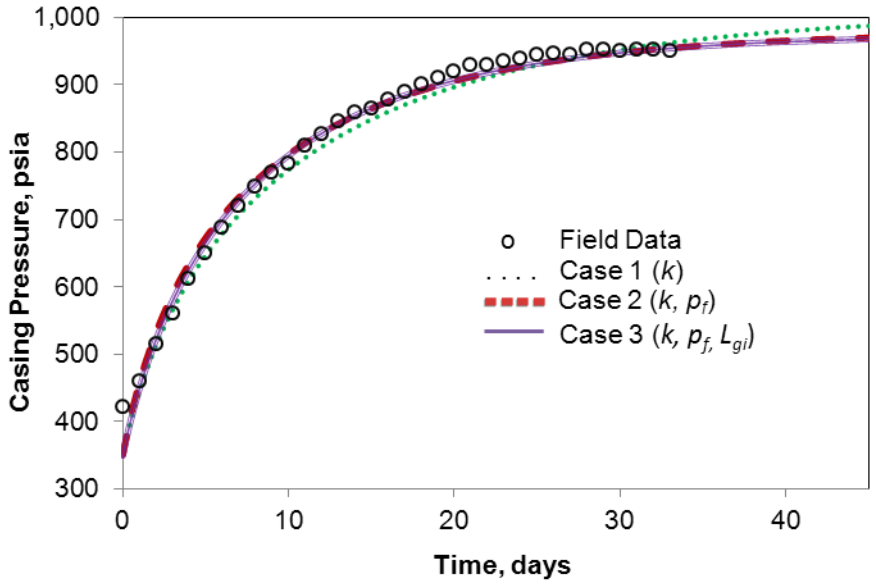

Figure 2.4. SCP modeling with multivariate regression, Well 24.

Next, we explored the notion of partial history matching, followed by future projection to minimize the test duration. We used the data set from Well 24 and estimated a series of k values using the first n number of data, where n = 3, 4, 5, etc. Figure 2.5 shows the sensitivity of k_s values estimated from the limited data showing only the maximum and minimum values of k_s estimated for and the number of points needed to obtain that value. Within Figure 2.5, the average error is shown; the average error is calculated by dividing the averaged k_s values of previous estimates with the k_s value estimated from the full set of data points. Figure 2.5 also helps demonstrate that the model can serve for early time diagnostic for $n \geq 3$ since thereafter, prediction accuracy does not increase significantly with the number of data points used to obtain the cement seepage factor, k_s.

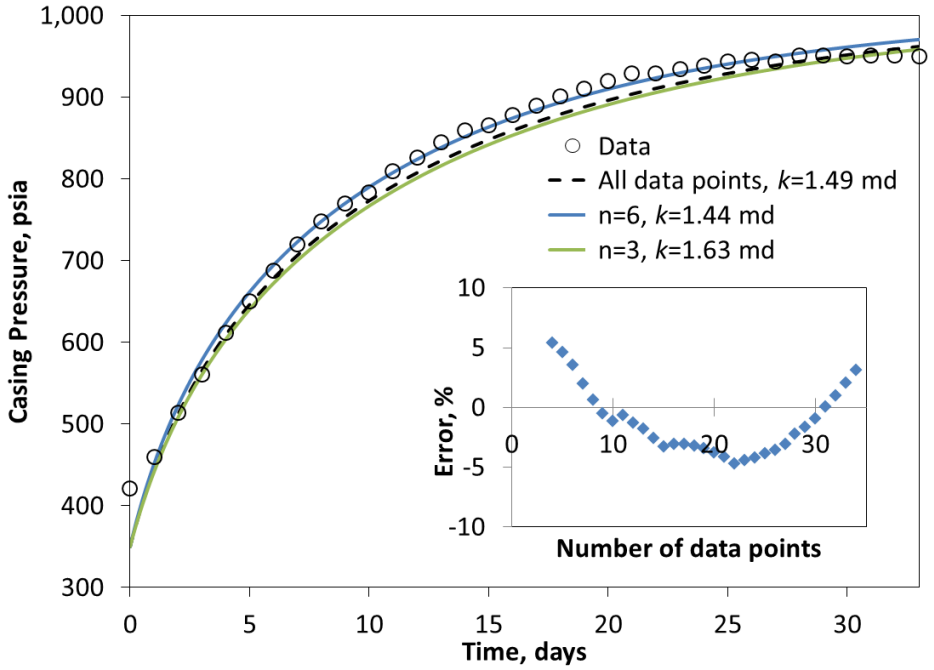

Figure 2.5. Pressure profiles from estimated *k* values with limited data.

2.3.2. Analysis of Gas Wells

In principle, the same SCP model should apply to any well; at least as a first approximation of the physical fact. The well integrity issue becomes a requirement, particularly where the environmental stakes are high, such as in a CO_2 sequestration project. Containment of the injected fluid within a given geologic horizon is of paramount importance during sequestration. For example, Aschehoug and Kabir (2013) have shown that fault breach occurred during CO_2 sequestration into a saline aquifer. Both supercritical-CO_2 lowering the formation-fracture gradient and encountering the unsuspected geologic confinement were cited as possible reasons for the fault breach.

Given the reservoir and/or well integrity issue, Huerta et al. (2009) and Tao et al. (2010) have used the SCP model in potential observation wells in gas reservoirs. The following three figures are examples from those studies. Figure 2.6 is taken from Buildup 4 of Case Study 1, as reported by Huerta et al. (2009). A high-quality match of the data is at hand. Figure 2.7 shows the results of Case Study 2 (by the same authors) and provides some clues about continuous gas influx over 200 days. The initial influx rate is comparable to those shown earlier in Figures. 2.2 and 2.3, although the total time periods vary markedly in all three cases. Our estimates of seepage constant for both these cases are in very good agreement with those of Huerta et al (2009).

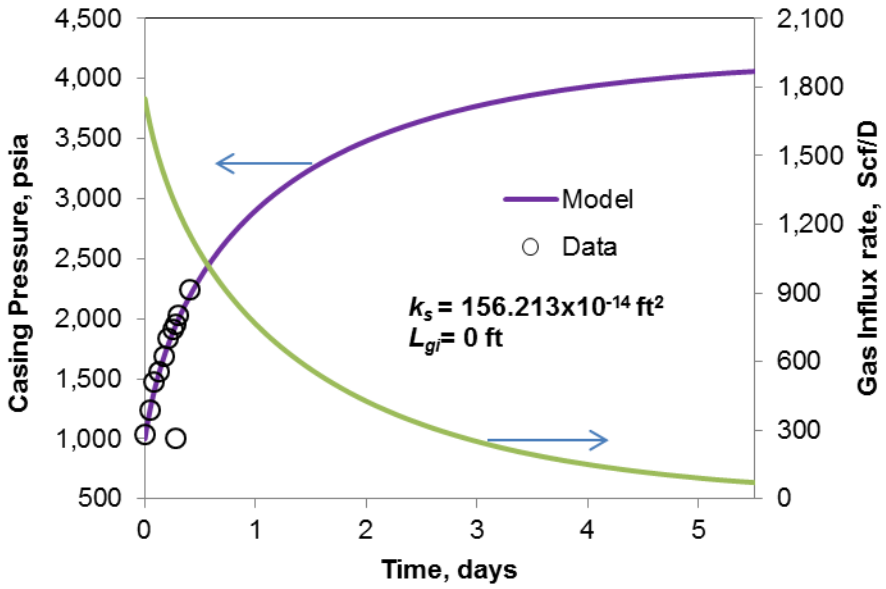

Figure 2.6. SCP modeling of field data, Case Study 1, Huerta et al. (2009)

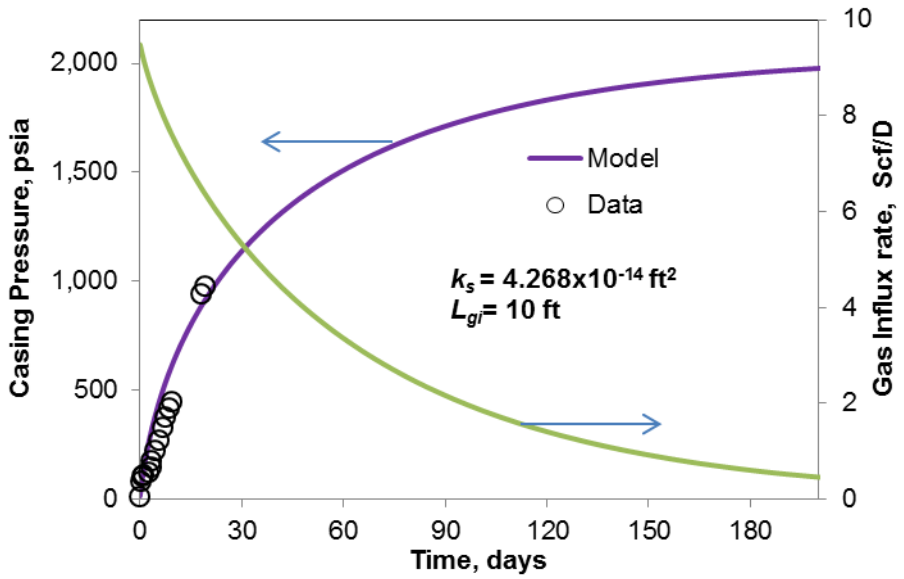

Figure 2.7. SCP modeling of field data, Case Study 2, Huerta et al. (2009)

Figure 2.8 is taken from Tao et al. (2010); it shows that the initial gas rate is two orders of magnitude lower than those of all the examples discussed thus far. This low rate is because of the seepage permeability of 0.01 md our model calculates, which compares favorably with that of 0.012 md, reported earlier by Tao et al. The gas rate estimation appears to provide significant insights into the leakage rate which, in turn, may be used to establish regulatory guidelines that are anchored in realistic data.

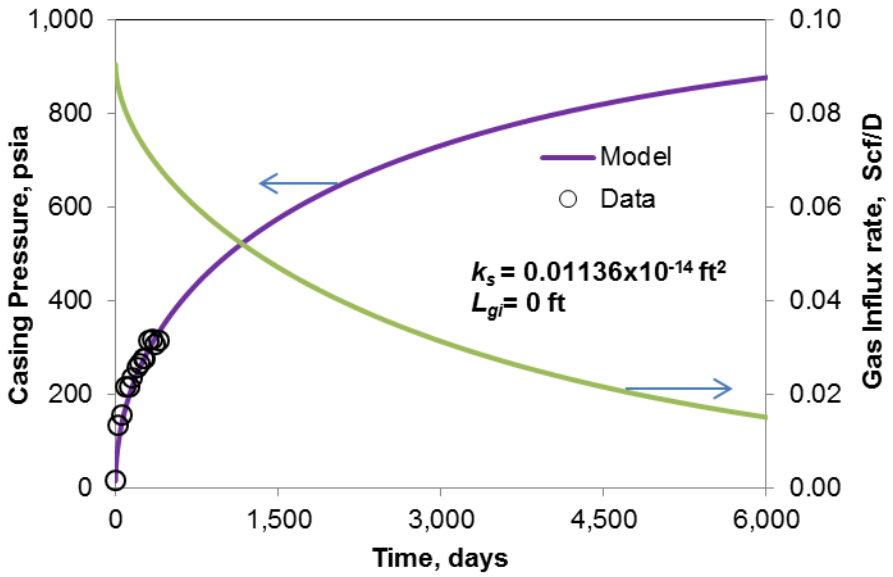

Figure 2.8. SCP modeling of field data, Tao et al. (2010)

The SCP profiles obtained using our model are in good agreement with the field data. Table 2.4 displays estimated parameters using our analytical model and those reported by Huerta et al. (2009) and Tao et al. (2010). We can see from comparing the permeabilities that both models give similar results.

2.4. Discussion

This study presents an analytical solution to Xu's (2002) formulation for studying SCP. There are several advantages of an analytical solution. First, the time to reach a certain pressure can be estimated rapidly without any information of the previous timestep. Second, this problem can be solved by a single-step calculation rather than

performing the same in an iterative fashion. Third, the gas rate estimation quantifies the leakage rate or the cumulative production over a certain time period.

Table 2.4 Study results for gas wells from Huerta et al. (2009) and Tao et al. (2010)

	Case 1		**Case 2**		**Case from Tao et al. (2010)**	
Model Parameters	Huerta et al. (2009)	This study	Huerta et al. (2009)	This study	Tao et al. (2009)	This study
p_f, psia	12041	12041	3200.7	3200.7	1860	1860
Initial L_t, ft	0	0	10	10	0	0
c_m, psi^{-1}	3.0E-6	3.0E-6	6.5E-6	6.5E-6	4.0E-6	4.0E-6
k, md	**140**	**147.08**	**4.0**	**4.01**	**0.012**	**0.0114**
k_s, ft^2		**156.21E-14**		**4.27E-14**		**1.14E-16**

The analytical solution presented in this work offers significant insights into the leakage rate, which may be used to establish regulatory guidelines. The model's ease of use and its ability to estimate the seepage constant and stabilized casing pressure at each timestep allows shortening of the SCP test duration, thereby reducing the test burden.

While studying the SCP problem, several authors (Huerta et al., 2009; Tao et al., 2010; Xu, 2002; Xu & Wojtanowicz, 2001) have used the term "permeability" assuming gas seepage occurs through the cement. While the notion of permeability has merit, it depends on the assumption that seepage only occurs through the cement sheath. A generalized term, such as "cement-seepage factor" or "effective permeability" as introduced here, may be more appealing because it includes leakage of all kinds.

Besides the usual source of cement and tubing integrity, the casing-shoe failure is recognized as one of the primary contributors to the casing-integrity problem. The formation leakoff test (Altun et al., 2001; Wang et al., 2011) can reveal whether the mud pressure at a certain depth exceeds that of the formation at the casing shoe after cementing. Recognizing the limitations of the current regulations, (Kinik & Wojtanowicz, 2011) proposed a probabilistic approach to the casing-shoe failure by adopting Xu's (2002) model. All the published statistics on well integrity issues revolve around old drilling and completion practices. In this context, the studies of Goodwin and Crook (1992) and Jackson and Murphey (1993) shed considerable light on the stress failure of cement. Proactive measures are being taken to mitigate SCP in modern completions such as the use of self-healing cement as described by Taoutaou et al. (2011).

2.5. Conclusions

The formulation of the transport processes for SCP has led to a first-order, linear-differential equation, resulting in an analytical solution. The resulting algebraic expressions for the casing pressure rise and the gas influx rate as a function of time are easy to apply in field-data analysis. Validations with field data from multiple sources lend credence to the model. This model may also be used to estimate the cement seepage factor from limited test data, thereby allowing rapid estimation of the leak's severity. In this context, gas rate estimation is valuable in assessing the total anticipated volume over the time period of interest. Limited testing indicates that the early-time data may be used

with high accuracy for this purpose, thereby curtailing the test duration significantly. A comparison of the model's performance with field data suggests that gas influx causes a casing pressure (Annulus-A) increase in wells. This model has the potential to be the basis for standardization of SCP testing.

3. INHERENTLY SAFER SUSTAINED CASING PRESSURE TESTING[*]

3.1. Introduction

SCP is indicative of compromised well integrity; the risks of not achieving well integrity can range from the activation of rupture disks to a blowout of oil or gas. Hence, SCP in one or more casing strings dictates wellbore safety concerns during hydrocarbon production and may indicate the need for temporary abandonment (Rocha-Valadez et al., 2014b). In addition to oil or gas producing wells, quantifying the CO_2 leakage rate during its sequestration has gained considerable interest recently because of possible emissions into the environment. Several studies (D'Alessio et al., 2011; Huerta et al., 2009; Loizzo et al., 2011; Tao et al., 2012; Tao et al., 2010) examine this subject and concur that the CO_2 leakage process is fundamentally similar and can lead to SCP phenomena with similar risks.

Current Federal Regulation, 30 CFR 250, dictate the mandatory monitoring, testing and corrective action for casings that present substantial SCP problems. Additionally, the MMS/ BOEMRE, provided general guidance in the development of the American Petroleum Institute recommended practice for Annular Casing Pressure Management for Offshore Wells (API RP-90). The current regulations and guidelines for SCP testing, although useful, are mostly qualitative and limited to arbitrary criteria relating to pressure buildup. For example, buildup tests and monitoring are bound to stop

[*]Part of this section is reprinted with permission from "Rocha-Valadez, T., Mentzer, R. A., Hasan, A. R., & Mannan, M. S. (2014). Inherently Safer Sustained Casing Pressure Testing for Well Integrity Evaluation. *Journal of Loss Prevention in the Process Industries, 29*, 209-215." Copyright 2014, Elsevier.

when the Maximum Allowable Wellhead Operating Pressure (MAWOP) is reached or the pressure stops increasing (reaching a stabilized casing pressure).

Figure 3.1 shows one of the flow diagrams for decision making for SCP as described by API-RP 90 (API, 2006). Waiting for those cycles to reach an end point and then make a diagnostic decision might not be the best approach. First, reaching the MAWOP can lead to accumulating large amounts of gas in the annular section of the wellhead which, if released, could have severe consequences from a safety and environmental risk perspective. Second, waiting until the pressure stops increasing, assuming the MAWOP is not reached, might imply that not much gas is present; however, the time to reach this stabilized casing pressure may take months during which time the annular components of the well could be unusable, with a consequent possible negative impact on production. This chapter presents an inherently safer approach to SCP testing using an analytical model as predictive tool that considers early time data to predict future pressure profile, gas accumulation and determine a seepage factor which is akin to permeability. The amount of time required for testing, pressure buildup and gas accumulation are calculated and compared.

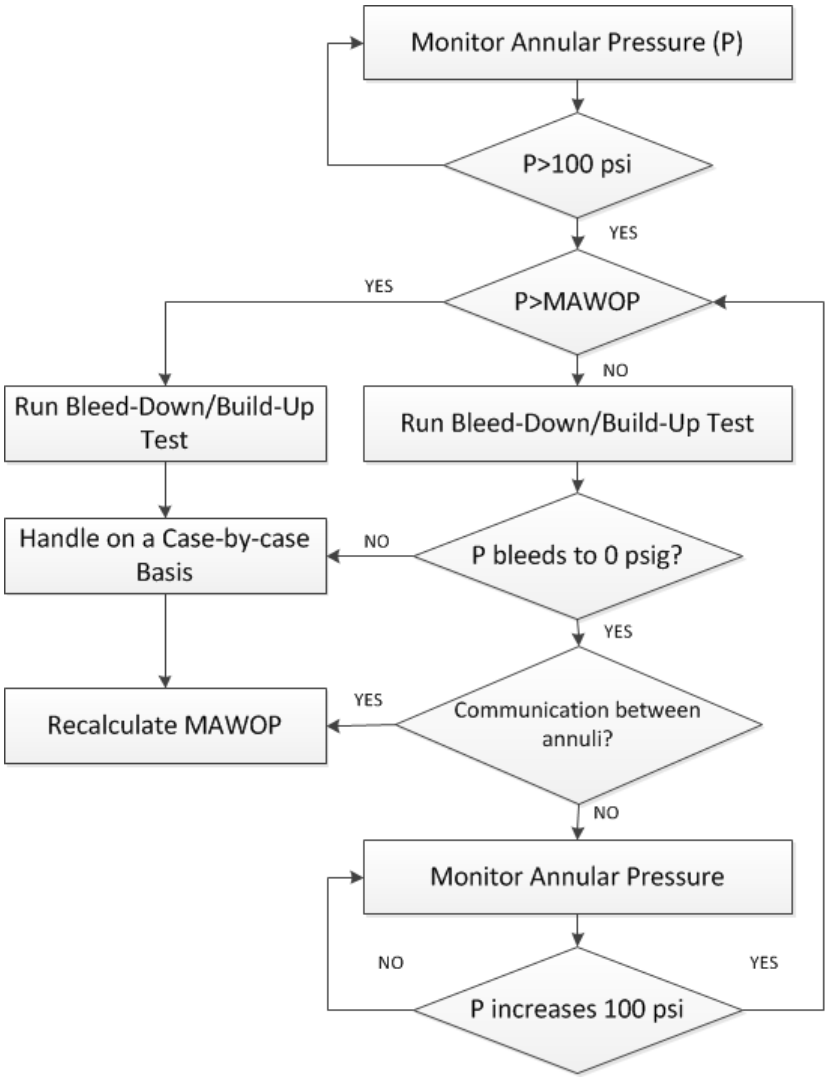

Figure 3.1. Flow chart for SCP decision making. Adapted from (API, 2006).

3.2. Inherently Safer Principles

Inherently safer design is an approach proposed by Kletz (1978). The concept involves a fundamental approach to hazard management that emphasizes reducing or completely avoiding the hazards at the source instead of requiring protective barriers or management systems to control them (Kletz, 1998). The inherent safety principles are:

1) Minimize (reduce the quantity of hazardous material), 2) Substitute (replace a hazardous material or process with a safer one), 3) Moderate (operate at less severe conditions or change the design and operation to minimize the effects of an incident), and 4) Simplify (avoid complexities in the system that can lead to human error or increase the probability of failure). Several authors agree that the benefits from inherently safer principles are maximized when applied as early in the process as possible (Crawley, 1995; Mannan, 2012; Warwick, 1998) and should come first in hierarchy before prevention systems, mitigation and response (Mannan, 2012). However, the application of inherently safer principles is not limited to the design stage and should be considered and pursued at any stage of the lifecycle of the process (Khan & Amyotte, 2002).

Much work has been done to implement the inherent safety principles in the oil and gas industry to reduce the risks. The main hazards on offshore installations, according to Khan and Amyotte (2002), are the process fluids and processing operations, the sea environment, and the process links between the reservoir and other installations. A clear example of inherently safer design is the automation of drilling-systems (Hansen & Abrahamsen, 2001; Kamphorst et al., 1999; Macpherson et al., 2013) which minimizes human involvement and proximity to the hazard; therefore minimizing the risk to the drilling crew. Casing while drilling is another inherently safer technology that, regardless of the complexity of the application, the proven benefits are related to borehole stability, wellbore integrity, a reduced number of casing/liner strings, personnel safety, among other advantages (Sanchez & Al-Harthy, 2011; Sanchez et al., 2012). An

example of simplification from inherently safer principles that reduces the risk between the reservoir and other installations includes the design of a structure for easy inspections which can result in costs of approximately 10% of the predicted savings in inspection costs (Hill Jr & Bhavsar, 1996).

The previous examples show that inherently safer designs and technologies, when developed and evaluated properly, are effective tools that not only reduce the risk and improve the overall process safety, but also improves the productivity and reduces operating or testing costs. It is important to mention that inherently safer principles could also, and should preferably, be applied to early design stages to prevent SCP from occurring, therefore eliminating the need to test for and quantify the problem (Rocha-Valadez et al., 2014c); for example, by using self-healing cement when placing the casings. These self-healing cements can either be activated when in contact with hydrocarbons (Le Roy-Delage et al., 2010) or without any fluid contact (Reddy et al., 2010). Nonetheless, a high percentage of wells around the world have already developed SCP and could benefit from this type of testing approach.

3.3. SCP Testing Methodology

In the proposed methodology we evaluate the risk from following the current practices as well as the risk from using the model described in this chapter. The methodology consists of quantifying the amount of gas that is accumulated in the casinghead for three different time periods. These three periods are 1) until the pressure is near stable conditions, 2) until the MAWOP is reached (if ever), and 3) until the

model can predict cement seepage factor within a 95% confidence interval. The data acquired for estimating the seepage factor is obtained from recording the annular wellhead pressure every 200 psia or every 12 hours, whatever occurs first. The gas contained in the casinghead, due to SCP or other sources, represents a safety and/or environmental risk; particularly if the gas is flammable. Most of the gases bled-off from the annulus are either purged to atmosphere or sent to a flare, depending on the quantity and regulations. The importance of proper purging procedures and use of flares to manage the risk from gases accumulated in the annuli is critical. If an unintended release of this gas were to occur, there are several possible outcomes; as described by the Center of Chemical Process Safety (CCPS, 2000) and summarized in Figure 3.2.

As a case study for this work we will assume that the gas contained in the annuli is released under conditions that achieve the worst case scenario outcome, which would be an explosion. To have a sense of the consequence component of the risk from accumulated gas, the mass of the gas is converted into an equivalent mass of TNT that would release a comparable amount of energy if an explosion would occur under certain conditions; the methodology followed is presented in the Peak Overpressure Estimation section. Figure 3.3 illustrates the methodology followed to compare the SCP testing methods discussed previously.

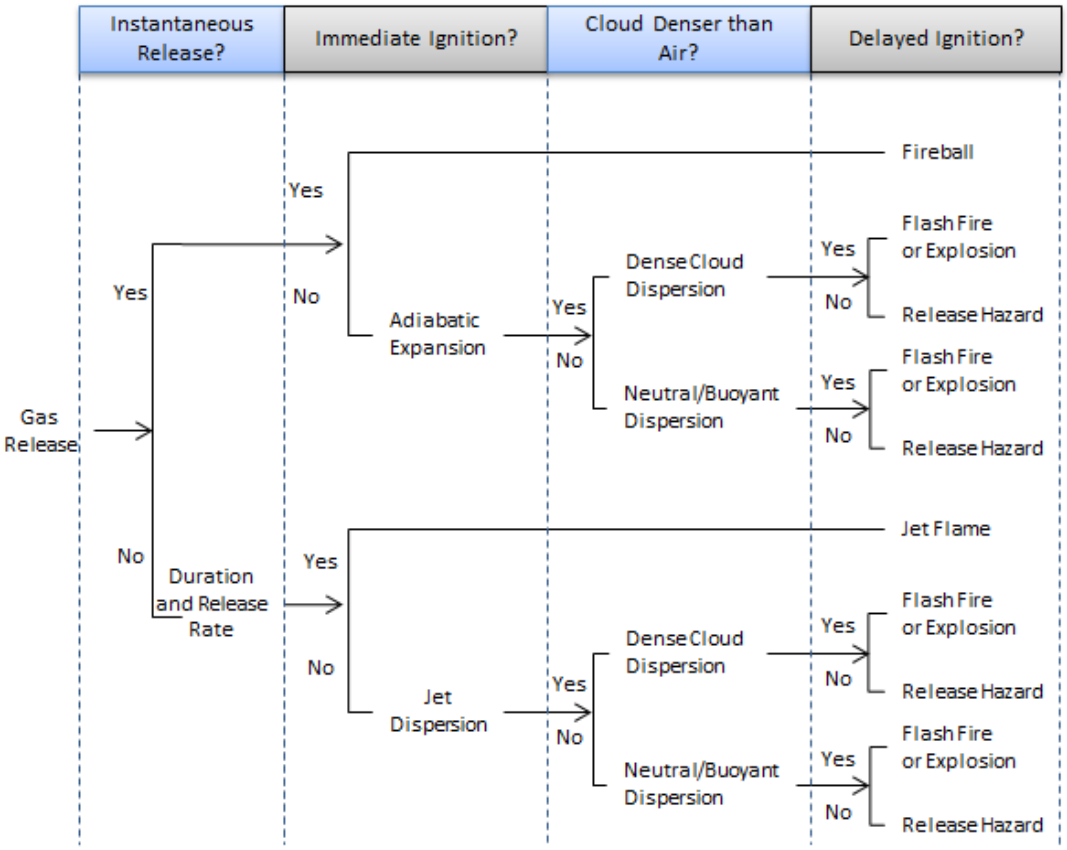

Figure 3.2. Event tree of gas release. Adapted from CCPS (2000).

3.4. SCP Model Formulation

In order to improve testing times and diagnostics for pressure buildup testing we use an analytical model developed by Rocha-Valadez et al. (2014b) that has been shown to provide similar results to existing numerical methods and field data; the model is described in section 2 of this dissertation, "MODELING THE SUSTAINED CASING PRESSURE PHENOMENA". The mentioned model has the advantage of having an

analytical solution from which the time to reach a certain pressure and the gas flow rate can be estimated.

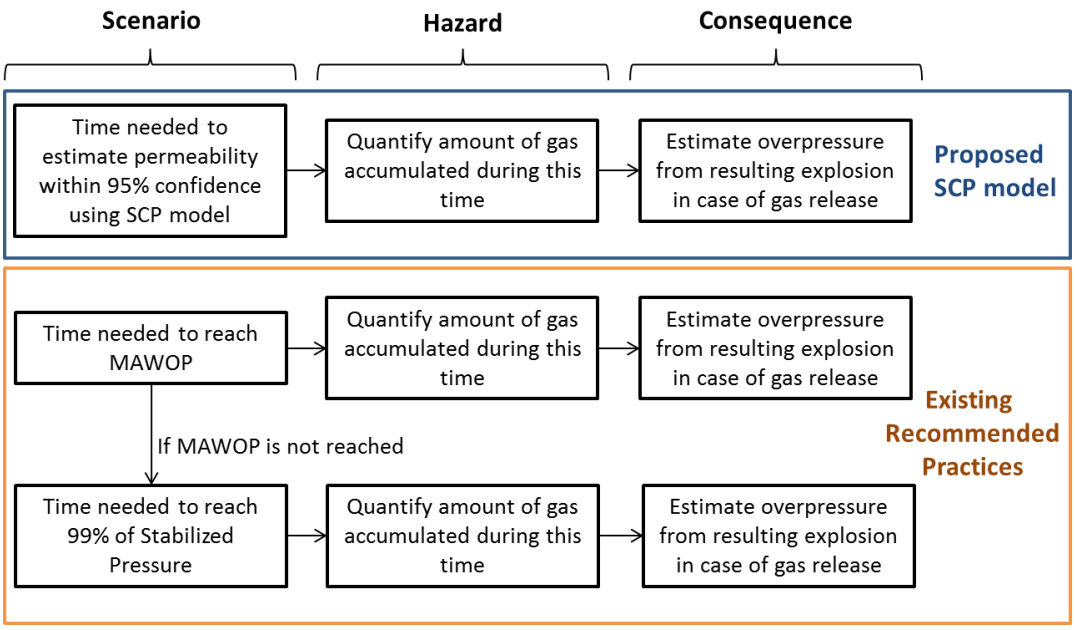

Figure 3.3. Hazard and consequence comparison flowchart for SCP testing.

3.5. Peak Overpressure Estimation

Natural gas was used as the explosive, this scenario is possible for an instantaneous release with delayed ignition or in case of a continuous release under conditions that allowed the formation of a vapor cloud that later ignited. The blast damage resulting from overpressure was estimated using an equivalent mass of TNT, m_{TNT}, and the distance from ground zero point, denoted as r, in this case being the center

top of the wellhead where the gas chamber is located. The empirically derived scaling law, as described by Crowl and Louvar (2011), is:

$$z_e = \frac{r}{m_{TNT}^{1/3}} \tag{3.1}$$

The estimation of the peak side-on overpressure is represented by the following empirical equation (Crowl & Louvar, 2011):

$$P_o = P_a \frac{1616\left[1+\left(\frac{z_e}{4.5}\right)^2\right]}{\sqrt{1+\left(\frac{z_e}{0.048}\right)^2}\sqrt{1+\left(\frac{z_e}{0.32}\right)^2}\sqrt{1+\left(\frac{z_e}{1.35}\right)^2}} \tag{3.2}$$

The TNT equivalency method assumes that an explosive fuel mass behaves similar to exploding TNT on an equivalent energy basis. The equivalent mass of TNT is estimated using the following equation from Crowl and Louvar (2011):

$$m_{TNT} = \frac{\eta m \Delta H_c}{E_{TNT}} \tag{3.3}$$

In Equation 3.3, η is the empirical explosion efficiency (unitless), m is the mass of natural gas (kg), ΔH_c is the energy of explosion of the flammable gas (54 kJ/kg for

natural gas); and E_{TNT} is the energy of explosion of TNT (4686 kJ/kg). Typical consequences from over pressure exposure are presented below in Table 3.1.

Table 3.1. Effect from overpressures. (Glasstone & Dolan, 1977; Sartori, 1983)

P_o	Effects on Structures	Effect on the Human Body
1 psi	Window glass shatters	Light injuries from fragments occur
2 psi	Windows and doors blown out and severe damage to roofs	People injured by flying glass and debris
3 psi	Residential structures collapse	Serious injuries are common, fatalities may occur

3.6. Case Studies and Results

We will take two wells, Case Study 1 and Case Study 2; Table 3.2 shows relevant parameters of these wells. Using the SCP model described earlier we can estimate the seepage factor with 95% confidence as soon as 3 hours after beginning testing for Case Study 1 and as soon as 4 days for Case Study 2.

To use these wells as examples, and given that not all the information is available, we will make the following assumptions: the gas contained in the casinghead is natural gas, the gas contained in the wellhead from the SCP testing is released under given circumstances that result in an explosion, which represents the worst case-scenario, the peak overpressure will be estimated at a distance from the explosion, *r*, of 30 meters and for an explosion efficiency of 5% since, according to Crowl and Louvar (2011), the most common values range between 1 and 10%. As mentioned previously, two criteria for stopping a buildup pressure test in the case of SCP are: 1) when the

wellhead pressure stabilizes and, 2) when it reaches the MAWOP. Additionally, the model presented herein permits establishing a new stopping criteria, 3) when the error of the average cement seepage factor changes by less than 5%.

Table 3.2. Input parameters for Case Study 1 and 2.

Parameter	**Case Study 1**	**Case Study 2**
A, ft^2	0.098	0.223
c_m, psi^{-1}	3.0E-6	1.5E-6
k_s, md	126.3	1.496
L_c, ft	4359	3217
Initial L_f, ft	8700	6433
Initial L_g, ft	3	0
p_f, psia	12041	6362
p_{sc}, psia	14.7	14.7
T, °R	770	584
T_{sc}, °R	491.7	491.7
T_{wh}, °R	539.7	520
Z-factor	0.86	0.92
μ, cp	0.02	0.015
ρ_m, lb/gal	17.4	16

Pressure ratio was normalized by dividing the current pressure by the stabilized pressure; the time to reach that pressure and amount of gas in the casinghead at that given time was estimated using the analytical SCP model in this chapter. Several different percentages were used ranging from the minimal value obtained from the analytical model up to 99% of stabilized pressure. Finally, the peak overpressure resulting from the ignition of that gas was estimated using the TNT equivalency method and the assumptions described above. These results are summarized in Table 3.3 for

Case Study 1 and Table 3.4 for Case Study 2. Red cells are over pressures where fatalities could occur, yellow cells represent conditions at which serious injuries could be sustained and green cells are conditions where only minor injuries might occur.

3.6.1. Case Study 1

We can observe from Table 3.3 that, if the stopping criterion was reaching a stabilized pressure it would take nearly 8.5 days; the consequences from an explosion after running a test for that period of time would be over 3 psi which could result in death of people in buildings within 30 meters. However, following the recommended API practice of stopping when reaching the MAWOP, and assuming that the MAWOP is around 3,000 psia, we can observe that the time of testing would be reduced to a little over 24 hours and reduce the peak over pressure to 2.2 psi, indicative of significant damage and potential injuries. Finally if we run the test for 4 hours, enough to successfully estimate the seepage factor, we would reduce the peak overpressure to only 1.2 psi, where only light injuries might occur. These three criteria points can be observed in Figure 3.4.

Table 3.3. Results for Case Study 1.

P/P_{stab}	Time, hour	Gas, scf	m_{TNT}, kg	P_o, psi
99%	209.0	2490	32.7	**3.15**
95%	118.1	2288	30.0	**3.04**
90%	78.2	2017	26.5	**2.87**
75%	34.5	1334	17.5	**2.41**
68%	24.7	1074	14.1	**2.23**
52%	**9.9**	531	7.0	**1.70**
49%	**8.1**	450	5.9	**1.57**
39%	**4.0**	240	3.1	**1.24**
37%	**3.2**	195	2.6	**1.15**

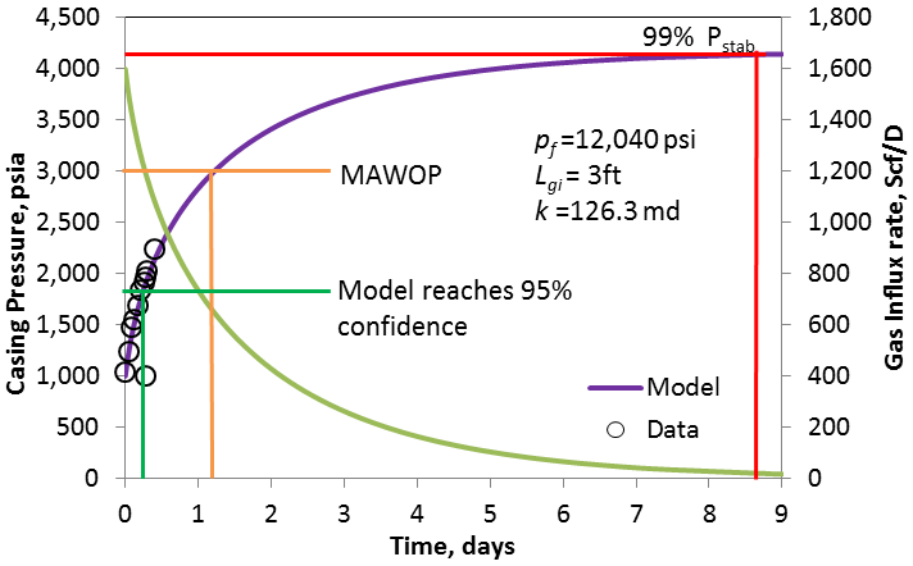

Figure 3.4. Wellhead pressure profile for Case Study 1.

3.6.2. Case Study 2

By observing Table 3.4, we can see that the resulting overpressures, even when reaching 99% of stabilized pressure are below 1 psi, meaning that even in the worst-case

scenario of release it is unlikely to have any fatalities or even major injuries. It is also unlikely that the MAWOP would be reached since the wellhead pressure is below 1000 psi. However, as observed in Figure 3.5, we can see a big difference between the time it takes to reach 99% of the stabilized pressure, 60 days, and the four days it would take to know the pressure profile by estimating the cement seepage factor with the analytical model. It would be a strong economic incentive to perform a quick test rather than waiting months to have a full pressure profile, especially if the casing should be needed for other activities which could affect production.

Table 3.4. Results for Case Study 2.

P/P_{stab}	**Time, days**	**Gas, scf**	**m_{TNT}, kg**	**P_o, psi**
99%	62.5	121	1.6	**0.97**
95%	33.5	111	1.5	**0.94**
90%	12.5	73	1.0	**0.81**
75%	9.5	61	0.8	**0.77**
73%	**8.0**	56	0.7	**0.74**
71%	**7.0**	52	0.7	**0.72**
68%	**6.0**	46	0.6	**0.69**
64%	**5.0**	40	0.5	**0.66**
60%	**4.0**	33	0.4	**0.62**

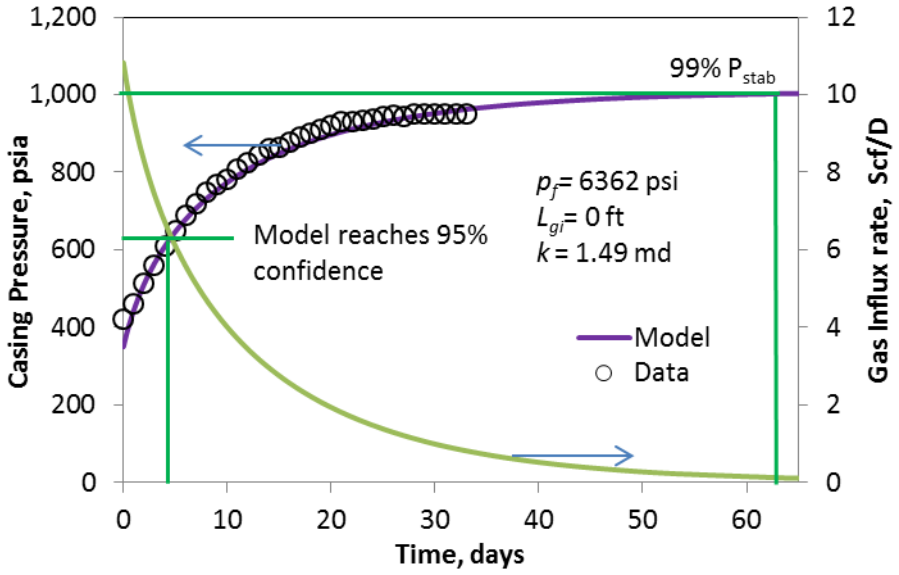

Figure 3.5. Wellhead pressure profile for Case Study 2.

3.7. Conclusions

The use of the SCP model, in the form of a first order, linear differential equation, allows for the estimation of the seepage factor and gas influx for wells with potential sustained casing pressure problems. Comparisons of the model against field data indicate that early-time data may be used with high accuracy for rapid estimation of the leak's severity. A comparison of the quantities of gas accumulated over different testing time periods was made. The amount of gas and the risk from the testing method proposed, showed that testing times and hazardous conditions such as high pressures and total accumulated gas can be reduced significantly. Besides practicing the inherently safer principles of minimize and moderate, this testing procedure could help reduce non-productive time. The model shows promise as a predictive tool and potential to be a basis for a standardization of SCP testing.

4. ESTIMATING ANNULAR GAS PROPERTIES IN GAS-LIFT WELLS*

4.1 Introduction

By definition, gas-lift valves (GLVs) are designed to allow influx of the annular gas into the tubing and prevent any backflow, even when there is a pressure differential with the annulus. However, elements such as erosion, corrosion, scale, fatigue, vibration, and temperature and pressure effects may cause the GLV to leak, thereby posing a serious safety issue. Because of the well integrity concern, suspected GLVs are often retrieved for inspection with a wireline from the side-pocket mandrel. Proactive testing is a way to minimize such costly intervention.

The use of gas-lift technology dates back to the 1940's. Recently, Decker (2008) provided some insights into modern design and use of injection-pressure-operated gas-lift valves. Accurate models are also available for calculating critical flow rate across Venturi valves, especially for high-pressure gas-lift systems, as proposed by (Almeida, 2011). Given the widespread use of gas-lift as an artificial-lift mechanism, integrity of GLV is of great interest to the industry. The UK's HSE highlighted the importance of integrity evaluation of mechanical barrier systems. In the Offshore Research priorities for the period 2009-2014, they request the determination of best practices for an effective in-service valve inspection strategy and reliability of acoustic technology as main tool of measurement (HSE, 2004). Accordingly, some operators (Carlsen et al.,

* Part of this section is reprinted with permission from "Rocha-Valadez, T., Hasan, A. R., Mannan, M. S., Crabtree, A., & Kabir, C. S. (2014). *Assessing Integrity of the Gas-Lift Valves by Analyzing Annular-Pressure-Transient Response* Paper presented at the SPE Artificial Lift Conference and Exhibition - North America, Houston, Texas". Copyright 2014, SPE.

2010; Xu et al., 2012) have taken proactive measures to ensure the GLV safety, beyond those suggested by the API recommended guidelines (API, 2008a, 2008b, 2008c, 2010). As stated by Grassick et al. (1992) the probability and consequence of a blowout can be amplified in some gas-lifted wells because of the large inventory of high pressure gas in the wells. To improve well safety, Gilbertson et al. (2013) offered a passive, thermally actuated safety valve for gas-lift operation in offshore wells. The valve adds redundancy to the system and improves overall safety. Loading and shut-in procedures were developed consistent with current practices and a real-size prototype was manufactured. Unfortunately, this technology has not yet been thoroughly tested.

The use of artificial intelligent agents, such as the one described by Stephenson et al. (2010) to diagnose the lift system has significantly helped manage data gathering and interpretation, and subsequent actions. Models have also been offered to design and analyze flow instability; the studies of Poblano et al. (2005), Blick et al. (1988), and Asheim (1988) are cases in point. More recently, several authors (Eikrem et al., 2008; Garcia, 2013; Posenato & Rosa, 2012) have offered stability analysis when cyclic variations in pressure and production rates occur resulting in significant disturbances to the downstream processing facility.

Despite the long operational history of the gas-lift system, methods for testing GLV integrity appear limited in the open literature. This chapter attempts to provide some insights into model development and interpretation of field data. Specifically, this study presents a methodology for computing liquid flow rate across the GLV into the annulus by drawing down the annular gas and the subsequent buildup of pressure

measured at the casinghead. These two tests allow estimation of the liquid leakage rate independently, thereby instilling confidence in the calculation.

To examine the integrity of GLVs, a number of tests were run on three wells. These tests included gathering acoustic-well sounding (AWS) data for annular liquid level and casinghead pressure at various times in accord with current field practice in an offshore setting. Appendix C provides more details regarding the AWS data and its interpretation. We used these data to validate the models developed in this study. These models are predicated upon the use of a mechanical energy-balance equation for estimating annular pressure and thermodynamic relations for estimating the annular gas temperature. Computations showed that the use of both the constant geothermal gradient and polytropic expansion/compression yielded comparable solutions.

4.2. Model Development

The model relies upon calculating the total amount of gas in the annulus at each timestep. By knowing the liquid level in the annulus and the casinghead pressure, the total volume of gas and its density can be calculated, leading to the computation of the total mass of gas. Because density varies nonlinearly with depth, the annulus is subdivided into 50 cells for numerical integration. The average pressure and temperature of a cell is used to calculate the gas density, which is then used to evaluate the mass in that cell, as well as the pressure difference across the cell. Figure 4.1 depicts a typical gas-lift system.

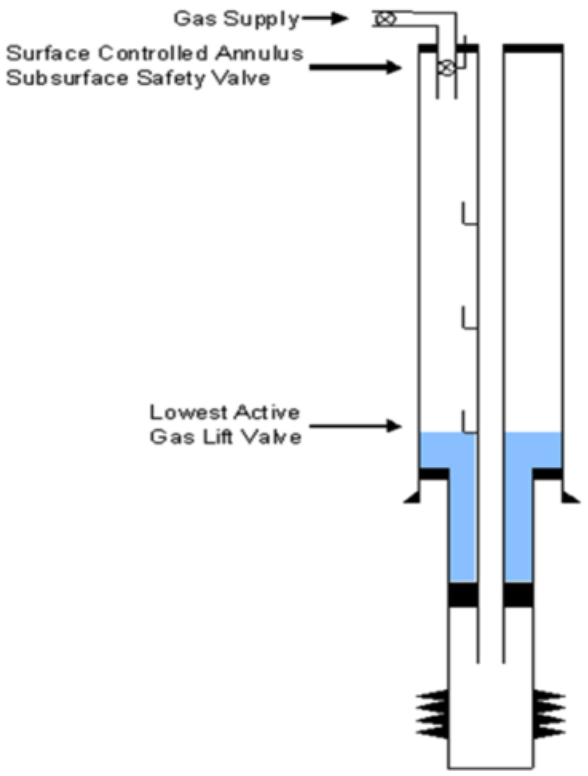

Figure 4.1. Schematic showing the GLV configuration in a typical well.

To represent the pressure, volume, and temperature (PVT) behavior of gas in the annulus, the generalized thermodynamic relation is given by:

$$pV = ZnRT \tag{4.1}$$

Equation 4.1 may be used to write an expression for gas density, which is needed to estimate the pressure profile in the annulus, which is given by:

$$\rho_f = \frac{29\gamma_g p}{\bar{Z}\bar{R}\bar{T}} \tag{4.2}$$

The model is based on the application of mechanical-energy balance to the annular gas. In integral form, the general mechanical-energy balance, neglecting work done and heat received, is written as (Watson et al., 2003):

$$\int_{p_1}^{p_2} \frac{dp}{\rho_f} + \frac{g}{g_c}(z_1 - z_2) + \frac{\rho_f\left(v_2^2 - v_1^2\right)}{2g_c} + \frac{fv^2(z_1 - z_2)}{2g_c d} = 0 \tag{4.3}$$

Although gas does flow up the annulus during a bleed-down test, the velocity is so small that energy losses owing to kinetic energy change and friction (less than 0.01% of the total) are neglected. In addition, we assume that the annular gas maintains a time-invariant, linear-temperature gradient (LTG). Calculations that allow for temperature change owing to polytropic expansion or compression in the case of pressure buildup will be discussed later. Under these conditions, the last two terms on the left side of Equation 4. 3 may be neglected. Therefore, one can solve Equation 4.3 to obtain pressure p_2 at depth z_2 from the known pressure p_1 at depth z_1, with the following expression:

$$p_2 = p_1 \exp\left[\frac{29\gamma_g(z_2 - z_1)}{\bar{Z}\bar{R}\bar{T}}\frac{g}{g_c}\right] \tag{4.4}$$

In Equation 4.4, $\overline{Z}$ and $\overline{T}$ represent average *Z*-factor and the temperature of the annular gas in the computational cell.

We use an iterative procedure to calculate pressure p_2 at depth z_2 with Equation 4.4, within a preset tolerance. Starting at the casinghead, this procedure calculates the gas-pressure profile in the annulus at any given time. Thereafter, the moles of gas in each cell are calculated using an average pressure and temperature for the cell and the following gas-law expression:

$$n_1 = \frac{(p_2 + p_1)V_1}{2\overline{Z}R\overline{T}} \tag{4.5}$$

The total mass of gas m_t in the annulus at time *t* is estimated by simply adding the mass in each cell, which is given by the following expression:

$$m_t = \sum_1^J \frac{(p_i + p_{i+1})V_i M}{2\overline{Z}_i R\overline{T}_i} \tag{4.6}$$

When gas is expelled from the annulus or compressed during a buildup test, adiabatic expansion or compression is possible. The short duration of the tests implies that the heat loss/gain from the system will be minimal, and the process may be treated as adiabatic. Even when the expansion/compression is not fully adiabatic, a polytropic (POLY) expression can represent the gas temperature change with pressure, which is given by Smith et al. (2005) as:

$$T_2 = T_1\left(\frac{p_2}{p_1}\right)^{\frac{\lambda-1}{\lambda}} \tag{4.7}$$

For an adiabatic process, $\lambda = cp/cv$ is the ratio of the specific heats of a gas; for a polytropic process, λ is an empirical constant with a slightly different value due heat transfer, ranging from 1.1 to 1.4. In our analyses, we used a value of 1.2.

Our general computational approach for various conditions relies upon the use of Equation 4. 6 to calculate the total mass of gas in the annulus at time *t* and compare that to the mass calculated at the next timestep *t*+1. When liquid-level data are available or can be interpolated from AWS readings, the mass calculated at the *t*+1 step can be used to determine the net gas flow rate. This approach is shown schematically in Figure 4.2, and specific applications of this methodology under various conditions are discussed below.

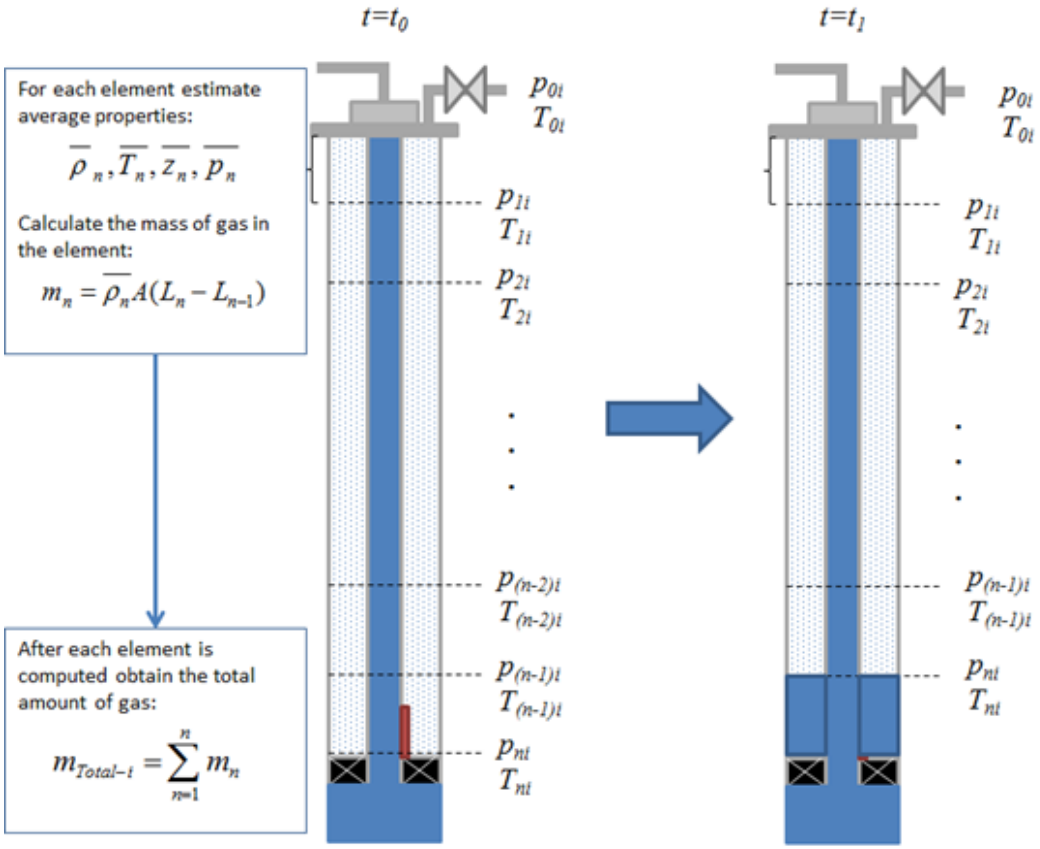

Figure 4.2. Schematic of computational algorithm.

Our general computational approach for various conditions relies upon the use of Equation 4. 6 to calculate the total mass of gas in the annulus at time *t* and compare that to the mass calculated at the next timestep *t*+1. When liquid-level data are available or can be interpolated from AWS readings, the mass calculated at the *t*+1 step can be used to determine the net gas flow rate. This approach is shown schematically in Figure 4.2, and specific applications of this methodology under various conditions are discussed below.

4.3. Model Validation with Field Data

This section discusses analysis of field data for three different types of tests; that is, drawdown (DD), pressure buildup (PBU), and constant-pressure bleed-down (CPB). Data from four independent tests conducted in three wells have been used to verify the models. In all cases, we present the data in both tabular and graphical forms so that one can easily replicate the results. Let us point out that the data gathered conform to the current industry practice in the North Sea. The models that are presented here suggest that changes in data gathering practice can bring about time and cost savings and improved analysis.

4.3.1. Drawdown (DD) Tests

The annular valve is opened during the drawdown (or bleed-down) tests, thereby allowing the gas to flow out of the annulus. In this test, no attempt is made to keep the casing pressure constant. The annular pressure decreases as the mass of gas contained in the casing is reduced. If the GLV is leaking or if it fails to close, the reduction in gas volume or pressure allows the tubing liquid to leak through the GLV into the annulus. During these tests, AWS measurements were also taken to determine the annular liquid level at various times. Note that annular gas venting was part of the AWS measurements in these tests.

We analyzed the DD data to estimate the gas efflux rate. With a known liquid level or gas volume, one can estimate the moles of gas n_t and n_{t+1} at two successive

timesteps, t_i and t_{i+1}, using Equation 4.5. The molar flow rate over that interval is then calculated as:

$$\dot{n} = \frac{n_t - n_{t+1}}{t_{i+1} - t_i} \tag{4.8}$$

Although fluid temperature variation in the annulus is not large, reasonable estimates of fluid temperature at various locations and times in the annulus is an important element of the calculation procedure. The initial fluid temperature in the annulus was reported to be approximately 20°C at the casinghead and about 60°C at the GLV location. In the case of the drawdown, we used two different assumptions—linear temperature gradient (LTG), and polytropic (POLY) expansion—for fluid temperature estimation along the well. The reported casinghead temperature did not appear to vary much, lending credence to this LTG assumption. However, polytropic expansion would not lead to a significant fluid temperature variation, either. Calculations based on both assumptions are shown in Table 4.1, and Figure 4.3 shows the calculated gas efflux rates (POLY with $\lambda = 1.2$) for the two drawdowns in Well 1.

Table 4.1. Estimation of flow rates during DD-1, Well 1.

				Polytropic		Linear Temp. Grad.	
Time minute	**Fluid Type**	**Annular Pressure psig**	**Liquid Level ft**	**Total Volume Mscf**	**Flow Rate Mscf/D**	**Total Volume Mscf**	**Flow Rate Mscf/D**
5	Gas	1,703	8,484	482		477	
15	Gas	1,685	8,388	474	1,234	467	1,505
30	Gas	1,652	8,203	457	1,569	447	1,905
60	Gas	1,614	7,994	439	880	425	1,061
120	Gas	1,527	7,511	397	1,001	375	1,187
180	Gas	1,446	7,061	359	913	331	1,056
240	Gas	1,368	6,626	324	860	291	967

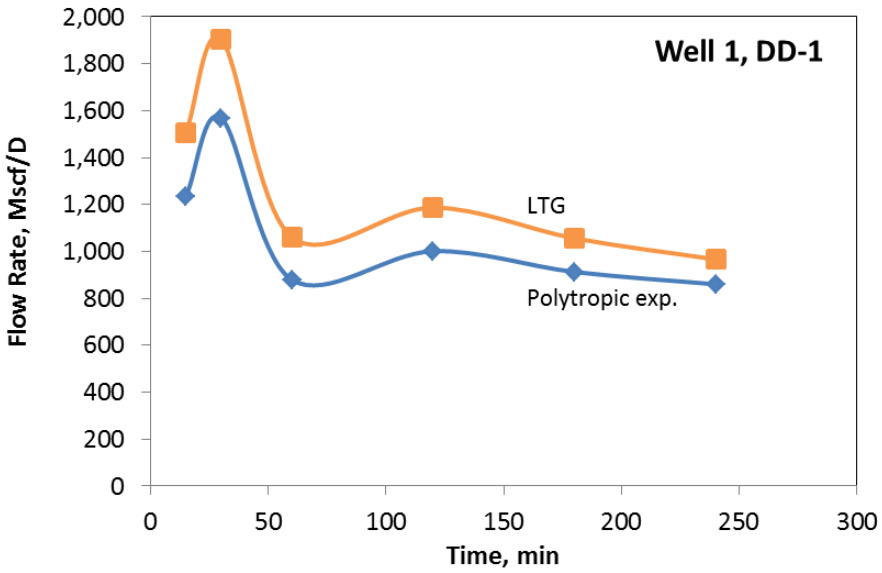

Figure 4.3. Estimation of flow rates during DD-1, Well 1.

Unfortunately, these calculated gas efflux rates are not directly comparable with those provided by the vendor because the vendor's rates were taken under very different conditions. Note that, considering the uncertainties involved, the differences in calculated flow rates for the two different assumed temperature profiles are small (between 3% to 22%) for both tests. Similar results were obtained for the second drawdown conducted for Well 1, as well as for the drawdowns for Well 2 and Well 3; these results are presented in Tables 4.2 through 4.4 and Figures 4.4 through 4.6.

Table 4.2. Estimation of flow rates during DD-2, Well 1.

				Polytropic		**Linear Temp. Grad.**	
Time minute	**Fluid Type**	**Annular Pressure psig**	**Liquid Level ft**	**Total Volume Mscf**	**Flow Rate Mscf/D**	**Total Volume Mscf**	**Flow Rate Mscf/D**
60	Gas	1,234	5,886	235		228	
120	Gas	1,167	5,516	210	605	199	691
180	Gas	1,086	5,066	180	703	167	779
240	Gas	1,017	4,680	157	573	141	611
300	Gas	929	4,197	130	647	114	667

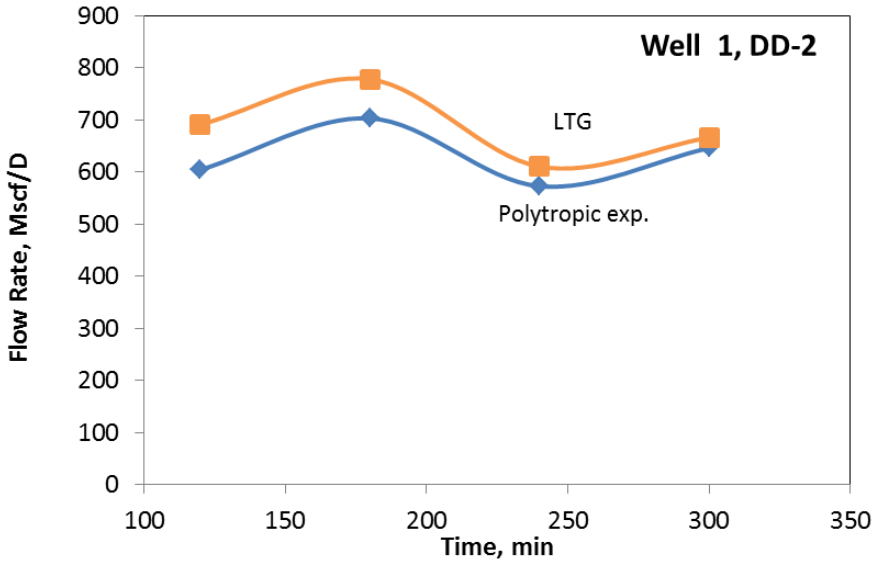

Figure 4.4. Estimation of flow rates during DD-2, Well 1.

Table 4.3. Estimation of flow rates during DD-1, Well 2.

				Polytropic		Linear Temp. Grad.	
Time minute	**Fluid Type**	**Annular Pressure psig**	**Liquid Level ft**	**Total Volume Mscf**	**Flow Rate Mscf/D**	**Total Volume Mscf**	**Flow Rate Mscf/D**
5	Gas	1,707	7,358	419		416	
20	Gas	1,678	7,233	407	1,125	401	1,390
50	Gas	1,627	7,015	387	972	376	1,197
110	Gas	1,566	6,754	369	578	347	701
230	Gas	1,407	6,070	301	736	275	866
390	Gas	1,314	5,672	267	310	236	348

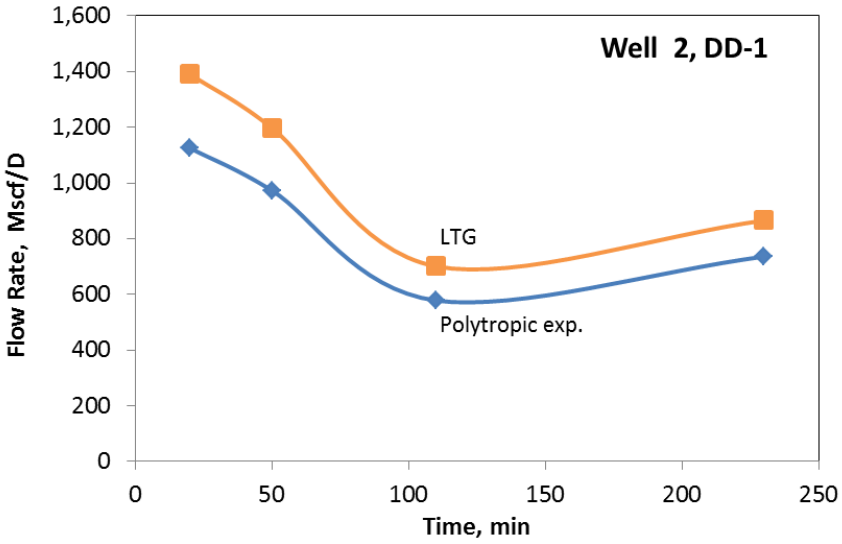

Figure 4.5. Estimation of flow rates during DD-1, Well 2.

Table 4.4. Estimation of flow rates during DD-1, Well 3.

				Polytropic		Linear Temp. Grad.	
Time minute	**Fluid Type**	**Annular Pressure psig**	**Liquid Level ft**	**Total Volume Mscf**	**Flow Rate Mscf/D**	**Total Volume Mscf**	**Flow Rate Mscf/D**
5	Gas	1,707	7,358	366.8		352	
15	Gas	1,678	7,233	354.9	1,718	334	2,528
30	Gas	1,627	7,016	341.0	1,331	314	1,934
60	Gas	1,566	6,754	312.3	1,382	274	1,947
120	Gas	1,407	6,070	225.2	2,090	169	2,518
142	Gas	1,314	5,672	198.5	1,747	143	1,702

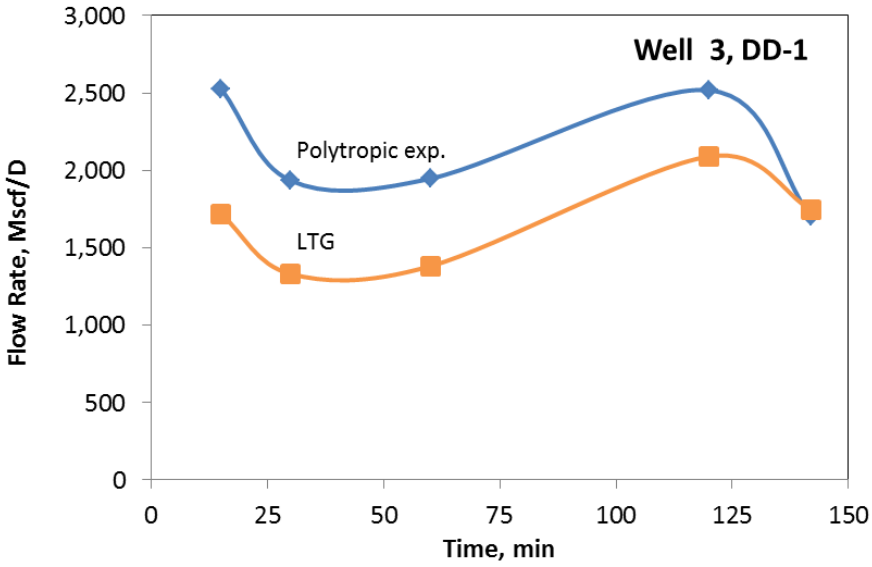

Figure 4.6. Estimation of flow rates during DD-1, Well 3.

4.3.2. Pressure-Buildup (BU) Test

For a buildup test, with the casinghead valve closed, the total mass of gas in the annulus must remain the same at all times. In other words, we are assuming that only liquid influx occurs across the suspected leaky valve in this undersaturated-oil reservoir. Therefore, at each timestep, our computation for a buildup test ends at a depth at which the total gas mass equals that of the previous (constant) step. This approach allows us to estimate the annular-liquid level as a function of time, as shown in Table 4.5. These results, which use both LTG and POLY, are shown in Figure 4.7, which also includes the results from the two simple analytical methods described later in this section. Note that Kabir and Hasan (1982) used a similar mass-balance approach while estimating

BHP in pumping-well annuli from the measured liquid-level and wellhead pressure (WHP) data.

For a closed system represented by a buildup test, we can derive a simple analytical expression for the annular liquid level as a function of casinghead pressure. We assume that the annular gas pressure *p* may be represented by the recorded pressure at the casinghead. In addition, if the annular gas maintains a constant LTG, we can write the material balance during buildup (no change in mass with time; that is, d*n*/d*t* = 0) as follows:

$$\frac{\mathrm{d}n}{\mathrm{d}t} = 0 = \frac{1}{\bar{Z}R\bar{T}}\left(p\frac{\mathrm{d}V}{\mathrm{d}t}+V\frac{\mathrm{d}p}{\mathrm{d}t}\right) \tag{4.9}$$

Minor variations in *Z* and *T* with time have been assumed and are represented by their average values for the entire annulus in Equation 4.9. In that case, we can rewrite Equation 4.9 as dp/p = - dV/V. If a constant cross-sectional area is assumed, one can develop the following simple expression for the liquid-level variation with casinghead pressure:

$$L = L_o(p_o / p) \tag{4.10}$$

In Eq. 4.10, as well as in Eq. 4.11, *L* is the length of gas column. When gas temperature changes with pressure and time, the polytropic compression assumption

holds. Under this circumstance, the gas temperature change is represented by Equation 4.7, in which the volumetric form is shown by:

$$V = V_o\left(\frac{p_o}{p}\right)^{\frac{1}{\lambda}} \qquad Or, \qquad L = L_o\left(\frac{p_o}{p}\right)^{\frac{1}{\lambda}} \tag{4.11}$$

A comparison of Equations 4.10 and 4.11 reveals that the liquid level L estimated during a buildup using the LTG assumption will always be shallower (smaller, or the liquid influx rate greater) than the corresponding POLY case because λ is greater than 1.0 as is p/p_o for a buildup. This observation is borne out by data analyses presented in Figures. 4.7 through 4.10.

Two annular buildup tests (BU-1 and BU-2) were conducted in Well 1. We analyzed the pressure-buildup data using both Equation 4.10 (LTG) and Equation 4.11 (POLY). Results from these analyses and the more rigorous analyses described before (Equation 4. 6), are shown in Figure 4.7. Note that the available liquid-level data, which were gathered during bleed down, were not useful for buildup analyses when casing pressure increased with the rise in liquid level. In this case, however, the initial liquid level at the start of the test was calibrated with the value measured prior to shut-in.

Table 4.5. Estimation of liquid levels during BU-1, Well 1.

Time min	Fluid Type	Tubinghead Pressure psig	Annular Pressure psig	Calculated Liquid Level, ft			
				LTG, rigorous	LTG, simplified	POLY, rigorous	POLY, simplified
0	Gas	394	1,356	6,748	6,748	6,748	6,748
5	Gas	394	1,363	6,706	6,712	6,720	6,722
10	Gas	393	1,370	6,665	6,677	6,693	6,696
15	Gas	393	1,373	6,649	6,663	6,682	6,685

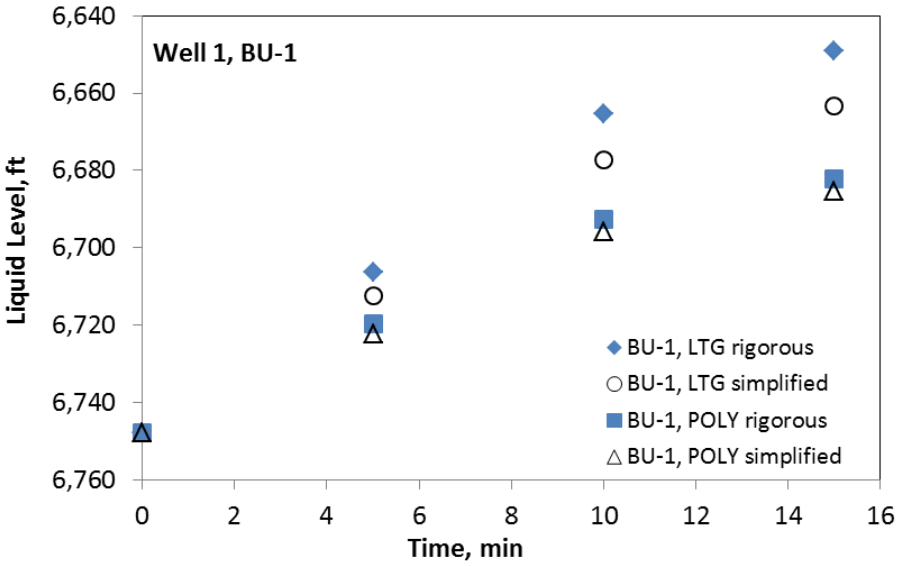

Figure 4.7. Estimated liquid levels during BU-1, Well 1.

During PBU-1, the casing pressure data were gathered at 5-minute frequencies, while those for PBU-2 were gathered at approximately 10-minute frequencies. The leak rates are estimated using the volumetric change with respect to the duration of the test. The calculated liquid level in the first buildup case implies a liquid influx (tubing to

annulus) rate of approximately 470 RB/D. However, PBU-2 indicates a liquid influx rate of approximately 250 RB/D. These influx rates compare with the reported influx rate of 380 RB/D, but under different circumstances, particularly considering that the leak rate is a declining function of time that approaches zero as pressure reaches hydrostatic equilibrium. The minimal change in the tubinghead pressure implies that the reservoir fluid preferentially migrated to the annulus via the leaky GLV.

Table 4.6. Estimation of liquid levels during BU-2, Well 1.

				Calculated Liquid Level, ft			
Time min	**Fluid Type**	**Tubinghead Pressure psig**	**Annular Pressure psig**	**LTG, rigorous**	**LTG, simplified**	**POLY, rigorous**	**POLY, simplified**
2	Gas	415	950	4,356	4,356	4,356	4,356
5	Gas	415	954	4,334	4,336	4,339	4,340
15	Gas	413	963	4,292	4,298	4,306	4,308
25	Gas	413	970	4,258	4,266	4,278	4,282

Both Figure 4.7 and Figure 4.8 clearly show that for either buildup, the liquid level, and therefore the influx rate, which was estimated by the simple analytic approaches (Equations 4.10 and 4.11), is very similar to those calculated by their more rigorous counterparts (Equation 4.6).

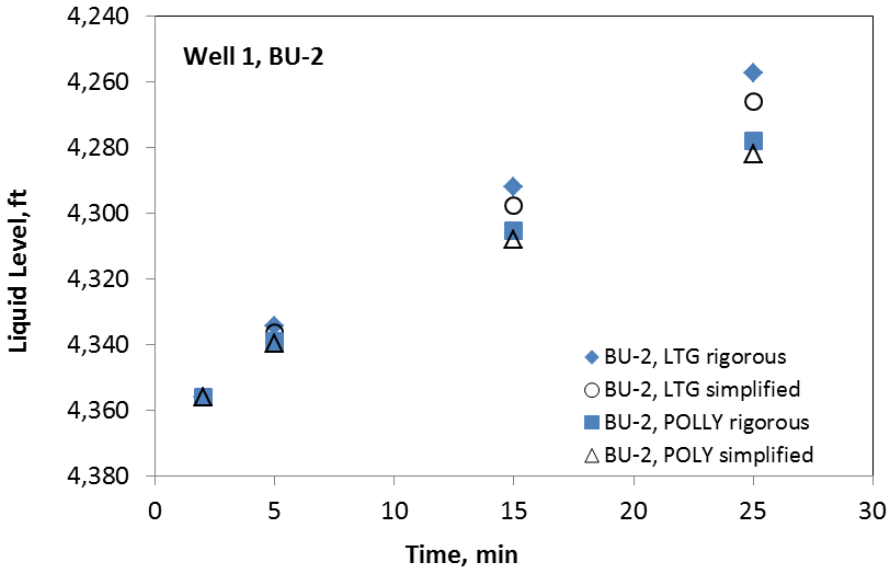

Figure 4.8. Estimated liquid levels during BU-2, Well 1.

We had access to three other test datasets belonging to different wells. Of these tests, one showed no buildup in annular pressure after the casing was bled off. This test clearly showed a GLV with no leak. The corresponding changes in liquid level, tubing pressure and annular pressure are presented in Table 4.7 and 4.8 for Well 2 and 3 respectively. The analyses of the buildup pressure data from the other two sets are shown in Figure 4.9 and Figure 4.10.

Table 4.7. Estimation of liquid levels during BU-1, Well 2.

				Calculated Liquid Level, ft			
Time min	**Fluid Type**	**Tubinghead Pressure psig**	**Annular Pressure psig**	**LTG, rigorous**	**LTG, simplified**	**POLY, rigorous**	**POLY, simplified**
0	Gas	397.2	1,457.4	6,332	6,332	6,332	6,332
2	Gas	395.8	1,466.1	6,290	6,305	6,295	6,301
5	Gas	394.3	1,473.4	6,254	6,282	6,264	6,276

Table 4.8. Estimation of liquid levels during BU-1, Well 3.

Time min	Fluid Type	Tubinghead Pressure psig	Annular Pressure psig	Calculated Liquid Level, ft			
				LTG, rigorous	LTG, simplified	POLY, rigorous	POLY, simplified
0	Gas	1,460	1,069	5,143	5,143	5,143	5,143
5	Gas	1,460	1,069	5,143	5,143	5,143	5,143
15	Gas	1,465	1,069	5,143	5,143	5,143	5,143
17	Gas	1,472	1,070	5,138	5,137	5,136	5,139
30	Gas	1,471	1,070	5,138	5,137	5,136	5,139
60	Gas	1,482	1,072	5,133	5,129	5,130	5,134
80	Gas	1,489	1,086	5,078	5,052	5,062	5,085

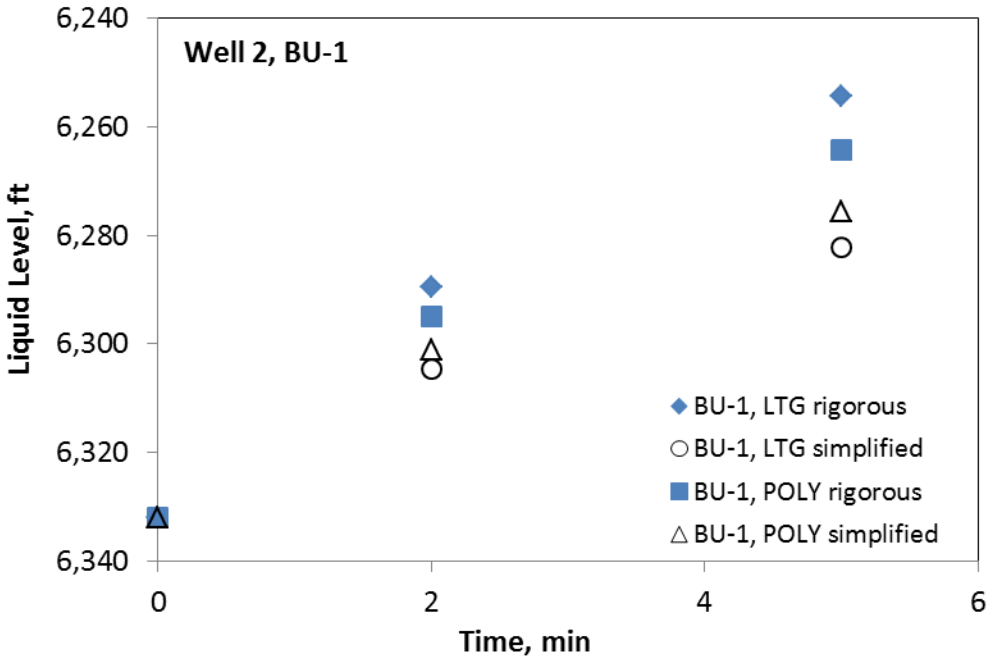

Figure 4.9. Estimated liquid levels during BU-1, Well 2.

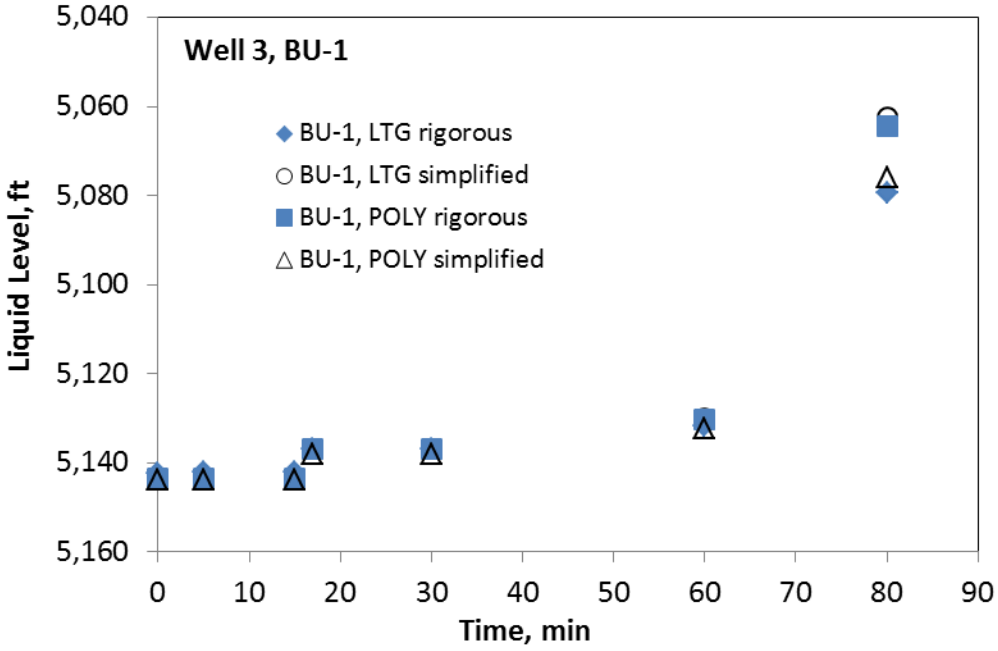

Figure 4.10. Estimated liquid levels during BU-1, Well 3.

Buildup data for the Well 2 shows a severely leaking GLV. The leak rate is approximately 1,400 RB/D. In contrast, the first hour of buildup data from Well 3 indicates a nearly leak-free valve. However, the last data point shows a significant increase in casing pressure, which implies a sudden development of a leak (~935 RB/D) if it is taken literally. Table 4.9 compares the results of all three tests with those measured in the field with AWS.

Table 4.9. Comparison of four test results.

Method	Well 1, BU-1	Well 1, BU-2	Well 2, BU-1	Well 3, BU-1
AWS Measurement, RB/D	540	n/a	986	<1
Model, RB/D	471	272	1,369	11.52

4.3.3. Constant-Pressure Bleed-down (CPB) Test

During the first test, data were also gathered at two different times when the casing was bled down, while keeping the casinghead pressure constant. The first such CPB was conducted for 30-minutes, but the second one was for a shorter, 10-minute period. When the casinghead pressure remains constant, Equation 4.9 can be rewritten (with $\mathrm{d}n/\mathrm{d}t = q \neq 0$ and $\mathrm{d}p/\mathrm{d}t = 0$) to obtain the following expression:

$$\frac{\mathrm{d}n}{\mathrm{d}t} = q = \frac{p}{\bar{Z}R\bar{T}}\left(\frac{\mathrm{d}V}{\mathrm{d}t}\right) = \frac{pA}{\bar{Z}R\bar{T}}\left(\frac{\mathrm{d}L}{\mathrm{d}t}\right) \tag{4.12}$$

When the gas flow rate at the casinghead is known, Equation 4.12 may be used to calculate the liquid influx rate from the tubing into the annulus through the GLV. For the first CPB test for Well 1 when the gas rate was reported at 142 Scf/D, we calculated the liquid influx rate to be 344 RB/D. Similarly, for the second CPB test, the liquid influx rate was estimated at 233 RB/D. Although rate estimation under CPB is feasible, buildup tests provide ample opportunity to do the same in a transparent way. That is because most of the flow from the formation into the annulus occurs directly across the leaky valve as minimal changes in the tubinghead pressure testify in Tables 4.5 and 4.6.

4.4. Discussion

We note that the traditional data acquired during the buildup test in sucker rod-pumped wells are fundamentally different from the data that is collected across the faulty

GLV. This difference happens because both gas and liquid (oil and water) are free to migrate into the annulus upon pump shut-in. In contrast, only liquid can flow back into the annulus upon depressurization in a gas-lift operation because gas, if any from the formation, will have a strong tendency to migrate into the tubing because of buoyancy. This fact explains why both the liquid-level data by way of AWS and the casinghead pressures are needed to estimate the bottomhole pressure for a two-phase mixture in pumping wells.

Pioneered by Godbey and Dimon (1977) and Brownscombe (1982), the AWS method remains a pragmatic approach for testing pumping wells. Subsequently, Hasan and Kabir (1985) and Hasan et al. (1988) have detailed how two-phase flow modeling was accomplished with AWS and WHP measurements for estimating BHP. In contrast, in a gas-lift situation, gas segregation in the tubing allows movement of only the liquid phase across the leaky GLV into the annulus when depressurization occurs, thereby posing fewer problems in modeling.

Based on the field tests discussed in this chapter, improvements in test procedures can be made because the integrity test demands creation of pressure differential across the GLV. Accordingly, a 10 to 40% pressure drawdown for the annulus may be required for the test to create sufficient perturbation. Let us elaborate on the test procedure and simplified analysis steps that can be enacted for efficiency that are less intrusive than those discussed here.

Ideally, the test can entail three simple steps.

1. After the cessation of gas injection, allow a few minutes so that the injected gas has had the time to escape the tubing.
2. Shut in the tubing and bleed off the annular gas so that the casinghead pressure is approximately 60% of the initial pressure. Monitor the pressure and rate with time. While a constant rate is not essential for the method to work, it is important to monitor the amount of mass exiting the annulus so that total gas inventory at the end of bleed off is known.
3. Shut in the annulus and monitor pressure evolution with time.

The last step involving pressure buildup can be analyzed to assess the gas volume. If the calculated annular gas volume remains essentially constant, no fluid exchange between the tubing and the annulus has occurred, and the integrity of the GLV is assured. On the other hand, if the casing pressure increases with shut-in time, it implies that the annular gas volume has decreased with time, meaning that liquid intrusion from the tubing has occurred. By subtracting the annular gas volume from the total volume, one obtains the total liquid influx into the annulus at any time. This step allows quantitative estimation of the leak's severity. One can also analyze the drawdown data in a similar manner using both the pressure and rate data. A proper material balance will allow us to calculate the rate of liquid influx from the tubing into the annulus.

4.5. Conclusions

This chapter presents simple models for analyzing transient-pressure data that is gathered at the casinghead during integrity testing of the GLV under various conditions.

Field data were used to validate the models. While direct validation of the model was not feasible for all test modes, the liquid-level data during acoustic well-sounding tests largely validated the model. Our analyses also pointed to the possibility of designing simpler tests to assess the GLV integrity. Specifically, we reached the following conclusions:

1. Newly developed interpretative models allow estimation of leakage rate from both drawdown and buildup tests of the annular gas, which have been indirectly verified for three wells. In this context, the current practice of gathering liquid-level data by acoustic well sounding can be avoided, largely because only the liquid intrusion is expected to occur in a gas-lift well.
2. The proposed two-step approach to data gathering (i.e., drawdown and buildup of the annular gas after the well shut-in) shortens the total test duration, thereby reducing the expense considerably.

5. LEAK TESTING METHODOLOGIES FOR GAS LIFT VALVES

5.1. Introduction

A current industry practice to measure liquid level in gas wells is Acoustic Well Sounding (AWS). This technology has also been used to measure liquid level in gas-lift settings, detect faulty gas-lift valves and even measure the influx rate over a given time (McCoy et al., 2009; Taylor et al., 2014). The importance of detecting and measuring leaks in gas-lift valves has been mentioned in previous chapters and is related to the risks inherent to gas-lift operations such as large inventories of gas (many cases flammable) and high operating pressures amongst others. Another important aspect that this technology enables is the capability to detect faulty valves *in-situ* rather than retrieving the valve and replacing without assessing if a leak existed. This is an important aspect as stated in the U.K. HSE's Offshore Division research priorities 2009-2014 (HSE, 2004). One of the downsides of using AWS is that it requires specialized equipment such as gas guns, computerized instrumentation, chart recorders, transducers, etc. making the test unsuitable for fast implementation. Most operations do not have their own AWS instrumentation. Therefore, whenever a diagnostic is required, the operator must contract a service company to perform this type of analysis. For the operator this leads to three problems: 1) the test is done as a corrective, rather than preventive, measure, 2) authorizing the time and expenses for the test becomes more difficult and, 3) the time it takes for the service company to arrive at location and set up the equipment can exacerbate the problem.

Several improvements in test procedures using AWS were suggested by Rocha-Valadez et al. (2014a). In summary, it involves a bleed-off or draw down (DD) test for the annulus to approximately 60% of its initial casinghead pressure while monitoring pressure and mass change of gas inventory. Once the casinghead pressure reaches 60% of the initial value, the annulus is shut off and the pressure buildup (BU) is monitored as a function of time. Additionally, Rocha-Valadez et al. (2014a) showed that the rate of change in gas pressure during a buildup could be used to estimate the rate of volume change, which could account for the rate of liquid influx through the GLV in the scenario where the packer and casings are undamaged. In this chapter, the same principles are applied and expanded. This offers a new testing methodology that allows the estimation of leak rates through a faulty GLV and identifying the extent of valve damage, potentially serving as quantitative criteria for GLV replacement. The test can be run in conjunction with AWS data gathering for increased accuracy or as a screening method before going on with contracting specialized sound-logging services.

5.2. Methodology

The basis of the proposed test methodology is depicted in Figure 5.1. As Figure 5.1a shows, even if the GLV has a leak, liquid from the tubing will not flow into the annulus if there is no pressure differential. If a positive pressure differential is created across a faulty GLV by venting some of the annular gas, liquid from tubing will flow into the annulus, as Figure 5.1b indicates. If the valve at the casinghead is closed after a period of venting, liquid coming in from the tubing will then compress the gas in the

annulus, resulting in pressure increase with shut-in time; Figures 5.1c and 5.1d illustrate this point. The rate of casing pressure rise can then be analyzed to obtain a quantitative measure of GLV damage.

This methodology suggests venting through an appropriate choke such that sonic velocity occurs, allowing the venting rate to be known (Figure 5.1b). To avoid a casing integrity issue arising from excessive pressure differential, venting is terminated when the casinghead pressure reaches a certain level, p_{risk} (Figure 5.1c). Obviously, if the initial annular pressure was not high enough, venting would cease when casinghead pressure nears atmospheric pressure (or venting line pressure) as shown in Figure 5.1d.

The test methodology and model formulation are described in the subsequent sections. However, to get a perspective we present how the gathered data can be used to determine the extent of GLV damage, if any. When a GLV is damaged and fluid flows through it from the tubing into the annulus, we can visualize the flow process as one through an orifice with ε fraction of the total valve area open. In this context, ε may be viewed as a damage coefficient, meaning a value of ε = 0% represents a fault-free GLV, while ε = 100% implies a wide-open GLV check valve.

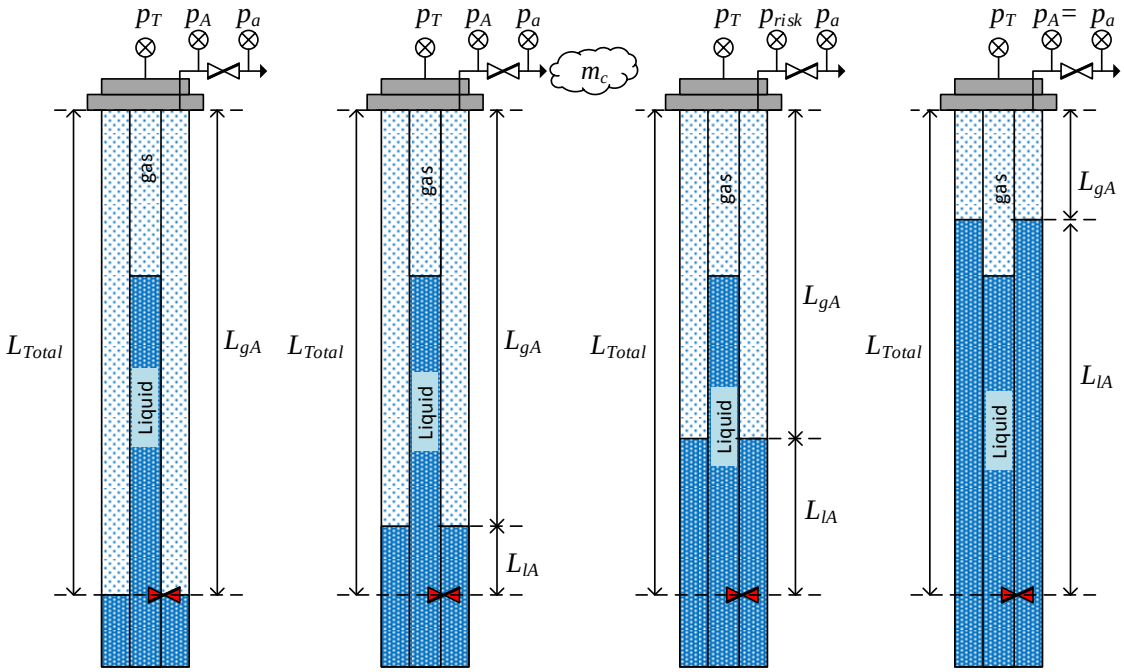

Figure 5.1. Changes in liquid level in the system due to flow through GLV during drawdown, followed by a buildup test.

In Figure 5.2, the y-axis represents the dependent variable (either pressure or liquid level). The solid lines represent simulated values of the dependent variable for various degrees of GLV damage. The open circles show data from an actual test. Figure 5.2, therefore, indicates that this GLV is faulty, and approximately 35% of the check valve area is "open."

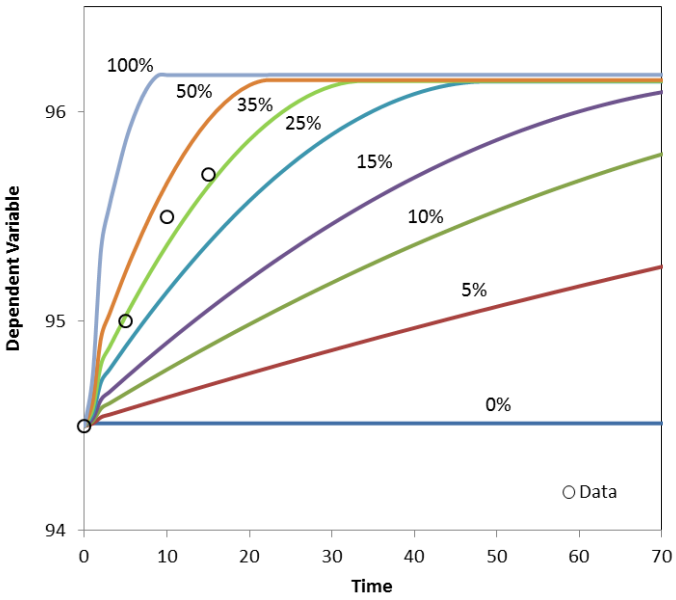

Figure 5.2. Dependent variable (pressure or liquid level) profiles for several ε values.

The test methodology consists of opening the casinghead valve, drawing down the annular gas (DD test), followed by a pressure buildup (BU) test, conducted by closing the casinghead valve. The methodology relies on calculating the mass of a known volume of gas in the annulus using the gas law and its pressure and temperature.

For a buildup test when gas mass does not change with time, rate of change of casinghead pressure is used to calculate the rate of change in gas volume, which is equal to the liquid ingress rate through the GLV. For a DD test, the rate at which gas is escaping the annulus needs to be known to set up a proper material balance to calculate liquid ingress rate into the annulus. We recommend the use of a flow-prover at the casinghead so that critical velocity is attained for the exiting gas, allowing estimation of

its rate. Note that the inside to outside pressure ratio for the annular gas is so high that attaining critical gas velocity through any choke will be easily attained.

The pressure differential across the GLV impacts the flow from the tubing into the annulus. Because any gas in the tubing fluid quickly moves up to the wellhead after well shut-in, we assume that only liquid flows from the tubing to the annulus through a faulty GLV. In addition, we note that after the tubinghead is closed, fluid will still flow (afterflow) from the reservoir into the well given the compressible wellbore fluid. The afterflow will either raise the tubinghead pressure or flow across the GLV and into the annulus. If the tubinghead pressure remains essentially constant, all of the fluid afterflow from the reservoir enters the annulus via the faulty GLV.

The approach just described can be used in conjunction with the AWS data acquisition to provide more confidence in the estimates. The steps for the testing procedures are below:

1. Begin the test by turning off gas injection and closing the tubinghead valve. Allow some time for the gas bubbles in the tubing to escape before shutting in the valve. We assume that the pressure in the annulus and that in the tubing at GLV depth will be essentially the same.
2. Initiate the DD test by opening the casinghead valve and letting gas flow through a choke (of known size) so that the critical sonic velocity is attained, thereby allowing estimation of the exiting gas flow rate.
3. Terminate the DD test when the annular pressure reaches 60% (p_{risk}) of its original value to maintain a safe operating pressure. The shortest possible time to

reach p_{risk} is calculated using the known gas rate and assuming that no liquid inflow from the tubing occurs into the annulus; that is, GLV damage coefficient is assumed to be zero. This step ensures sufficient pressure differential across the GLV for the BU test that follows.

4. Begin BU test by monitoring the annular wellhead pressure after closing the casinghead valve (Step 3). Perform pertinent gas compression calculations and liquid influx estimation.
5. Compare the pressure profile from DD and/or BU test with theoretical pressure isopleths, described later. The match obtained with the test data and theoretical pressure isopleths allows damage coefficient ε determination. The coefficient ε indicates the extent of GLV damage.

5.3. Model Formulation

The test begins when pressure in the tubing and in the annulus across the GLV is equal. If there is a leak in the GLV, the liquid originally in the tubing, will enter into the annulus upon depletion of the annular gas because of the pressure differential. Our experience with a number of such tests indicates that the wellhead tubing pressure p_T remains practically constant even when liquid moves from the annulus into the tubing. The operating envelope of the tubinghead pressure during the complete testing period (DD, BU and AWS measurements) remained within 415±15 psi for Well 1, 418±15 psi for Well 2 and 1474±30 psi for Well 3; varying only around 2% from the average value.

The compressible tubular fluid column masks any subtle perturbation triggered downhole.

We have observed that if a leak exists, the liquid column above the GLV depth in the tubing remains unchanged and that the liquid entering the annulus originates from the formation. Therefore, the tubing pressure at GLV depth can be assumed constant. We assume that the flow of gas from the annulus through a choke to a flow line will occur at the critical rate. Critical gas flow conditions exist when the inlet to outlet pressure ratio is about 1.7, which is very likely to be satisfied during these tests. Our model is based on a mass and volume balance of the annular gas and liquid, and estimation of hydrostatic pressures exerted by the gas and liquid columns.

5.3.1. Mass Balance

The mass conservation for the liquid and the gas in the system are represented by Equations 5.1 and 5.2 below:

Mass of liquid in the annulus:

$$m_{lA} = \rho_l L_{lAo} A_A + \int \dot{m}_l dt = \rho_l L_{lA} A_A \tag{5.1}$$

Mass of gas in annulus:

$$m_{gA} = m_{gAo} - \int \dot{m}_g dt \tag{5.2}$$

In these equations m represents mass, $\dot{m}$ is mass rate, L represents measured depth above GLV, and subscripts A, c, l, g, and o, represent annulus, critical, liquid, gas, and values at initial conditions, respectively.

The initial mass of gas in the annulus is calculated using the gas law. However, because the pressure in the annulus varies significantly over the well depth, we discretize the annulus into n sections and calculate the mass and pressure in each section iteratively. Equation 5.2, therefore, is rewritten in the following form that sums the mass of gas in each cell:

$$m_{gA} = \sum_{i=0}^{n_o} \frac{29\gamma_g \left(L_{gA,i+1} - L_{gA,i}\right) A_A \left(p_{gA,i} + p_{gA,i+1}\right)}{2\overline{Z}_i R \overline{T}_i} - \int \dot{m}_g dt \tag{5.3}$$

Equation 5.1 and 5.3 represent the mass balance of each component of the system and are valid at any given time. To obtain the initial gas mass in the annulus, we use Equation 5.3 by treating the entire length above the GLV as being gas. At any other time, because of liquid ingress from the tubing, the lengths of the liquid and gas columns add up to the same total length, L_T:

$$L_{Total} = L_{gA} + L_{lA} \tag{5.4}$$

5.3.2. Hydrostatic Pressure

The density of a gas can be related to its pressure and temperature by, ρ = (pM)/(ZRT). Therefore, the hydrostatic pressure, dp, of a gas column of vertical height dz is given by the following equation:

$$dp = \rho \frac{g}{g_c} dz = \frac{pM}{ZRT} dz \tag{5.5}$$

where $M = 29\gamma_g$, is the molecular weight of the gas and γ_g is the specific gravity of gas with respect to air and g is the gravitational acceleration. In addition, dz is the vertical depth that can be related to measured depth L, as dz = dL (cos θ) where θ is the deviation angle from the vertical. Equation 5.5 may be easily integrated over a short depth using average temperature and Z-factor for the depth, yielding:

$$p_2 = p_1 \exp\left(\frac{29\gamma_g \left(z_2 - z_1\right)}{R\bar{Z}\bar{T}} \frac{g}{g_c} \right) \tag{5.6}$$

We compute the annular-gas pressure from the known pressure at the casinghead, and march downward in n steps to the gas/liquid interface. Therefore, the gas pressure at this position p_{GA} in terms of the hydrostatic pressure of the liquid and gas columns is given by:

$$p_{GA} = \rho_L z_{lA} \frac{g}{g_c} + \sum_{i=0}^{n} p_{gA,i} \exp\left[\frac{29g\gamma_g \left(z_{gA,i+1} - z_{gA,i}\right)}{\bar{Z}_i R\bar{T}_i} \frac{g}{g_c} \right] \tag{5.7}$$

We use the same iterative solutions approach to estimate the mass of gas in the annulus, m_{gA} at each time step. However, there is an added complexity for computations for $t > 0$, because the length of the gas column changes with time as liquid enters the annulus from the tubing. Because p_{GA} depends on the liquid level above it, and the liquid influx rate, which, in turn, depends on p_{GA}, the computation becomes iterative. We need to solve for mass of gas remaining in the annulus, represented by Equation 5.8 below, simultaneously with Equation 5.7 for annular pressure at the GLV to obtain p_{GA}, z_{LA} and m_{GA}

$$m_{gA} = \sum_{i=0}^{n} \frac{29\gamma_g \left(L_{gA,i+1} - L_{gA,i}\right) A_A \left(p_{gA,i} + p_{gA,i+1}\right)}{2\overline{Z}_i R \overline{T}_i} \tag{5.8}$$

5.3.3. Computational Scheme

One of the objectives of this model is to allow for estimating the time t_{60} needed for the annular pressure to go down to 60% of its initial value, p_{risk}, through a known (critical) rate of gas drawdown. The idea is to allow annular pressure to decrease to a minimum allowable annular wellhead pressure (MAAWP). If annular wellhead pressure decreases beyond p_{risk}, the risk of damaging the casing becomes a possibility. The time at which p_{risk} is reached will vary according to the damage coefficient of the GLV. We assume that the damage coefficient is zero; that is, GLV is intact ($\varepsilon = 0$), to obtain a

conservative estimate of t_{60}. Flow through GLV is calculated using the following general expression for flow through orifices:

$$\dot{m}_l = \varepsilon A\sqrt{2\rho_l\left(p_{GT} - p_{GA}\right)} \tag{5.9}$$

Because pressure is a continuous variable and the methodology proposed discretizes the variable, the annular pressure at the GLV depth should use an average pressure between the previous time step and the current one; $(p_{GA,i}+p_{GA,i-1})/2$.

The magnitude of pressures at the casinghead is much higher than the outside pressure where gas will be discharged, thereby making the gas flow from the casinghead critical. Therefore, we calculate the casinghead gas flow rate $\dot{m}_g$ by using the following critical flow equation (Crowl & Louvar, 2011):

$$\dot{m}_l = C_o A\sqrt{\rho_g P_A\left(\frac{2}{\lambda+1}\right)^{\frac{\lambda+1}{\lambda-1}}} \tag{5.10}$$

In Equation 5.10, C_o is the valve's orifice discharge coefficient, A is its cross-sectional area, ρ_g, λ, and p_A are the gas density, its specific heat ratio, and its pressure at the casinghead. All of these properties are known from the top-down calculation and should be used at each time step.

In the following section, we discuss the computational scheme used. At initial conditions, hydrostatic equilibrium exists and there is no flow through the GLV. At these conditions the pressure at GLV depth in both the annulus and tubing can be established. The procedure to calculate the mass and pressure of the gas column is as follows:

1. We assume that initially there is no liquid above the GLV in the annulus; thus, the length of the gas column is the same as the depth of the GLV, $L_{gA} = L_T$. Because the casinghead initial pressure p_A is known, we estimate the total mass of annular gas m_{gA} and the pressure at GLV depth p_{GA} using Eqs. 5.7 and 5.8.
2. With the known annular initial mass, we proceed to estimate these quantities at later times allowing for gas bleed-off. The reduction in the amount of annular gas, with consequent pressure reduction, allows liquid to flow from the tubing into the annulus through a faulty GLV. This and several important stages of the test are sketched in Figures 5.1 and 5.3 for DD and BU tests, respectively.

The damage coefficient can range from $0 \geq \varepsilon \geq \varepsilon_{max}$. We used $\varepsilon = 0$ to calculate t_{60}. For a damaged GLV when liquid coming in from the tubing will support the annulus pressure, t_{60} calculated this way will lead to lesser drawdown, leading to a safer test environment.

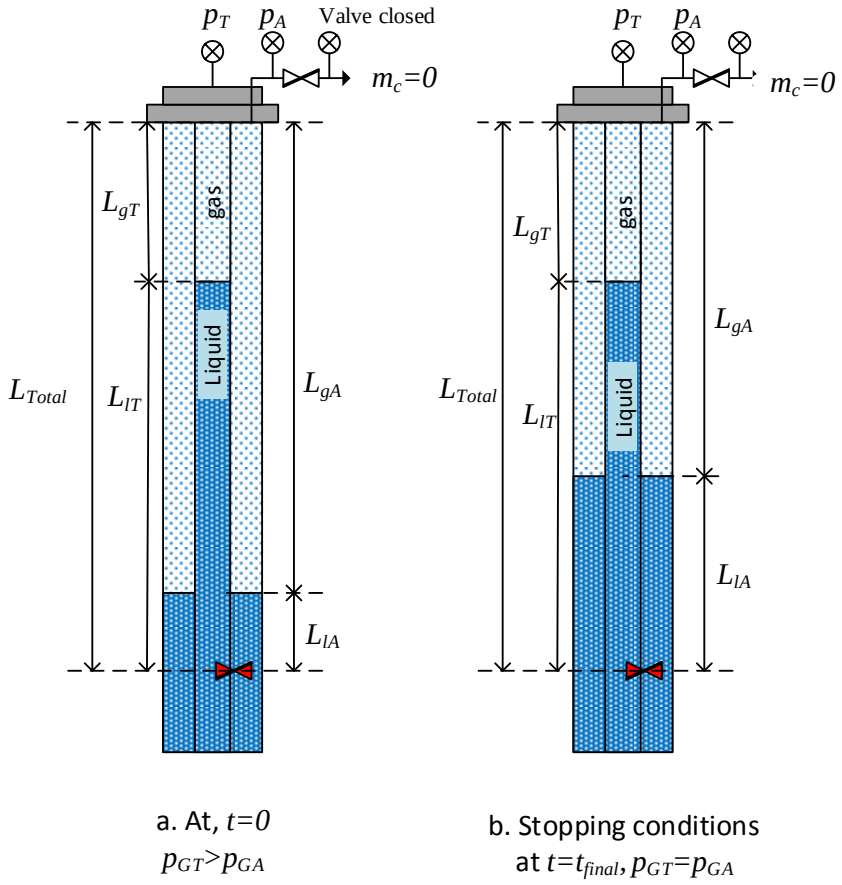

Figure 5.3. Changes occurring in the system due to flow through GLV during BU test.

The procedure to estimate time needed for 40% annulus pressure reduction is the following:

1. Estimate the mass of gas in the annulus after a given time-step Δt for $\varepsilon = 0$.
2. For the next time-step, use an initial p_A value, smaller than in the previous time-step.

3. Verify that p_A satisfies gas properties for mass $m_{gA} = pV/(29\gamma_g RT)$ and length of gas chamber L_{gA}.
4. Repeat Steps 3 and 4 until convergence is achieved.
5. Estimate new p_{GA} using Equation 5.5 along with $z_{Total} = z_{gA} + z_{lA}$ and use Equation 5.7 to estimate amount of mass of liquid that entered the annular section.
6. Use density of the oil (ρ_L) and geometry of the annulus to estimate the height occupied by liquid (L_{lA} and z_{lA})
7. Calculate the change in gas and liquid columns with Equation 5.3. and 5.4 and use as input for next timestep
8. Repeat steps 2 through 8 until $t = t_{final}$, $p_A = p_{risk}$ or $p_A = 0$ psig

The procedure for a buildup test is same as that for a drawdown test except that the gas mass, m_{gA}, remains constant during the entire test. In the Appendix we present a flow diagram for the methodology presented above. Figure 5.4 shows a flow diagram for this methodology.

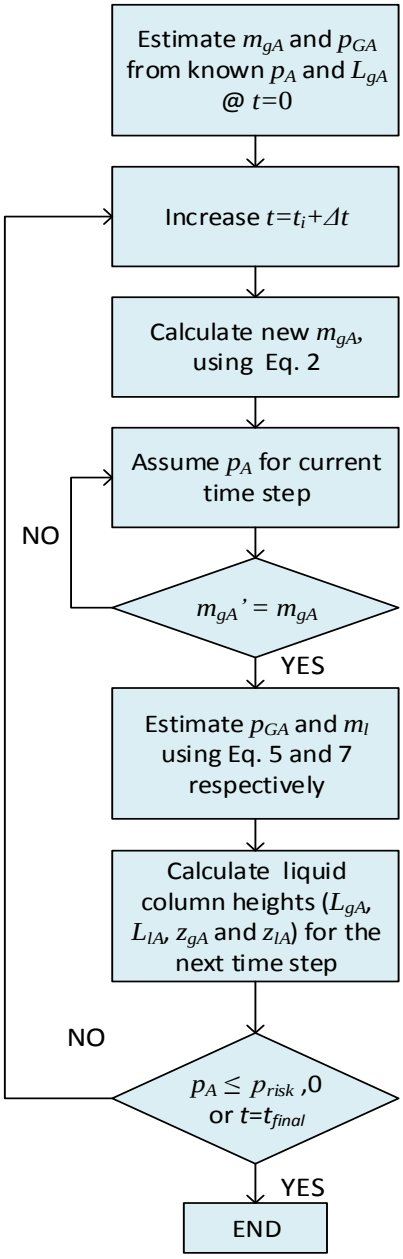

Figure 5.4. Solution methodology for estimating GLV test duration.

5.4. Model Validation

We compared our theoretically simulated pressure versus time profiles from BU test with those performed in three gas-lift wells using AWS data. The DD test data acquired by the vendor could not be used to validate the model because the bleed-off rate for gas discharge was not measured. The gas discharge rate is a required parameter in the model and the reason for recommending a flowmeter at the casinghead for DD tests.

We used the liquid level measured by AWS and annular pressure data at the beginning of the BU test as initial conditions; the proposed model was used thereafter to track all changes. The initial conditions of Wells 1, 2, and 3 are given in Table 5.1.

Table 5.1. Initial well conditions for BU Tests.

	p_A, psi	Liquid Level, ft	p_{GT}, psi
Well 1	1370.6	6,747.7	2371.4
Well 2	1472.1	6,332.0	2644.0
Well 3	1083.4	5,143.4	2339.5

We simulated pressure buildup over a time for several GLV damage coefficients, and compared the estimated values with the pressure reported from the field tests. Figures 5.5 through 5.7 show the pressure contours for these BU tests. In these figures, the open circles represent data while the solid lines represent annular pressures calculated using various ε values. For all these wells, the GLV aperture was 0.5-in. ID.

Figure 5.5 shows that the pressure buildup for Well 1 is similar to the profile resulting from an orifice of 35% of the cross-sectional area of the GLV. A 35% damaged

area would be the equivalent to having a completely open valve with a diameter of 0.3 inches or 7.25 mm. Figure 5.6 represents the pressure response for Well 2. The data indicated a damage of 60% for the GLV, equivalent to having an orifice of 0.39 inches, almost 80% of the original diameter. The severity of the calculated leak matches the field test using AWS for this well where the vendor noted "…there was a severe leak".

.

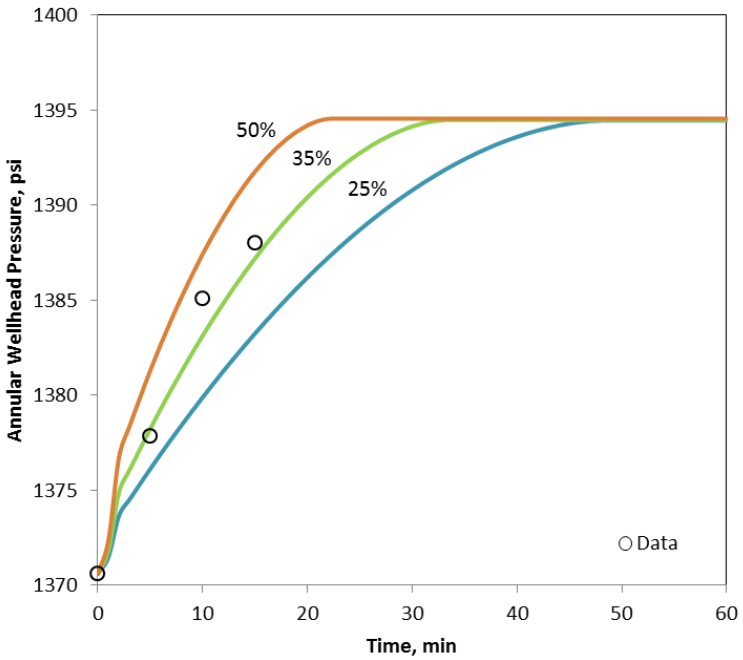

Figure 5.5. Comparison of pressure profiles during BU Tests, Well 1.

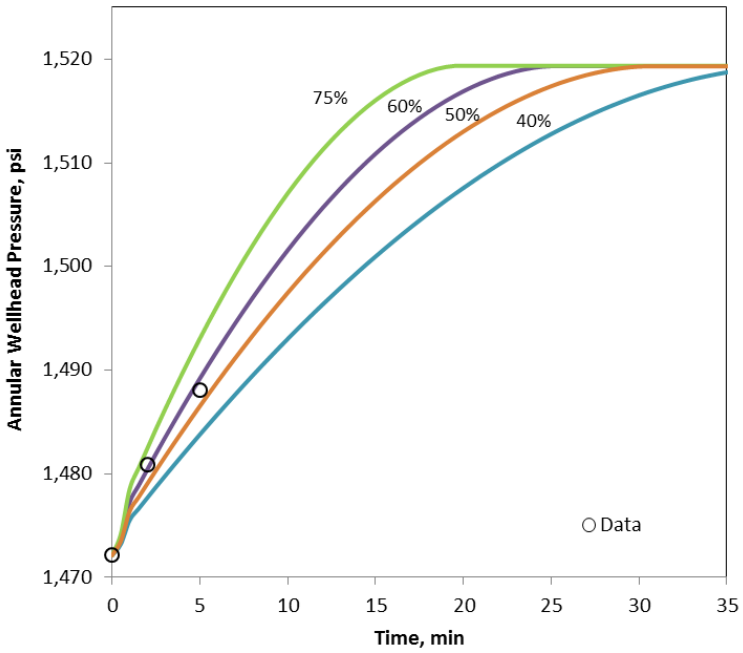

Figure 5.6. Comparison of pressure profiles during BU Tests, Well 2.

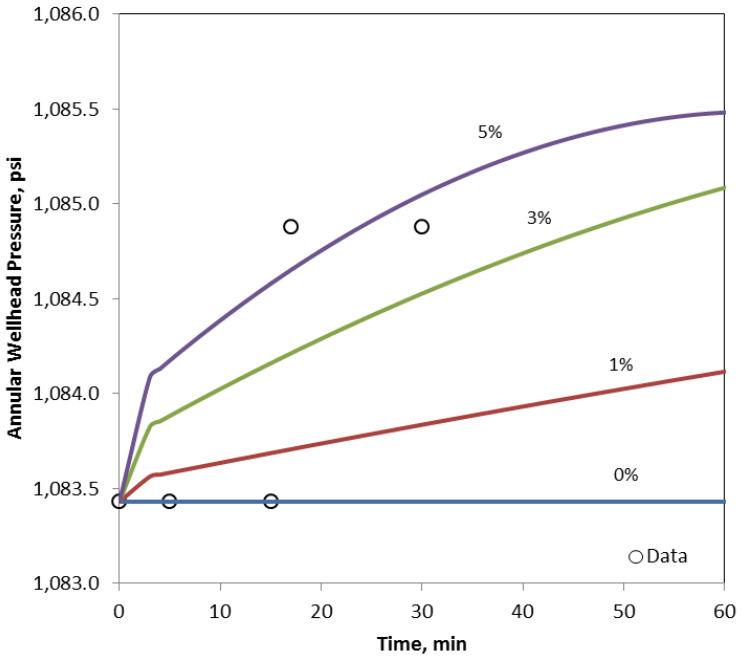

Figure 5.7. Comparison of pressure profiles during BU Tests, Well 3.

Figures 5.8 through 5.10 show the liquid-level profiles from these tests and serve as a basis for calculating flow through the GLV. The solid lines are model generated values for various degrees of GLV damage. Although direct measurements in these tests are lacking, values estimated following the method of Rocha-Valadez et al. (2014a), are plotted to show the similarities in the estimated liquid-level profiles. Rocha-Valadez et al. accounted for temperature variation by using a polytropic (POLY) and a linear temperature gradient (LTG).

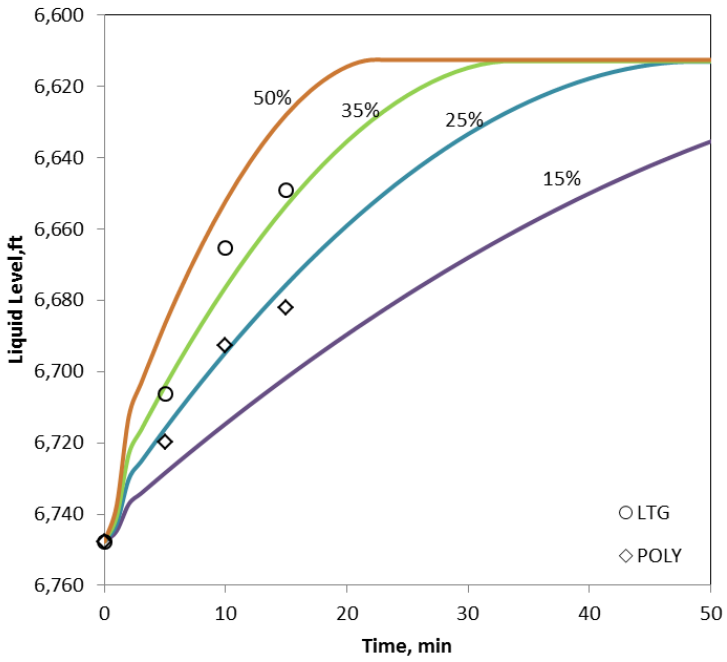

Figure 5.8. Calculated liquid level profiles for several ε values, Well 1.

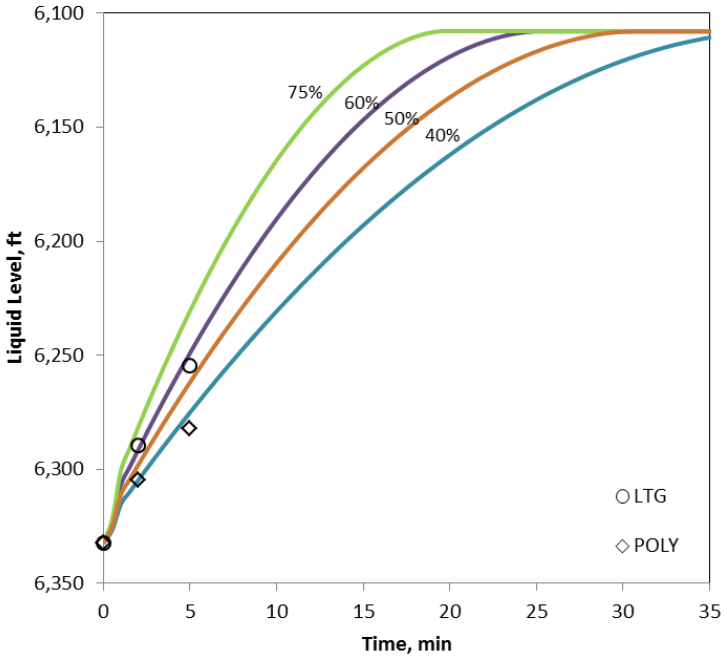

Figure 5.9. Calculated liquid level profiles for several ε values, Well 2.

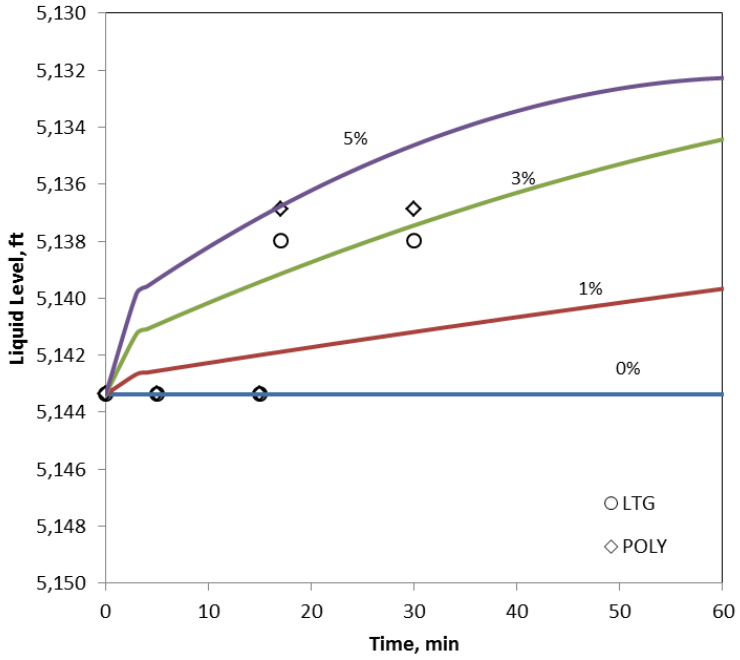

Figure 5.10. Calculated liquid level profiles for several ε values, Well 3.

Figures 5.8 through 5.10 support the conclusions of those shown in Figs. 5.5 through 5.7. The GLV in Well 1 is moderately (35%) damaged, Well 2 has a severe leak, and Well 3 is probably leak-free. We used the average flow rate reported during the test period to estimate and compare calculated flow rates with those reported by the AWS test for these wells. The flow rate estimations for all wells for various damage coefficient values are presented in Table 5.2. A comparison of the best fit, according to the pressure profile contours, is given in Table 5.3. In Table 5.2, the bolded damage coefficients correspond to the profile that had the best match to the pressure data reported by the vendor.

Table 5.2. Estimated flow rates for several GLV damage coefficients in three wells.

WELL 1			**WELL 2**			**WELL 3**		
ε,	**Effective Time, min.**	**Flow rate, RB/D**	***ε,***	**Effective Time, min.**	**Flow rate, RB/D**	***ε,***	**Effective Time, min.**	**Flow rate, RB/D**
5%	15	99.9	0%	-	0.0	0%	-	0.0
10%	15	192.5	25%	5	657.3	1%	60	5.4
15%	15	277.5	40%	5	1,023.2	**3%**	**60**	**12.1**
25%	15	424.2	50%	5	1,239.3	5%	60	13.3
35%	**15**	**538.7**	**60%**	**5**	**1,467.3**	25%	12	67.9
50%	15	645.0	75%	5	1,769.6	50%	4	111.7
100%	8	981.6	100%	5	2,212.4	100%	3	212.9

Table 5.3. Comparison of flow rates from this model and AWS vendor.

Well	Modeled Flow Rate, RB/D	Vendor Estimated Flow Rate, RB/D	Modeled ε
1	538.7	540	35%
2	1467.3	986	60%
3	0-12.1	<1	0-3%

Well 1 and Well 3 flow rate estimates match well with those reported by the vendor. This test helps us conclude that a leak exists in Well 1 with a 35% GLV damage. The difference in Well 3 vendor data and model estimation most likely corresponds to temperature fluctuations or noise in the equipment. We conclude that there is probably no leak in the GLV of this well. Well 2 appears to have a severe leak which represents a damaged area of 60%. The difference between our estimate and the vendor data could be related to the fact that the vendor's test was terminated because of severe liquid leak after just 5 minutes of testing, allowing insufficient time for a proper test. Due to the experience obtained by performing these tests, we recommend buildup times of at least 15 minutes.

5.5. Case Studies

Two case studies are presented in this section. The first one shows the general application of the test procedure for a vertical well. In this case we assume that only initial conditions are known and that there is no data to compare with the simulated

values. This case study shows how the simulated pressure and liquid level profiles can be examined to assess actual data.

The second case is based on Well 1, for which we have the most complete set of data. Data from the BU test from this well has already been used to validate the model. In this section, we show the full simulated pressure profiles for both the DD and BU tests, as well as choke size needed to achieve comparable pressure profile as the reported data.

5.5.1. Case Study 1

One objective of this study is to avoid the complications of running an AWS test for measuring annular liquid level. Avoiding an AWS test, however, necessitates the knowledge of the initial amount of annular gas; that is, the initial liquid level in the annulus. We assume that at the beginning of the drawdown test, the liquid level is just below the GLV. The mass of gas in the annulus is tracked during DD test and serve as input for the following buildup test where flow rates are calculated to assess the GLV damage.

For this well, the initial wellhead annular pressure p_A is 1,727 psig, the initial-liquid level depth L_{lA} is 8,740 ft and calculated pressure at GLV depth, p_{gA} is 2,312 psig. These input parameters return an initial amount of annular gas of 493 Mscf. From that point forward the gas is released through a 0.375-in. ID choke with a discharge coefficient, C_o, of 0.61 under the critical-flow condition. The DD continues until the pressure reaches 60% of the original p_A, which is about 1,037 psig in this case. Table 5.4

shows important parameters for the well at the end of the DD test, which also serves as the initial condition for the BU test.

Table 5.4. Parameters at the end of DD-1.

ε	**Testing time, min**	P_A**, psi**	p_{gA}**, psi**	**Final** m_{ga}**, Mscf**	**Final Liquid Level, ft**
0%	144	1,038.9	1,369.4	273.7	8,740
5%	144	1,067.6	1,554.9	270.9	8,345
10%	144	1,093.1	1,712.4	268.4	8,012
15%	144	1,115.0	1,843.2	266.2	7,737
25%	144	1,147.8	2,033.3	262.5	7,338
50%	144	1,181.3	2,229.4	257.6	6,923
100%	144	1,190.3	2,291.6	255.2	6,784

Note that Table 5.4 shows simulation results for 144 minutes of drawdown for all ε values. This is the t_{60} (MAAWP) only for $\varepsilon = 0$ (a faultless GLV); for all other ε values the annular pressure drop will be less than 60% after 144 minutes of drawdown, resulting in a safer conduct of the GLV test. Figures 5.11 through 5.13 show the variation in pressures at the casinghead p_A and at the GLV depth p_{gA} with time. The left-hand side of these figures corresponds to the DD portion of the test while the right-hand side corresponds to the BU section of the test.

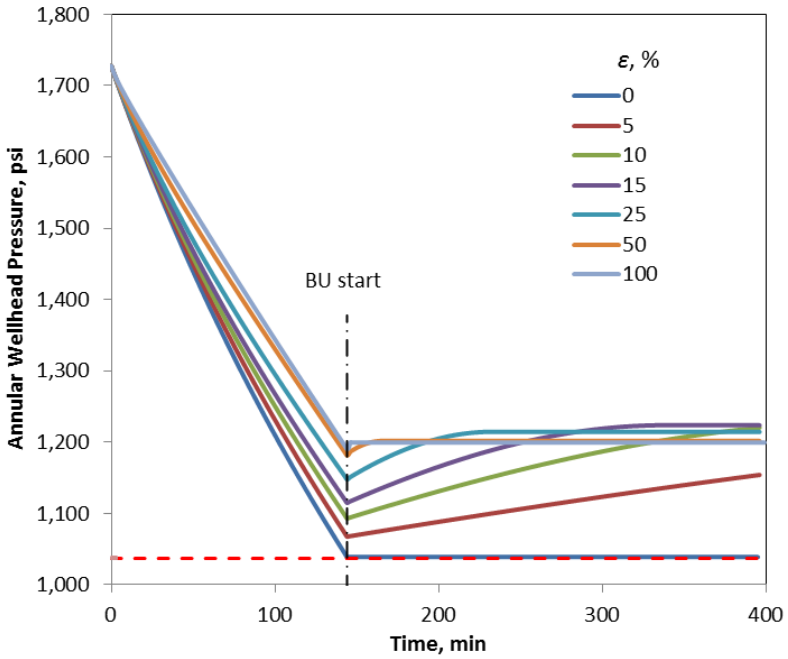

Figure 5.11. Annular wellhead pressure profile of full GLV test.

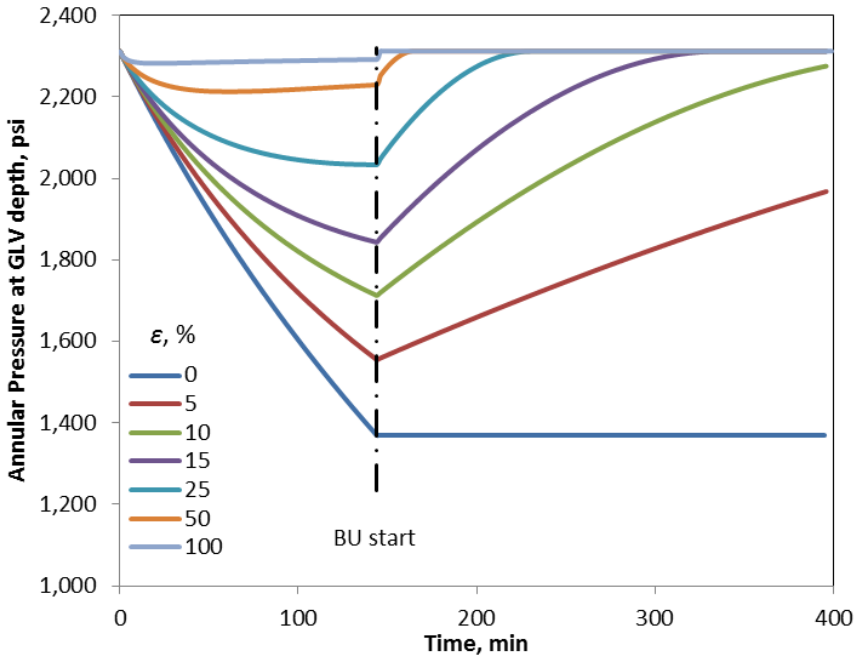

Figure 5.12. Annular pressure profile at GLV depth of full GLV test.

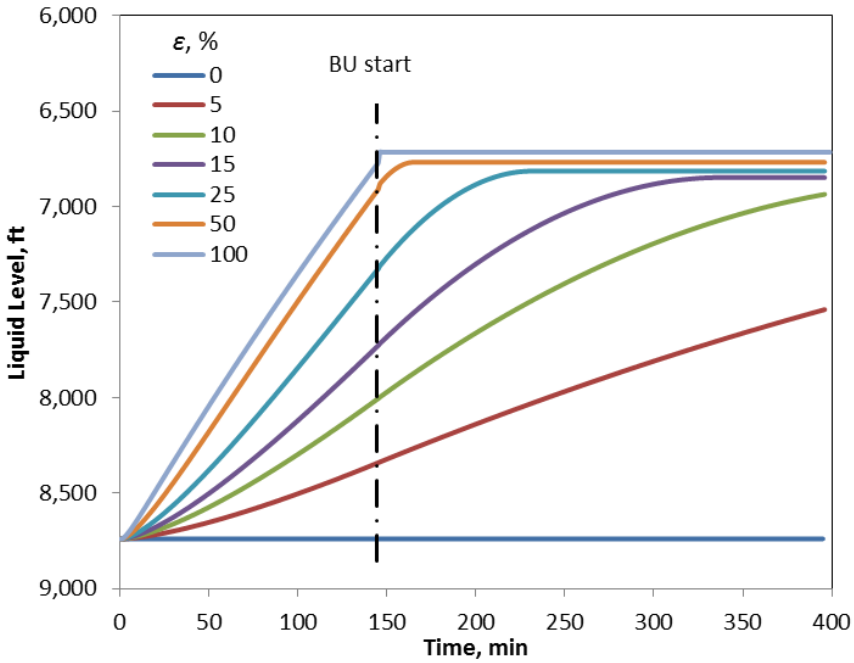

Figure 5.13. Liquid level profile of full GLV test.

During a GLV test, the casinghead pressure versus time data for both DD and BU tests, can be plotted and compared in Figure 5.11 against the simulated values. Matching field data will help obtaining a ε value, which is a measure of valve damage. Alternatively, the "preliminary" results from a DD test can be used to design a better and shorter BU test. A DD test that indicates severe leak in a GLV, can be used to terminate the test because valve retrieval and replacement has become obvious.

5.5.2. Case Study 2

Well 1 was selected for this case study because it has the most complete set of data. The vendor did not specify the rate of gas exiting the annulus or the choke size at

the casinghead. However, the high inside/outside pressure ratio allows us to presume that critical flow was achieved. The simulated results are based on critical flow for a choke valve with a diameter such that the initial conditions for the BU test at the end of the DD test was matched. The initial p_A was 1,748 psig and the faulty GLV was located at a depth of 8,286 ft, giving a pressure in the annulus at GLV depth p_{GA} of about 2,400 psig. This result is similar to the estimated p_{GT} obtained with AWS data, as reported in Table 5.1. This outcome reaffirms that the initial hydrostatic equilibrium assumption is reasonable. The unmodified data reported in the test is shown in Table 5.5. We note that there are some discrepancies between the BU and DD tests in the reported data.

Table 5.5. Unmodified AWS test data, Well 1.

	Raw Data				
	Time	**Relative Time, min**	**p_T, psi**	**p_A, psi**	**Liquid Level, ft.**
DD Period	1:45	0	407.6	1,747.7	-
	1:50	5	401.8	1,717.2	-
	2:00	15	413.4	1,699.8	-
	2:15	30	410.5	1,666.5	-
	2:45	60	407.6	1,628.8	-
	3:45	120	400.3	1,541.8	-
	4:45	180	404.7	1,460.5	-
	5:45	240	403.2	1,382.2	-
	6:40	300	410.5	1,380.8	-
BU Period	6:20	275	-	1,370.6	6,747.7
	6:25	280	407.6	1,377.9	-
	6:30	285	409.0	1,385.1	-
	6:35	290	409.0	1,388.0	-

To use that data for our methodology we needed to make the following adaptations. First, we decided to ignore the test point at the end of the DD period because it was unreliable. Second, because the proposed methodology only requires a valve closure, we decided to reduce the time gap before the last DD test duration (240 minutes) and the first BU test duration (275 minutes) from 35 minutes to 5 minutes. These modifications are shown in Table 5.6 and represent the data used for comparison and choke diameter estimation. Using the data in Table 5.6, and a discharge coefficient of 0.61 (Crowl & Louvar, 2011), we estimated that the choke size was 0.225 in. corresponding to a casinghead pressure of 1,368 psig and the liquid level of 6,742 ft. Other choke valve sizes and their corresponding casinghead pressures and liquid level depths are shown in Table 5.7.

Table 5.6. Data used for GLV leak estimation with proposed methodology.

	Processed Data			
	Relative Time, min	**p_T, psi**	**p_A, psi**	**Liquid Level, ft.**
DD Period	0	407.6	1,747.7	-
	5	401.8	1,717.2	-
	15	413.4	1,699.8	-
	30	410.5	1,666.5	-
	60	407.6	1,628.8	-
	120	400.3	1,541.8	-
	180	404.7	1,460.5	-
	240	403.2	1,382.2	-
BU Period	245	-	1,370.6	6,747.7
	250	407.6	1,377.9	-
	255	409.0	1,385.1	-
	260	409.0	1,388.0	-

Table 5.7. Well properties at t=240 min. of DD for several d_{choke} values.

D_{choke} inches	Time, min	p_A, psi	Liquid Level, ft.
0.185	240	1,524.9	7,352.4
0.2	240	1,488.6	7,209.4
0.21875	240	1,454.8	7,068.2
0.225	**240**	**1,368.0**	**6,742.4**
0.25	240	1,274.9	6,259.7

With the data from Table 5.6 and assuming a choke-valve with diameter 0.225 inches, we computed the casinghead pressure for the drawdown test followed by the buildup test. Figure 5.14 suggests good agreement between the model (solid line) with data (open circles).

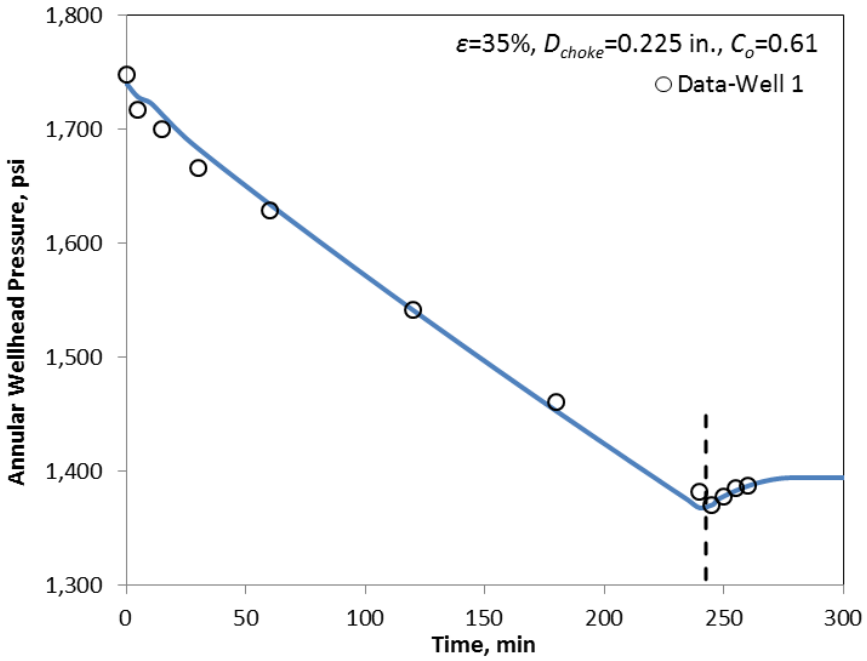

Figure 5.14. Pressure profile from current methodology and field data.

Figure 5.15 shows the liquid level profile when the two tests are performed sequentially. Similar to the validation section of this chapter, we plot our calculated liquid level against point estimates using the methodology described by Rocha-Valadez et al. (2014a).

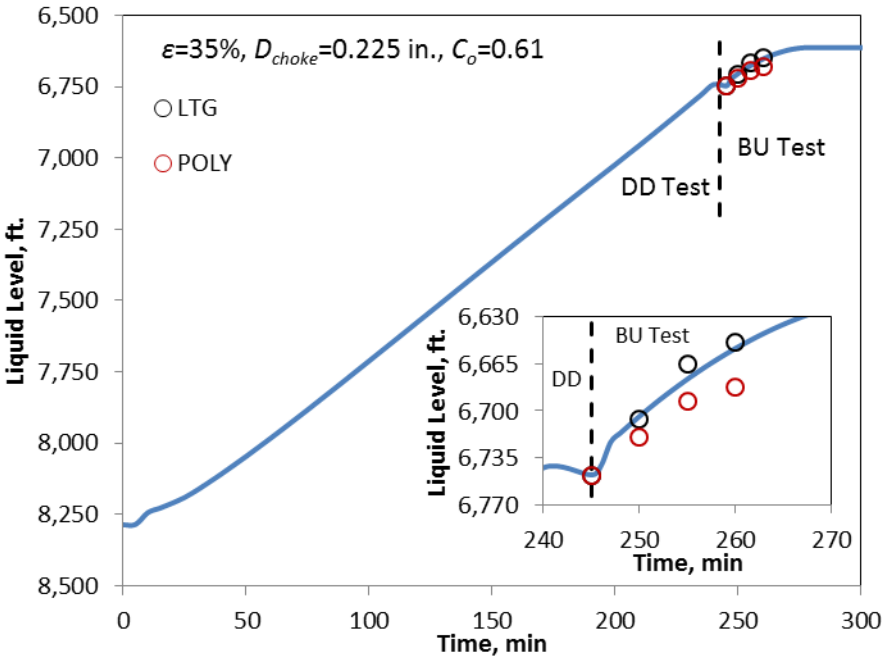

Figure 5.15. Liquid level profile with proposed methodology with two different thermodynamic models.

Because we obtained good quality match with the data using critical gas damage rate in the proposed model, we think that critical flow conditions prevailed during the AWS test for Well 1. As mentioned earlier, critical flow is likely to occur given the magnitude of pressure ratio between the annulus and the flow line. Finally, given specific parameters and variability between valves, such as the flow coefficient, one

cannot be sure that the vendor actually used a valve of 0.225 in. diameter. However, given the pertinent information, the process of bleeding off a well followed by pressure buildup test can be modeled and the damage to a gas-lift valve evaluated.

5.6. Conclusions

A testing methodology to measure flow rate through faulty gas-lift valves and track pressure profiles and liquid levels for the annulus gas is presented. The model also allows for an estimate of the damage for the faulty GLV in terms of the discharge coefficient which can be used as a quantitative parameter for GLV replacement. The methodology eliminates the need for AWS measurements as long as choke flow conditions are established for the DD tests and the test begins from hydrostatic pressure equilibrium between the pressure in the tubing at GLV depth and the annulus pressure at the same depth. The presented testing methodology can also be improved by combining with AWS measurements, particularly before starting the BU test to corroborate initial conditions of the pressure buildup test. If AWS testing is preferred, this method could still be useful as a screening test, before hiring specialized services, or after a test is performed to improve credence of the AWS test. This test has the advantages of being easy and almost immediate to implement, accurate, does not require any specialized equipment and provides a quantitative damage parameter to the GLV, making it a strong candidate for GLV integrity evaluation.

6. CONCLUSIONS AND RECOMMENDATIONS

6.1 Conclusions

This dissertation focuses on modeling the pressure transient response of oil and gas wells affected by well integrity issues and develops strategies for well integrity testing. Fundamental transport phenomena and thermodynamic properties are used to model the gas properties in the annular section of wells and across the different settings, such as cement for sustained casing pressure, and under choke velocity for the gas-lift valve problems. Based on these models, testing procedures are recommended for estimating the damage to the cement in the annulus, for SCP, and the damage coefficient, for GLV problems.

The formulation of the transport processes for SCP led to a first-order, linear-differential equation, with an analytic solution. The resulting algebraic expressions for the casing pressure rise and the gas influx rate as a function of time can be easily implemented in field-data analysis. This model was validated with field data from multiple oil and gas wells that were known to exhibit SCP problems, giving credence to the model. This model may also be used to estimate the cement seepage factor from limited test data, allowing rapid estimation of the leak's severity. This model was used to develop a new procedure for SCP testing.

The use of the SCP model, allows estimating the seepage factor, gas influx, and casinghead pressure increase, for wells with potential sustained casing pressure problems. A comparison of the amount of gas accumulated during tests of different

durations was made. The amount of gas and the risk from the proposed testing procedure showed that testing times and hazardous conditions such as high pressures and total accumulated gas can be reduced significantly in comparison to current standards. This very well can fit within the inherently safer principles of minimizing and moderating the hazards. Furthermore, this testing procedure could help reduce non-productive time which, in offshore operations, is very costly.

Simple models for analyzing transient-pressure data in gas-lift operations were developed. The model requires gathering pressure data at the casinghead during integrity testing of the GLV under various conditions. While direct validation of the model was not feasible for draw down periods, the liquid-level data during acoustic well-sounding tests largely validated the model. The estimation of amount of gas in the annulus in gas lift wells, served as a starting point in designing simpler tests to assess the GLV integrity. In this context, the current practice of gathering liquid-level data by acoustic well sounding can be avoided, largely because only the liquid intrusion is expected to occur in a gas-lift well. Additionally, the proposed two-step approach to data gathering (i.e., drawdown followed by buildup of the annular gas) shortens the total test duration, thereby reducing the testing expenses considerably

This dissertation presents a gas-lift valve integrity test that is useful when the suspected intrusion occurs predominantly from the GLV. The test is non-intrusive, of short duration, and does not require GLV retrieval. Indeed, any time a gas injection is suspended in a gas-lifted well, this test can be run with minimal expenditure of time and effort to determine the health of the gas-lift valves in the system. A forward model for

the analyses of the annulus pressure transients forms the backbone of the test design procedure. By developing isopleths, a "type-curve matching" approach of the annulus pressure transients is recommended, which conveniently determines the existence and magnitude of GLV damage. Validation of the proposed approach shows the ease with which test design can be carried out.

6.2 Recommendations

The scope of this work has focused on modeling well integrity issues inside the wellbore. For SCP integrity issue arises from the annulus cement, while for the GLV this represents the gas-lift valve. However, during the lifecycle of a production well, which can range from a few years to over 50 years (Tveit et al., 2014), the reservoir properties can change due to changes in the rate of production or well stimulation. Hence, coupling the models presented in this thesis with reservoir models would be beneficial in order to estimate the parameters that serve as input for this model, during the lifecycle of the test or of the well.

In some cases, casing pressure increase is a slow process that can take months to present itself. The model to extrapolate SCP could benefit from using the formation pressure variation with time. One of the assumptions of the SCP model is that the mud and the gas are immiscible fluids. While this might be the case for most water based muds, solubility might be an issue in some oil-based drilling fluids, according to their composition. A comparison of the effects of gas solubility in the mud column versus the

assumption of immiscible fluids would bring more credence to the model or broaden the area of usage.

The GLV model uses the pressure in the tubing at the gas-lift valve depth as the driving force for the liquid to enter the annulus through a faulty gas-lift valve. This pressure might not necessarily remain constant over long periods of time, particularly if there is high sandface flow rate combined with an almost leak-free gas-lift valve, the pressure inside the tubing might vary over time. This phenomenon would manifest itself as build up of pressure in the tubing side of the well rather than in the annulus during buildup periods. Coupling a reservoir model that can predict after flow with the GLV model could increase the accuracy of damage coefficient predictions and leakage rate.

NOMENCLATURE

The following notations are used for the SCP and GLV models:

SCP Model – Chapters 2 and 3

A	Cross sectional annular area, ft^2
c_m	Mud compressibility, psi^{-1}
D_1	Outer diameter of annulus, ft
D_2	Inner diameter of annulus, ft
K	Cement permeability to gas, md
k_s	Cement seepage factor, ft^2
L_c	Length of cement column, ft
L_f	Length of mud column, ft
L_g	Gas-column length, ft
L_{gi}	Initial gas-column length, ft
p	Casinghead pressure, psia
p_o	Initial casinghead pressure, psia
p_c	Cement-top pressure, psia
p_f	Formation pressure, psia
p_{max}	Maximum casinghead pressure, psia
p_{sc}	Standard condition pressure (=14.7), psia
q_{sc}	Gas rate at the cement top, Scf/D
R	Gas constant (=10.731), ft^3 psi / ^oR lb_{mol}

T	Reservoir temperature, ^{o}R
T_{sc}	Standard condition temperature (=491.7), ^{o}R
T_{wb}	Average wellbore temperature, ^{o}R
T_{wh}	Wellhead temperature, ^{o}R
V	Gas chamber volume, ft^3.
V_i	Initial gas chamber volume, ft^3
V_m	Mud volume, ft^3
Y_i	True value vector, variable units
$\hat{Y}_i$	Prediction value vector, variable units
Z	Gas-law deviation factor, dimensionless
μ_g	Gas viscosity, cp
ρ_m	Mud density, lbm/gal

GLV Model – Chapters 4 and 5

A	GLV bellow cross-sectional area, ft^2
A_A	Annular cross-sectional area, ft^2
A_T	Tubular cross-sectional area, ft^2
g	Gravitational acceleration, 32.174 ft/sec^2
g_G	Geothermal gradient, 0.0353°F/ft
L_{gA}	Measured depth of gas column in the annulus, ft
L_{lA}	Measured depth of liquid column in the annulus, ft
L_T	Total Measured Depth length from casinghead to GLV, ft

n	Number of cells for calculation to liquid level, dimensionless
m_{gA}	Mass of gas in the annulus at any given time, lbm
m_l	Total mass of liquid in the system, lb
$\dot{m}_c$	Mass flow of gas from choke flow on wellhead, Scf/hr
$\dot{m}_l$	Mass flow rate of liquid through GLV, lbm/hr
p_a	Pressure of choke flow outlet (=14.7), psia
p_A	Annulus wellhead pressure, psi
p_{GT}	Tubing pressure at GLV depth, psi
p_{GA}	Annulus pressure at GLV depth, psi
p_{risk}	Minimum allowable annular wellhead pressure, psi
p_T	Tubing wellhead pressure, psi
R	Gas constant (=10.731), ft^3psi/(°R lbmol)
T	Temperature, °R
T_{wh}	Wellhead temperature, °R
v	Fluid velocity, ft/s
Z	Gas compressibility factor, dimensionless
z_{gA}	True vertical depth of gas column in the annulus, ft
z_{lA}	True depth of liquid column in the annulus, ft
z_T	Total true vertical depth from casinghead to GLV, ft
ε	Gas-lift valve damage coefficient, dimensionless
γ_g	Gas gravity, dimensionless
ρ_{gA}	Density of gas in annulus, lbm/ft^3

ρ_l	Density of liquid, lbm/ft^3
θ	Well inclination (to horizontal) angle, degree
λ	Heat capacity ratio, dimensionless

REFERENCES

Almeida, A. (2011). A Model To Calculate the Theoretical Critical Flow Rate Through Venturi Gas Lift Valves. *SPE Journal, 16*(1), 134-147.

Altun, G., Langlinais, J., & Bourgoyne Jr., A. T. (2001). Application of a New Model To Analyze Leak-Off Tests. *SPE Drilling & Completion, 16*(2), 108-116.

Anders, J., Cismoski, D., Daniel, R., Dube, A., Engel, H., Hughes, A., Norene, T., Hamilton, R., & Mohr, W. (2008). *Prudhoe Bay Well P2 15 Surface Casing Collapse*. Paper presented at the SPE Annual Technical Conference and Exhibition, Denver, Colorado.

API. (2006). RP 90 - Annular Casing Pressure Management for Offshore Wells: American Petroleum Institute.

API. (2008a). SPEC 11V1 - Specification for Gas Lift Equipment: American Petroleum Institute.

API. (2008b). RP 11V7 - Recommended Practice for Repair, Testing, and Setting Gas Lift Valves: American Petroleum Institute.

API. (2008c). RP 11V5 - Operation, Maintenance, Surveillance, and Troubleshooting of Gas-Lift Installations. Washington, DC: American Petroleum Institute.

API. (2010). RP 19G2 - Flow-Control Devices for Side-Pocket Mandrels. Washington, DC: American Petroleum Institute.

Aschehoug, M., & Kabir, C. S. (2013). Real-Time Evaluation of Carbon Dioxide Production and Sequestration in a Gas Field. *SPE Reservoir Evaluation & Engineering, 16*(2), 134-143.

Asheim, H. (1988). Criteria for gas-lift stability. *Journal of Petroleum Technology, 40*(11), 1452-1456.

Azzola, J. H., Tselepidakis, D. P., Patillo, P. D., Richey, J. F., Tinker, S. J., Miller, R. A., & Segresto, S. J. (2007). Application of Vacuum-Insulated Tubing to Mitigate Annular Pressure Buildup. *SPE Drilling & Completion, 22*(1), 46-51.

Bellarby, J., Kofoed, S. S., & Marketz, F. (2013). *Annular Pressure Buildup and Methodology with Examples From Multifrac Horizontal Wells and HPHT Reservoirs*. Paper presented at the SPE/IADC Drilling Conference and Exhibition, Amsterdam, The Netherlands.

Blick, E. F., Enga, P. N., & Lin, P. C. (1988). Stability Analysis of Flowing Oil Wells and Gas Lift Wells. *SPE Production Engineering, 3*(4), 508-514.

Bourgoyne Jr., A. T., Scott, S. L., & Regg, J. B. (1999). *Sustained Casing Pressure in Offshore Producing Wells*. Paper presented at the Offshore Technology Conference Houston, Texas, USA.

Bourgoyne Jr., A. T. J., Scott, S. L., & Manowski, W. (2000). *A Review of Sustained Casing Pressure(SCP) Ocurring on the OCS*. Final Report Submiteted to MMS.

BP. (2010). Deepwater Horizon Accident Investigation Report *BP Incident Investigation Team*.

Carlsen, J. A., Stokka, Ø., & Kleppa, E. (2010). *Taking the gas lift valves to a new level of reliability*. Paper presented at the Offshore Technology Conference, Houston, TX.

CCPS. (2000). *Guidelines for Chemical Process Quantitiative Risk Assessment*. New York.

Crawley, F. (1995). Offshore loss prevention. *Chemical Engineer* (592), 24-25.

Crowl, D. A., & Louvar, J. F. (2011). *Chemical Process Safety Fundamentals with Applications* (3rd ed.): Prentice Hall.

D'Alessio, P., Poloni, R., Valente, P., & Magarini, P. A. (2011). Well-Integrity Assessment and Assurance: The Operational Approach for Three CO2-Storage Fields in Italy. *SPE Productions and Operations, 26*(2), 140-148.

Decker, K. L. (2008). IPO Gas Lift Design With Valve Performance. *SPE Production & Operations, 23*(4), 464-467.

Deepwater Horizon Study Group. (2011). Final report on the investigation of the macondo well blowout *Center for Catastrophic Risk Management, University of California at Berkeley*.

Dranchuk, P. M., & Abou-Kassem, H. (1975). Calculation of Z Factors for Natural Gases Using Equations of State. *Journal of Canadian Petroleum Technology, 14*(3), 34-36.

Economides, M. J., Hill, D. A., & Ehlig-Economides, C. (1993). *Petroleum Production Systems*: Prentice Hall Petroleum Engineering Series.

Eikrem, G. O., Aamo, O. M., & Foss, B. A. (2008). On Instability in Gas-Lift Wells and Schemes for Stabilization by Automatic Control. *SPE Production & Operations, 23*(2), 268-279.

Garcia, A. P. (2013). *Stability Analysis and Stabilization of Gas-Lift Systems*. Paper presented at the 22nd International Congress of Mechanical Engineering, Riberao Preto, SP, Brazil.

Gilbertson, E. (2010). *Gas lift valve failure mode analysis and the design of a thermally-actuated positive-locking safety valve.* (M. Sc. Thesis), Massachusetts Institute of Technology, Boston, Massachusetts.

Gilbertson, E., Hover, F., & Freeman, B. (2013). A Thermally Actuated Gas-Lift Safety Valve. *SPE Production & Operations, 28*(1), 77-84.

Glasstone, S., & Dolan, P. J. (1977). *The Effects of Nuclear Weapons*. (ADA087568). Washington, DC.

Goodwin, K. J., & Crook, R. J. (1992). Cement Sheath Stress Failure. *SPE Drilling Engineering., 7*(4), 291-296.

Grassick, D. D., Kallos, P. S., Dean, S., & King, S. D. J. (1992). Blowout risk analysis of gas-lift completions. *SPE Production Engineering, 7*(02), 172-180.

Hansen, M., & Abrahamsen, E. (2001). *Improving safety performance through rig mechanization*. Paper presented at the SPE/IADC Drilling Conference, Amsterdam, The Netherlands.

Hasan, A. R., Izgec, B., & Kabir, C. S. (2010). Sustaining Production by Managing Annular-Pressure Buildup. *SPE Production & Operations, 25*(2), 195-203.

Hill Jr, T., & Bhavsar, R. (1996). *Development of a self-equalizing surface controlled subsurface safety valve for reliability and design simplification.* Paper presented at the Offshore Technology Conference, Houston, TX.

Hopkins, A. (2012). Safety Indicators for Offshore Drilling- A Working Paper for the CSB Inquiry of the Macondo Blowout: CSB.

HSE. (2004). Offshore Division research priorities 2009-2014. *Health and Safety Executive, UK* Retrieved Feb 2014, from http://www.hse.gov.uk/offshore/researchpriorities2009-2014.htm

HSE. (2012). Gas release hazards from gas-lifted oil wells. *Health and Safety Executive, UK* Retrieved Feb 2014, from http://www.hse.gov.uk/foi/internalops/hid_circs/technical_osd/spc_tech_osd_46.htm

Huerta, N., Checkai, D., & Bryant, S. (2009). *Utilizing sustained casing pressure analog to provide parameters to study CO2 leakage rates along a wellbore.* Paper presented at the SPE International Conference on CO2 Capture, Storage, and Utilization.

Jackson, P. B., & Murphey, C. E. (1993). *Effect of Casing Pressure on Gas Flow Through a Sheath of Set Cement*. Paper presented at the APE/IADC Drilling Conference, Amsterdam.

Kamphorst, G., Van Wechem, G., Boom, W., Bottger, D., & Koch, K. (1999). *Casing Running Tool*. Paper presented at the SPE/IADC Drilling Conference, Amsterdam, The Netherlands.

Khan, F. I., & Amyotte, P. R. (2002). Inherent safety in offshore oil and gas activities: a review of the present status and future directions. *Journal of Loss Prevention in the Process Industries, 15*(4), 279-289.

Kinik, K., & Wojtanowicz, A. (2011). *Identifying environmental risk of sustained casing pressure.* Paper presented at the SPE Americas E&P Health, Safety, Security, and Environmental Conference.

Kletz, T. (1978). What you don't have, can't leak. *Chemistry and Industry, 6*, 287-292.

Kletz, T. (1998). *Process plants: A handbook for inherently safer design* (2nd ed.). Philadelphia: Taylor & Francis.

Le Roy-Delage, S., Comet, A., Garnier, A., Presle, J., Bulte-Loyer, H., Drecq, P., & Rodriguez, I. (2010). *Self-Healing Cement System-A Step Forward in Reducing Long-Term Environmental Impact*. Paper presented at the IADC/SPE Drillng Conference and Exhibition, New Orleans, Louisiana, USA.

Loizzo, M., Akemmu, O. A. P., Jammes, L., Desroches, J., Lombardi, S., & Annunziatelliz, A. (2011). Quantifying the Risk of CO2 Leakage Through Wellbores. *SPE Drilling & Completion, 26*(3), 324-331.

Macpherson, J., de Wardt, J., Florence, F., Chapman, C., Zamora, M., Laing, M., & Iversen, F. (2013). Drilling-Systems Automation: Current State, Initiatives and Potential Impact. *SPE Drilling & Completion, 28*(04), 296-308.

Mannan, M. S., Mentzer, R. A., Rocha-Valadez, T., & Mims, A. (2014). OFFSHORE DRILLING RISKS-1: Risk Indicators have varying impact on mitigation. *Oil & Gas Journal, 112.5*(05), 64-69.

Mannan, S. (2012). *Lee's loss prevention in the process industries: hazard identification, assessment, and control* (4th ed. Vol. 1): Elsevier.

McCoy, J. N., Rowlan, O. L., & Podio, A. (2009). *Acoustic Liquid Level Testing of Gas Wells*. Paper presented at the SPE Production and Operations Symposium, Oklahoma City, Oklahoma.

National Oil Spill Commission. (2011). Deep Water: The Gulf Oil Disaster and the Future of Offshore Drilling *Presidential Report*.

Nishikawa, S. (1992). *Mechanisms of Gas Migration after Cement Placement and Control of Sustained Casing Pressure. Master Thesis.* (M. Sc. Thesis), Louisiana State University, Baton Rouge, Louisiana.

NORSOK. (2004). Well Integrity in Drilling and Well Operations, Rev. 3 (Vol. D-010). Norway.

Oudeman, P., & Kerem, M. (2006). Transient Behavior of Annular Pressure Buildup in HP/HT Wells. *SPE Drilling & Completion, 21*(4), 234-241.

Poblano, E., Camacho, R., & Fairuzov, Y. V. (2005). Stability Analysis of Continuous-Flow Gas Lift Wells. *SPE Production & Facilities, 20*(1), 70-79.

Posenato, A., & Rosa, V. (2012). *Unload Procedure With Control of Liquid Flow Rate Through Gas Lift Valve*. Paper presented at the SPE Latin America and Caribbean Petroleum Engineering Conference, Mexico City, Mexico.

Reddy, B., Liang, F., & Fitzgerald, R. (2010). Self-Healing Cements That Heal Without Dependence on Fluid Contact: A Laboratory Study. *SPE Drilling & Completion, 25*(3), 309-313.

Rigzone. (2012). How Does Artifical Lift Work? Retrieved July 29, 2013

Rocha-Valadez, T., Hasan, A. R., Mannan, M. S., Crabtree, A., & Kabir, C. S. (2014a). *Assessing Integrity of the Gas-Lift Valves by Analyzing Annular-Pressure-Transient Response* Paper presented at the SPE Artificial Lift Conference and Exhibition - North America, Houston, Texas.

Rocha-Valadez, T., Hasan, A. R., Mannan, M. S., & Kabir, C. S. (2014b). Assessing Wellbore Integrity in Sustained Casing Pressure Annulus. *SPE Drilling & Completion, 29* (01), 131-138.

Rocha-Valadez, T., Mentzer, R. A., Hasan, A. R., & Mannan, M. S. (2014c). Inherently Safer Sustained Casing Pressure Testing for Well Integrity Evaluation. *Journal of Loss Prevention in the Process Industries, 29*, 209-215.

Sanchez, F., & Al-Harthy, M. H. (2011). Risk analysis: Casing-while-Drilling (CwD) and modeling approach. *Journal of Petroleum Science and Engineering, 78*(1), 1-5.

Sanchez, F., Said, H., Turki, M., & Cruz, M. (2012). Casing While Drilling (CwD): A New Approach To Drilling Fiqa Formation in he Sultanate of Oman--A Success Story. *SPE Drilling & Completion, 27*(2), 223-232.

Sartori, L. (1983). The effects of nuclear weapons. *Physics Today, 36*(3), 32-38.

Skogdalen, J. E., Utne, I. B., & Vinnem, J. E. (2011). Developing safety indicators for preventing offshore oil and gas deepwater drilling blowouts. *Safety Science, 49*, 1187-1199.

Smith, J. M., Van Ness, H. C., & Abbott, M. M. (2005). *Introduction to Chemical Engineering Thermodynamics* (7th ed.): McGraw-Hill.

Stephenson, G., Molotkov, R., De Guzman, N., & Lafferty, L. (2010). Real-Time Diagnostics of Gas Lift Systems Using Intelligent Agents: A Case Study. *SPE Production & Operations, 25*(1), 111-123.

Sutton, R. P. (1985). *Compressibility factors for high-molecular-weight reservoir gases*. Paper presented at the SPE Annual Technical Conference and Exhibition, Las Vegas, Nevada.

Takacs, G. (2005). *Gas Lift Manual*: Pennwell Corporation.

Tao, Q., Bryant, S., Meckel, T. A., & Luo, Z. (2012). *Wellbore Leakage Model for Above-Zone Monitoring at Cranfield, MS*. Paper presented at the Carbon Management Technology Conference, Orlando, Florida, USA.

Tao, Q., Checkai, D., Huerta, N., & Bryant, S. (2010). *Model to Predict CO2 Leakage Rates Along a Wellbore.* Paper presented at the SPE Annual Technical Conference and Exhibition.

Taoutaou, S., Vargas Bermea, J. A., Bonomi, P., Elatrache, B., Pasturel, C., & Brangetto, M. (2011). *Avoiding Sustained Casing Pressure in Gas wells using Self Healing Cement.* Paper presented at the International Petroleum Technology Conference.

Taylor, C., Rowlan, O. L., & McCoy, J. (2014). *Acoustic Techniques to Monitor and Troubleshoot Gas-Lift Wells*. Paper presented at the SPE Western North American and Rocky Mountain Joint Regional Meeting, Denver, Colorado, USA.

Tveit, E., Sivertsen, H., & Hernæs, S. (2014). *Experience from Field Life Extension*. Paper presented at the Offshore Technology Conference, Houston, Texas.

U.S. CSB. (2014a). Explosion and Fire at the Macondo Well - Investigation Report (Vol. 2): U.S. Chemical Safety Board.

U.S. CSB. (2014b). Explosion and Fire at the Macondo Well - Investigation Report (Vol. 1): U.S. Chemical Safety Board.

Vignes, B., & Aadnoy, B. (2010). Well-Integrity Issues Offshore Norway. *SPE Productions and Operations, 25*(2), 145-150.

Vinnem, J. E. (2010). Risk indicators for major hazards on offshore installations. *Safety Science, 48*, 778-787.

Wang, H., Soliman, M., Shan, Z., Meng, F., & Towler, B. (2011). Understanding the Effects of Leakoff Tests on Wellbore Strength. *SPE Drilling & Completion, 26*(4), 531-539.

Warwick, A. (1998). *Inherently safe design of floating production, storage & offloading vessels(FPSOs).* Paper presented at the OMAE 1998: 17th International Conference on Offshore Mechanics and Arctic Engineering.

Watson, D., Brittenham, T., & Moore, P. L. (2003). *Advanced Well Control*. Richardson, TX: SPE.

Watson, T. L., & Bachu, S. (2009). Evaluation of the Potential for Gas and CO2 Leakage Along Wellbores. *SPE Drilling & Completion, 24*(1), 115-126.

Wojtanowicz, A. K., Nishikawa, S., & Rong, X. (2001). Diagnosis and remediation of sustained casing pressure in wells. *final report, United States Minerals Management Service (July 2001)*.

Xu, J., Scott, S. L., Mabry, W., & Gamboa, J. (2012). *High Reliability Gas Lift Flow Control Device Technology and Erosion/Endurance Tests*. Paper presented at the SPE Annual Technical Conference and Exhibition, San Antonio, TX.

Xu, R. (2002). *Analysis of Diagnostic Testing of Sustained Casing Pressure in Wells.* (Ph. D. Dissertation), Louisiana State University, Baton Rouge, Louisiana.

Xu, R., & Wojtanowicz, A. (2001). *Diagnosis of sustained casing pressure from bleed-off/buildup testing patterns.* Paper presented at the SPE Production and Operations Symposium, Oklahoma City, Oklahoma.

Zhu, H., Lin, Y., Sun, Y., Zeng, D., Zhang, Z., & Shi, T. (2011). Coupled Mathematical Model of Gas Migration in Cemented Annulus with Mud Column in Acid Gas Well *Carbon Dioxide Sequestration and Related Technologies* (pp. 449-462): John Wiley & Sons, Inc.

Zhu, H., Lin, Y., Zeng, D., Zhang, D., & Wang, F. (2012). Calculation analysis of sustained casing pressure in gas wells. *Journal of Petroleum Science, 9*, 66-74.

APPENDIX A

SCP MODEL DERIVATION AND ANALYTICAL SOLUTION*

A.1. Gas Influx Rate

Using Darcy's law, an expression for gas flow rate through the cemented section, considered a porous medium can be written as follows:

$$\frac{\mathrm{d}p}{\mathrm{d}z} = \frac{\mu v}{k} = \frac{\mu q}{Ak} \tag{A.1}$$

The gas velocity (or flow rate) will change with cement depth, z while flowing through the cement column. To account for that change, the in-situ flow rate q can be substituted in terms of q_{sc}, the flow rate at standard pressure p_{sc}, standard temperature T_{sc}, in-situ pressure p, and temperature T. These substitutions allow rewriting Equation A.1 as follows:

$$q_{sc} = \frac{kAT_{sc}}{\mu ZTp_{sc}} p \frac{\mathrm{d}p}{\mathrm{d}z} \tag{A.2}$$

In flowing through the cement column, changes in gas temperature, viscosity, and Z-factor are likely to be small and expected to be well represented by the average

* Part of this section is reprinted with permission from "Rocha-Valadez, T., Hasan, A. R., Mannan, M. S., & Kabir, C. S. (2014). Assessing Wellbore Integrity in Sustained Casing Pressure Annulus. *SPE Drilling & Completion*, *29* (01), 131-138". Copyright 2014, SPE.

values evaluated at the initial condition, T_i, μ_i, and Z_i. Under these assumptions, integration of Equation A.2 leads to the following relation between gas seepage rate q_{sc}, formation pressure, p_f and pressure at the top of cement, p_c:

$$q_{sc} = \frac{kAT_{sc}}{2L_c\mu_i Z_i p_{sc} T_i}\left(p_f^2 - p_c^2\right) \tag{A.3}$$

In oilfield units, Equation A.3 is rewritten as:

$$q = \frac{0.003164kAT_{sc}}{L_c\mu_i Z_i p_{sc} T}\left(p_f^2 - p_c^2\right) \tag{A.4}$$

Equation A.4 was used by Xu (2002) and others without showing its roots.

A.2. Governing Equation and Solution for SCP

By use of the gas law, $n = pV/(ZRT)$, and neglecting the variation of gas-deviation factor with time, the molar rate of gas into the casinghead can be written as:

$$\frac{\mathrm{d}n}{\mathrm{d}t} = \frac{1}{ZRT_{wh}}\left(V\frac{\mathrm{d}p}{\mathrm{d}t} + p\frac{\mathrm{d}V}{\mathrm{d}t}\right) \tag{A.5}$$

The gas accumulation rate, $\mathrm{d}n/\mathrm{d}t$, can also be related to the volumetric flow rate, q, by:

$$\frac{dn}{dt} = \frac{q_{sc} p_{sc}}{ZRT_{sc}} \tag{A.6}$$

Because the rate equation is written in terms of gas rate at standard conditions, Equation A.6 has standard pressure, p_{sc}, in the numerator. Xu (2002) used pressure at the top of cement (bottom of the mud column), p_c, which may be imprudent. Equations A.5 and A.6 are combined to obtain the following expression for the change of pressure with time:

$$\left(\frac{q_{sc} p_{sc}}{ZRT_{sc}}\right) = \frac{1}{ZRT_{wh}}\left(V\frac{dp}{dt} + p\frac{dV}{dt}\right) \tag{A.7}$$

Since the change in the length of the mud column is compensated by the change in mud density, the pressure exerted by the mud column is constant. In other words, the pressure increase at the cement top will be attributed solely to the gas chamber pressure increase as follows:

$$p_c = p + 0.052\rho_m L_f \tag{A.8}$$

The gas-chamber volume increases with time as the mud column is compressed. The decrease in mud volume is given by:

$$V = V_i + c_m V_m (p - p_{atm}) \tag{A.9}$$

where c_m is the mud compressibility at gauge pressure. The variation of gas volume with respect to time can be written as:

$$\frac{\mathrm{d}V}{\mathrm{d}t} = c_m\left(V_m \frac{\mathrm{d}p}{\mathrm{d}t} + p\frac{\mathrm{d}V_m}{\mathrm{d}t}\right) \tag{A.10}$$

Because the change in the mud volume represents the equal and opposite change of the gas-cap volume, the second term on the right-hand side of Equation A-10, [p ($\mathrm{d}V_m/\mathrm{d}t$)], can be written as [$-p$ ($\mathrm{d}V/\mathrm{d}t$)]. This step allows for the rearrangement of Equation A.10 in explicit form for ($\mathrm{d}V/\mathrm{d}t$):

$$\frac{\mathrm{d}V}{\mathrm{d}t} = \left(\frac{c_m V_m}{1 + c_m p}\right)\frac{\mathrm{d}p}{\mathrm{d}t} \tag{A.11}$$

Substituting Eqs. A.4, A.9, and A.11 into Equation A.7 the following equation, with the derivation shown, is obtained:

$$\frac{0.003164kAT_{sc}}{L_c\mu_i Z_i p_{sc} T}\frac{p_{sc}}{ZRT_{sc}}\left(p_f^2 - p_c^2\right) = \frac{1}{ZRT_{wh}}\left[V\frac{\mathrm{d}p}{\mathrm{d}t} + p\frac{\mathrm{d}V}{\mathrm{d}t}\right]$$

$$\frac{0.003164kAT_{wh}}{L_c\mu_i Z_i T}\left(p_f^2 - p_c^2\right) = \left[\left(V_i + c_m V_m p\right)\frac{\mathrm{d}p}{\mathrm{d}t} + p\frac{\mathrm{d}V}{\mathrm{d}t}\right]$$

$$= \left[\left(V_i + c_m V_m p\right)\frac{\mathrm{d}p}{\mathrm{d}t} + p\left(\frac{c_m V_m}{1 + c_m p}\right)\frac{\mathrm{d}p}{\mathrm{d}t}\right]$$

$$\frac{0.003164kAT_{wh}}{L_c\mu_i Z_i T}\left(p_f^2 - p_c^2\right) = \left[V_i + c_m V_m p\left(1 + \frac{1}{1 + c_m p}\right)\right]\frac{\mathrm{d}p}{\mathrm{d}t} \tag{A.12}$$

Substitution and regrouping leads to the differential equation governing the transient behavior of casing pressure:

$$\frac{\mathrm{d}p}{\mathrm{d}t} = \frac{\dfrac{0.003164kAT_{wh}}{L_c\mu_i Z_i T}\left(p_f^2 - (p + 0.052\rho_m L_f)^2\right)}{V_i + c_m V_m p\left(1 + \dfrac{1}{1 + c_m p}\right)} \tag{A.13}$$

For simplification, we group constants in the following form:

$$b = 0.052\rho_m L_f \quad ; \qquad d = \frac{0.003164kAT_{wh}}{L_c\mu_i Z_i P_{sc} T}; \tag{A.14}$$

Using these lumped parameters and separating the variables allow us to solve Equation A.13 as follows:

$$\begin{aligned} t = {} & \frac{\{(\alpha - 1)V_i - \alpha\beta V_m\}\tanh^{-1}\left(\dfrac{p + b}{p_f}\right)}{p_f d(\alpha - 1)} \\ & + \frac{c_m V_m\left\{2\ln[1 + c_m p] + (2 - \alpha)\ln\left[p_f^2 - (p + b)^2\right]\right\}}{2d(\alpha - 1)} \end{aligned} \tag{A.15}$$

where α and β represent the following groups of constants:

$$\alpha = 2bc_m - b^2c_m^2 + c_m^2 p_f^2 \quad ; \quad \beta = bc_m - 1 \tag{A.16}$$

The time, t to reach a certain pressure, p can be obtained by evaluating Equation A.15:

$$t = t(p) - t(p_o) \tag{A.17}$$

APPENDIX B

NATURAL GAS PROPERTIES ESTIMATION

An accepted practice in the oil and gas industry is to use Sutton's correlations to estimate the mixture's pseudocritical properties. These correlations are based on the mixture's specific gravity and using the Dranchuk and Abou-Kassem equation of state to estimate the gas compressibility factor. Since the gas in the annulus is a mixture, the mixture specific gravity, γ_g, is used. Sutton (1985) used a second order regression analysis to fit pseudocritical properties from hydrocarbon mixture data. The formulas are as follows (Sutton, 1985):

$$p_{pc} = 756.8 - 131.07\gamma_g - 3.6\gamma_g^2 \tag{B.1}$$

$$T_{pc} = 169.2 + 349.5\gamma_g - 74.0\gamma_g^2 \tag{B.2}$$

These equations are valid over the range of specific gravities from $0.57 < \gamma_g < 1.68$. The pseudo-reduced pressure and temperature are relative to the pseudocritical properties:

$$p_{pr} = \frac{p}{p_{pc}} \tag{B.3}$$

$$T_{pr} = \frac{T}{T_{pc}} \tag{B.4}$$

The compressibility factor, Z, for real gases is obtained from the (Dranchuk & Abou-Kassem, 1975) equation of state. This equation of state was fitted to over 1,500 data points and is valid over the ranges of $0.2<p_{pr}<30$ with pseudoreduced temperature range between 1 and 3; and for $p_{pr}<1.0$ with pseudoreduced temperature between 0.7 and 1.0. The equation of state is as follows (Dranchuk & Abou-Kassem, 1975):

$$Z = 1 + \left(A_1 + \frac{A_2}{T_r} + \frac{A_3}{T_r^3} + \frac{A_4}{T_r^4} + \frac{A_5}{T_r^5} \right) \rho_r + \left(A_6 + \frac{A_7}{T_r} + \frac{A_8}{T_r^2} \right) \rho_r^2 - A_9 \left(\frac{A_7}{T_r} + \frac{A_8}{T_r^2} \right) \rho_r^5 + A_{10} \left(1 + A_{11} \rho_r^2 \right) \left(\frac{\rho_r^2}{T_r^3} \right) \exp\left[- A_{11} \rho_r^2 \right] \tag{B.5}$$

where the values of the constants are A_1= 0.3265, A_2= −1.07, A_3= −0.5339, A_4= 0.01569, A_5= −0.05165, A_6= 0.5475, A_7= −0.7361, A_8= 0.1844, A_9= 0.1056, A_{10}= 0.6134, A_{11}= 0.721 and:

$$\rho_r = \frac{0.27 p_r}{Z T_r} \tag{B.6}$$

Equations B.5 and B.6 need to be solved iteratively. Generally an initial value of Z=1 can be used to begin iterating by solving B.6 and then B.5 until convergence. An alternative is to use nonlinear-equation solver algorithms. The absolute error of the compressibility factor obtained by this equation of state, is reported by their authors as 0.486% with a standard deviation of 0.00747.

APPENDIX C

ACOUSTIC WELL SOUNDING TEST PROCEDURE USED FOR DATA COLLECTION[*]

Four tests were conducted on three gas-lift wells that were suspected to have leaking GLVs in an offshore setting. The first of these tests followed the most elaborate procedure for data gathering at the surface; the other three tests followed some of the same procedure. The steps for the procedure for Test-1 in Well 1 are:

1. Gathered acoustic data over a 6-hour period to determine the liquid level in the annulus at various times. The data clearly showed that the liquid level moved up with time, indicating a leaking GLV.
2. Conducted a drawdown (DD-1) test over a 4-hour period, with monitoring of annular pressure that declined with time.
3. The first drawdown was followed by a 15-minute buildup (PBU-1), which raised the annular pressure by 17.4 psig.
4. Followed the PBU-1 with a CPB test of the annulus by keeping the annular pressure constant to meter leakage through the GLV for an hour.
5. Followed the CPB with a second drawdown test (DD-2), which was initiated over a period of 5 hours and resulted in a decrease of the annular pressure with time.

[*] Part of this section is reprinted with permission from "Rocha-Valadez, T., Hasan, A. R., Mannan, M. S., Crabtree, A., & Kabir, C. S. (2014). *Assessing Integrity of the Gas-Lift Valves by Analyzing Annular-Pressure-Transient Response* Paper presented at the SPE Artificial Lift Conference and Exhibition - North America, Houston, Texas". Copyright 2014, SPE

6. Conducted another CPB to meter the leakage rate through the GLV for a 50-minute period.
7. Conducted a second buildup (PBU-2) for 25 minutes.

These seven steps appear to be too cumbersome and time-consuming for gathering required information on the leakage rate. As pointed out in the Discussion of section 4, the three-step test procedure proposed should yield the desired information.

While analyzing the test data, we made the following assumptions:

1. Figure C.1 shows the acoustic liquid-level data from Well 1 that was gathered during the drawdown period. These and other data show that the liquid level behaves linearly with annular pressure. The liquid-level data are also essentially linear with time, but pressure offers a more reasonable correlation. Some of the acoustic data were taken after a short buildup period; therefore, the liquid-level data are only approximately linear. However, this assumption allows us to estimate the movement of liquid level with time, and the volume of gas in the annulus. The annular gas volume is needed for the analysis of drawdown data.
2. Gas occupies the annulus from the casinghead to the liquid level. When needed, we interpolated the liquid level from the acoustic data. When acoustic measurements are unavailable, the initial-liquid level may be assumed to be at the lowest GLV.

3. Only single-phase liquid flows from the tubing into the annulus. This assumption is reasonable because any gas in the tubing will quickly migrate upward and therefore will not be available for flow into the annulus.
4. The reported flow rates (for comparison purposes) are from the two metered drawdown periods.

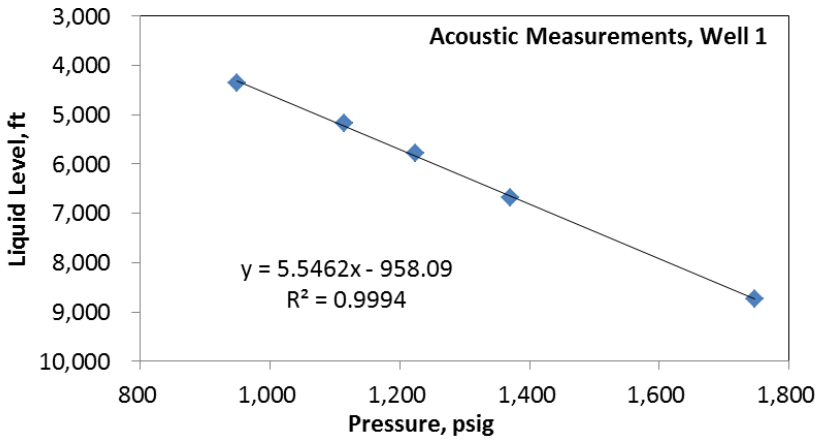

Figure C.1. Liquid level changes linearly with casinghead pressure, Well 1.